

Novel α -olefin polymer systems

by

Lufuno Siphuma

Dissertation presented for the Degree

Doctor of Philosophy (Polymer Science)

at the

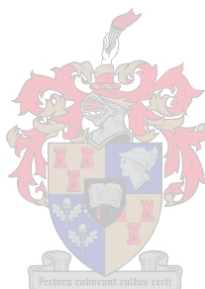
University of Stellenbosch

Promotor

Dr. A. J. van Reenen

Stellenbosch

March 2005



DECLARATION

I, Lufuno Siphuma, hereby declare that the work contained in this dissertation is my own original work and that I have not previously in its entirety or in part submitted it at any university for a degree.

Abstract

Propylene oligomers with unsaturated chain endgroups were synthesized using metallocene catalysts activated with methylalumoxane (MAO). The complexes *rac*-*et*(Ind)₂ZrCl₂/MAO (**1**) and Me₂Si[2-Me-Benzo(Ind)]₂ZrCl₂/MAO (**2**) produced propylene oligomers containing a large amount of vinylidene terminated endgroups. From ¹H NMR the presence of vinyl and butenyl endgroups could be seen, although in very low amounts. The metallocene (**1**) produced lower molecular weight oligomers than the metallocene (**2**) under similar conditions.

Regio-irregular 2,1-misinsertions were observed by using ¹³C NMR spectroscopy in both catalyst systems (**1** and **2**).

The synthesized oligomers generally had low tacticity, especially those produced from complex (**1**).

The stereoerrors found in these propylene oligomers decreased with an increase on the molecular weight of the material. As reaction temperatures were increased, tacticities decreased. Polydispersities and molecular weight could be altered by varying parameters, such as catalyst and co-catalyst concentrations, temperature and time of reactions.

Selected propylene oligomers were used in copolymerization reactions with ethylene as the second monomer using metallocene catalysts: *i*-pr(9-Flu)CpZrCl₂ (syndiotactic) and Me₂Si[(Cp*)][(tert-Bu)N]TiMe₂ (constrained geometry) activated with MAO. From ¹³C NMR evidence of small fraction of propylene oligomer in the copolymer could be found. This means the only reactive endgroup towards the selected metallocene was the vinyl endgroups.

The copolymers showed broad molecular weight distribution and in some instances, where there was notable incorporation of the propylene oligomers, a bimodal molecular weight distribution was observed.

Further studies involved the hydration of propylene oligomers via their unsaturated chain end-groups, using *oxymercuration-demercuration* reactions. This resulted in a tertiary hydroxyl group at the end of the polymer

chain. The hydroxyls were converted to acrylate esters by reactions with acryloyl chloride to form oligopropenylacrylates.

The oligopropenylacrylates were then homopolymerized, and copolymerized with methyl methacrylate (MMA), using a free radical initiator (AIBN).

Mechanical studies on the copolymers were done using DMA. For the oligopropenylacrylate copolymer with MMA, there was an additional transitional peak at $-50^{\circ}\text{C}.$, indicating that phase separation occurred at molecular level in these copolymers.

Opsomming

Propileen oligomere met onversadigde endgroepe is gesintetiseer deur gebruik te maak van metalloseen-kataliste wat met metiel-alumoksaan (MAO) geaktiveer is. Die verbindings *rac*- $\text{et}(\text{Ind})_2\text{ZrCl}_2/\text{MAO}$ (**1**) en $\text{Me}_2\text{Si}[2\text{-Me-Benzo}(\text{Ind})]_2\text{ZrCl}_2/\text{MAO}$ (**2**) het propileen oligomere gelewer wat 'n groot hoeveelheid vinilideen-endgroepe bevat het. Deur die gebruik van ^1H KMR spektroskopie is die teenwoordigheid van viniel en buteniël endgroepe oof waargeneem, alhowel in baie klein hoeveelhede. Die metalloseen (**1**) het oor die algemeen laer molekulêre massa oligomere gelewer as die metalloseen (**2**) onder soortgelyke reaksietoestande.

Regio-onsimmetriese 2,1-mis-invoegings is deur ^{13}C KMR spektroskopie waargeneem vir beide katalissisteme (**1** en **2**).

Die oligomere het oor die algemeen lae taktisiteit gehad, veral die deur verbinding (**1**) vervaardig

Die stereo-foute wat in die propileen oligomere gevind is, het oor die algemeen afgeneem met 'n toename in die molekulêre massa van die materiaal. Taktisiteit het oor die algemeen ook afgeneem met toenemende reaksietemperatuur. Molekulêre massa sowel as molekulêre massa verspreidingswaardes kon beheer word deur die manipulasie van reaksieparameters soos katalis en ko-katalis konsentrasies, reaksietemperatuur en reaksietye.

Geselekteerde propileen oligomere is gebruik in kopolimerisasie-reaksies met etileen as tweede monomeer. Metalloseen kataliste, nl. $i\text{-pr}(9\text{-Flu})\text{CpZrCl}_2$ (syndiotactic) en $\text{Me}_2\text{Si}[(\text{Cp}^*)[(\text{tert-Bu})\text{N}]\text{TiMe}_2]$ is gebruik vir die reaksies. ^{13}C KMR het aangedui dat klein hoeveelhede van die oligomere in die kopolimere ingevoeg is. Slegs die klein persentasie viniel endgroepe teenwoordig kon aan hierdie reaksies deelneem.

Die kopolimere het breë molekulêre massa verspreiding geopenbaar, met selfs bimodale verspreidings in gevalle waar opmerkbare hoeveelhede van die oligomeer in die kopolimeer ingevoeg is.

Verdere studies het die hidrasie van die oligomere via hulee onversadigde endgroepe deur gebruik te maak van *oksiemerkurasie-demerkurasie* reaksies. Sulke reaksies het gelei tot die vorming van 'n tersiêre hidroksie-groep op die ketting-endpunt. Hierdie hidroksie-groep is chemies omgesit in akrilaat-esters deur reaksie met akriloïel chloride om oligopropenielakrilate te vorm.

Die oligopropenielakrilate is deur 'n vrye radikaal meganime gepolimeriseer, beidie as homopolimeer en as kopolimeer met metielmetakrilaat.

Meganistiese studies is op die kopolimere gedoen deur DMA. Die kopolimere het 'n addisionele oorgang by -50°C getoon, wat aandui dat fase-skeiding op molekulêre vlak in die kopolimere plaasvind.

Acknowledgements

There are many people who shared their thoughts and made valuable contributions during the study of this degree. As the list will be very long I will not be able to list all of them by names. I would like to thank Dr. A. J. van Reenen, my study leader and promotor who guided me through the study and gave me encouragement when I lost motivation. Dr. M. W. Bredenkamp, for his scientific input regarding the organic synthesis work. Financial sponsors: The National Research Foundation, Sasol, and Institute for Polymer Science at the University of Stellenbosch. Prof. Sanderson, staff and students at the Institute for Polymer Science who assisted me in any form during the studies. My colleagues at the Olefin Research Laboratory, not forgetting the encouragement we had, Siya, Charl, Liezel, Nyambeni and Marietjie thanks a lot. Prof. Mathias of Polymer Science department, University of Southern Mississippi, who allowed me to work in his group and gave me valuable information on scientific understanding of polymer macromolecules.

My family especially my mother who gave me support during the study. Friends outside the department (amongst others Victor, Memory) who helped share their ideas and support.

Table of contents

	Page
List of contents	I
List of figures	VII
List of schemes	XII
List of tables	XIV
List of abbreviations	XV

List of Contents

Chapter 1. Introduction and Objectives	1
1.1 <i>Introduction</i>	1
1.2. <i>Objectives</i>	2
1.2.1 Synthesis of propene oligomers	2
1.2.2 Copolymerization of the propene oligomers	3
1.2.3 Investigation of microstructure of the oligomers	4
1.2.4 Functionalization and copolymerization of the functionalized oligomers	4
1.3. <i>References</i>	5
Chapter 2. Background and Theory	7
2.1 <i>Metallocenes in General</i>	7

2.1.1	Introduction	7
2.1.2	Tacticity and catalyst symmetry	8
2.2	<i>Polypropylene by metallocene catalyzed polymerization.</i>	13
2.2.1	Mechanism of polymerization	13
2.2.1.1	Formation of the active species	13
2.2.1.2	Olefin coordination	14
2.2.1.3	Olefin insertion	16
2.2.1.4	Stereocontrol	18
2.3	<i>Effect of cocatalysts: The alumoxanes</i>	22
2.3.1	Other cocatalysts	24
2.4	<i>Chain transfer reactions</i>	25
2.5	<i>Effect of the transition metal on catalyst productivity</i>	27
2.6	<i>Effect of the ligand</i>	28
2.6.1	Ligands for elastomeric PP	33
2.5.2	Halogenated ligands	36
2.7	<i>Copolymerization of higher α-olefins</i>	38
2.8	<i>Long-chain branching in polyolefins</i>	40
2.9	<i>Temperature</i>	42
2.10	<i>Dimerization and oligomerization of olefins</i>	42
2.11	<i>Polymerization of functionalized monomers</i>	44
2.11.1	Functionalized polyolefins	45

2.12	<i>Mechanical properties</i>	46
2.13	<i>References</i>	48
	Chapter 3. Experimental	55
3.1	<i>Oligomerization</i>	55
3.1.1	Chemicals	55
3.1.2	Preparation of catalyst solutions (typical)	55
3.2.3	Oligomerization procedure (typical)	56
3.2	<i>Copolymerization of oligomers with ethylene</i>	56
3.2.1	Materials	56
3.2.2	Preparation of catalyst solutions	57
3.2.3	Copolymerization reactions	57
3.3	<i>Functionalization and block copolymerization reactions of propylene oligomers</i>	58
3.3.1	Hydration reactions	58
3.3.2	Synthesis of acryloyl esters of the propylene oligomers	59
3.3.4	Polymerization of oligomer acryloyl esters by free radical initiators	60
3.4	<i>Characterization techniques</i>	60
3.4.1	NMR spectroscopy	60
3.4.1.1	Spectroscopy for room temperature samples	60
3.4.1.2	Spectroscopy for high temperature samples	60
3.4.2	Infrared spectroscopy	61
3.4.3	Differential Scanning Calorimetry	61
3.4.4	Size exclusion chromatography	62

3.4.4.1	Size exclusion chromatography for room temperature samples	62
3.4.4.2	High temperature size exclusion chromatography	62
3.4.5	Crystallization analysis by fractionation	62
3.5	<i>References</i>	63
Chapter 4. Oligomerization		64
4.1	<i>Solution Oligomerization</i>	64
4.1.1	Oligomer Synthesis	64
4.1.2.	NMR Spectroscopy	67
4.1.2.1	^1H NMR	67
4.1.2.2	^{13}C NMR	68
4.2	<i>Microstructure of the Oligomers</i>	68
4.2.1	Regiochemistry	72
4.2.2	The Development of stereoerrors	76
4.2.3	Tacticity	81
4.3	<i>Attempted oligomerization reactions in bulk</i>	82
4.4	<i>Conclusions</i>	84
4.5	<i>References</i>	85
Chapter 5. Reactions of the propene oligomers		86
5.1	<i>Copolymerization</i>	86
5.2	<i>Products and yields</i>	90
5.3	<i>Copolymer Molecular weight</i>	99

5.4.	<i>Crystallization analysis by fractionation (CRYSTAF)</i>	101
5.5	<i>Thermal characterization</i>	105
5.6	<i>Conclusions</i>	107
5.7.	<i>References</i>	107
 Chapter 6. Functionalization and block copolymerization reactions of propylene oligomers		 109
6.1	<i>Introduction</i>	109
6.2	<i>Hydration of oligomers</i>	110
6.2.1	NMR Studies	111
6.2.1.1	¹H NMR	111
6.2.1.2	¹³C NMR	112
6.2.2	Infrared spectra	114
6.2.3	Mechanism of hydration	115
6.3	<i>Esterification of the hydrated oligomers</i>	116
6.3.1	Reactions of methacryloyl chloride in THF	116
6.3.2	The reaction of acryloyl chloride with oligomer in ether as a solvent	119
6.4	<i>Polymerization of the acrylate ester oligomer</i>	124
6.4.1	¹³C NMR of the polymer	125
6.4.2.	Molecular weight of polymers	126
6.4.3	Dynamic mechanical properties	127
6.5.	<i>References</i>	129

Chapter 7. Conclusions and recommendations	130
7.1 <i>Introduction</i>	130
7.2 <i>Oligomerization</i>	130
7.3 <i>Copolymerization of oligomers with ethylene using metallocene catalysts</i>	131
7.4 <i>Functionalizaion and block copolymerization</i>	132
7.4.1 Hydration of propylene oligomers	132
7.4.2 Synthesis of oligomer acrylate esters	133
7.4.3 Polymerization of acrylate esters	133
7.5 <i>Recommendations</i>	134
7.6 <i>References</i>	134

List of Figures

Chapter 1

- Figure 1: Propylene oligomer with vinylidene end-group 3
- Figure 2: Proposed structure of ethylene and propylene oligomer copolymer 3
- Figure 3: Proposed structure of oligopropenylacrylate formed by esterification of vinylidene-terminated oligopropene 4

Chapter 2

- Figure 1: Different configurations of polypropylene 8
- Figure 2: The symmetry arrangements of metallocene catalysts, with description of the coordination and tacticities of the polymers formed by these symmetries 9
- Figure 3: Examples of C_2 -symmetric metallocenes 11
- Figure 4: Examples of C_s -symmetric catalysts 12
- Figure 5: Examples of C_1 -symmetric catalysts 12
- Figure 6: Inner layer of triple-layer cage structure of MAO 22
- Figure 7: Structure of silyl-bridged metallocene with benzindenyl ligands 30
- Figure 8: Substituted ligands for C_1 -symmetric bridged catalysts 32
- Figure 9: The Waymouth compounds and their rotation to synthesize elastomeric PP 34
- Figure 10: Cyclopentadienyl zirconocene with alkenyl substituents 35
- Figure 11: Phenyl substituted biscyclopentadienyl zirconocenes 36
- Figure 12: Zirconocene with substituted ligands 37
- ### Chapter 4
- Figure 1: Metallocenes used for oligomerizations 64

Figure 2:	¹H NMR of propene oligomer synthesized using Et(Ind)₂ZrCl₂ at 100°C	67
Figure 3:	¹³C NMR spectrum of propene oligomers (I) synthesized using catalyst (1) and (II) synthesized using catalyst (2)	68
Figure 4:	¹³C NMR spectra of oligomers prepared with three different catalysts	70
Figure 5:	¹³C NMR of the region 14 – 23 ppm of a propylene oligomer prepared with EBI catalyst. The arrows indicate the “vinylidene” “n-propyl methyls associated with chain ends (refer to Table 2)	71
Figure 6:	¹³C NMR spectrum illustrating the position of peaks arising from <i>threo</i>- 2,1-misinsertions in polypropylene. Refer to Scheme 4 for carbon numbering	73
Figure 7:	¹³C NMR spectra of the “aliphatic” region of two oligomers prepared by EBI catalyst (bottom trace) and MBI catalyst (top trace)	73
Figure 8:	Oligomer prepared with a C_{2v}-symmetric metallocene catalyst	74
Figure 9:	¹³C NMR spectra of oligomers prepared by the MBI catalyst and 80, 90, 100°C	75
Figure 10:	¹³C NMR spectra of a polymer and oligomer of propylene prepared by the same catalyst ((MBI) catalyst	76
Figure 11:	¹³C NMR of polypropylene prepared at 100°C using the MBI catalyst. The expansion shows the microstructure	77
Figure 12:	Stereoerrors present in two oligomers	79
Figure 13:	¹³C NMR of polypropylene with Mw of 90 000 prepared at 100°C using MBI catalyst	80
Figure 14:	DSC thermogram of the oligomer	83
Figure 15:	Crystallization curves of the materials synthesized in bulk	83

Chapter 5

- Figure 1:** ^1H NMR of an oligomer prepared with the MBI catalyst; vinylidene, vinyl and 2-butenyl endgroups are indicated 87
- Figure 2:** Catalysts used for the copolymerization reactions 88
- Figure 3:** ^{13}C NMR spectra of reaction products 272 and 274 (Table 1); no extraction 91
- Figure 4:** ^{13}C NMR spectra of reaction products 282 and 295 (Table 1) 91
- Figure 5:** ^{13}C NMR spectra of reaction product 174 before and after extraction with hexane 92
- Figure 6:** ^{13}C NMR spectra of hexane extract (top) and remaining material (bottom) of product 174 93
- Figure 7:** ^{13}C NMR spectrum of reaction product 302 (Table 2) 94
- Figure 8:** ^{13}C NMR spectrum of reaction product 306 (Table 2) 95
- Figure 9:** ^{13}C NMR spectra of reaction product 307 (Table 2) before and after hexane extraction 96
- Figure 10:** ^{13}C NMR spectrum of reaction product 347 (Table 2) 97
- Figure 11:** ^{13}C NMR spectra of reaction products 358 and 359 (Table 2) after hexane extraction 98
- Figure 12:** ^{13}C NMR spectra of the oligomer (ii) in deuterated chloroform, and its homopolymer (i) in trichlorobenzene synthesized using catalyst (2) 99
- Figure 13:** GPC curve of ethylene copolymer with propylene oligomer ($M_w \cong 4\,200$) synthesized using catalyst (1) at 70°C 100
- Figure 14:** GPC curve of ethylene copolymer with propylene oligomer ($M_w \cong 1\,800$) using catalyst (2) at 60°C 101
- Figure 15:** Crystallization curves of the copolymers, Δ and * were synthesized using catalyst 1 at polymerization temperatures of 60 and 80°C , and +, o, and x were synthesized using catalyst 2 at 60°C , while – was synthesized using catalyst 1, at room temperature 102

- Figure 16:** Influence of polymerization temperatures on the crystallinity of the copolymers synthesized using catalyst 1, *, \diamond , Δ at polymerization temperatures of 60, 70 and 80°C respectively 103
- Figure 17:** ^{13}C NMR spectrum of xylene soluble fraction of copolymer in toluene- d^8 . The large peak at 20 ppm is due to solvent 104
- Figure 18:** DSC thermogram of the ethylene copolymer with propylene oligomer ($M_w \cong 4\,500$) synthesized using catalyst 1 at 70°C 105

Chapter 6

- Figure 1:** ^1H NMR spectra of propylene oligomers ($M_w \cong 500$): (i) after hydration and (ii) before hydration 110
- Figure 2:** ^{13}C NMR spectra of propylene oligomers ($M_w \cong 500$): (i) shows the spectrum of the oligomer after it was hydrated and (ii) before it was hydrated 112
- Figure 3:** Infrared spectra of propylene oligomers ($M_w \cong 700$), (A) before hydration and (B) after hydration process 113
- Figure 4:** ^1H NMR of the methacrylate ester of a propylene oligomer ($M_w \cong 800$). 116
- Figure 5:** ^{13}C NMR spectrum of the methacrylate ester of a propylene oligomer ($M_w \cong 800$) 117
- Figure 6:** Infrared spectrum of the methacrylate ester of the propylene oligomer ($M_w \cong 800$). 118
- Figure 7:** ^1H NMR spectra comparing the unreacted acryloyl chloride (ii) and acrylate ester of a propylene oligomer (i) ($M_w \cong 350$) 120
- Figure 8:** ^{13}C NMR spectra of acryloyl chloride (2) in toluene- d_8 and the acrylate ester of propylene oligomer (1) ($M_w \cong 350$) in CDCl_3 121
- Figure 9:** Infrared spectrum of the acrylate ester of a propylene oligomer ($M_w \cong 350$) 122
- Figure 10:** ^{13}C NMR spectra of the oligopropenylacrylate (i) and its homopolymer (ii) 125

Figure 11: GPC curves of the acrylates synthesized using AIBN at 80°C, \diamond is the homopolymer of the acrylate ester of propylene oligomer, Δ is the copolymer of acrylate ester of propylene oligomer and \times is the homopolymer of MMA **126**

Figure 12: DMA curves of the PMMA (Δ) and a copolymer of PMMA with oligopropenylacrylate (\diamond) **127**

List of Schemes

Chapter 2

Scheme 1: Reactivation of the dormant site	14
Scheme 2: Control of monomer coordination	15
Scheme 3: Types of stereoerrors determined by stereocontrol mechanism	15
Scheme 4: Cossee-Alrman mechanism for olefin insertion	17
Scheme 5: Green-Rooney mechanism for olefin polymerization	17
Scheme 6: Mechanism of stereoregulation for both syndiotactic and isotactic chain-end controlled propylene polymerization	18
Scheme 7: Enantiomorphic site control mechanism	20
Scheme 8: Depiction of β -hydride transfer reactions	25
Scheme 9: Regeneration of the dormant sites by H_2	26
Scheme 10: Chain-end formation by β - CH_3 transfer and H transfer reactions	26
Scheme 11: Formation of internal vinylidene	27

Chapter 4

Scheme 1: Oligomerization of propylene	65
Scheme 2: The schematic representation of polymeryl transfer to the Al center	71
Scheme 3: <i>Threo</i> 2,1-insertion during propylene polymerization	72

Chapter 5

Scheme 1: A schematic representation of a propylene oligomer with vinylidene and n-propyl endgroups. The methyls discussed in the text are circled	86
Scheme 2: Copolymerization of ethylene with propylene oligomers	89

Chapter 6

Scheme 1: Hydration of oligomers using mercuric acetate	114
Scheme 2: Removal of mercury from the oligomers	115
Scheme 3: Esterification of oligomers using methacryloyl chloride	116
Scheme 4: Reaction of hydrated oligomer with acryloyl chloride	119
Scheme 5: Assignment of vinyl protons of the acrylate ester of propylene oligomer	119
Scheme 6: Homopolymerization of acrylate ester of oligomer with AIBN	123
Scheme 7: Copolymerization of acrylate ester of oligomer with methyl methacrylate	124

List of Tables

Chapter 4

Table 1:	Oligomerization of propylene: Representative results.	65
Table 2:	Common endgroups and ^{13}C NMR shifts for propylene polymers.	69
Table 3:	Chemical shifts of different stereoerrors in polypropylene.	78
Table 4:	Tacticity as measured by mmmm% of oligomers prepared with three different catalysts.	81

Chapter 5

Table 1:	Attempted copolymerization of propylene oligomers with ethylene using catalyst 1.	89
Table 2:	Attempted copolymerization of oligomers with ethylene using catalyst 2.	90
Table 4:	Enthalpy values of copolymers from DSC and their melting temperatures.	106

Chapter 6

Table 1:	The molecular weights of the oligomers which were hydrated.	111
----------	---	-----

List of abbreviations

Al:	aluminium
Benz:	benzene
Cp:	cyclopentadienyl
Crystaf:	Crystallization analysis by fractionation
DMA:	dynamic mechanical analyzer
DSC:	differential scanning calorimetry
Elpp:	elastomeric polypropylene
Et:	ethylene
Flu:	fluorenyl
FTIR:	fourier transform infra-red
GPC:	gel permeation chromatography (size exclusion chromatography)
H:	hydrogen
Ind:	indenyl
<i>i</i> -pr:	iso-propyl
MAO:	methyl alumoxane
Me:	methyl
Mn:	number average molecular weight
Mt:	metallocene
Mw:	molecular weight
MWD:	molecular weight distribution
NMR:	nuclear magnetic resonance
PDI:	polydispersity index
Ph:	phenyl
PP:	polypropylene
TEA:	tiethyl aluminum
THF:	tetrahydrofuran
Tm:	melting temperature
TMA:	trimethyl aluminum
Tp:	polymerization temperature

Chapter 1

Introduction and Objectives

1.1 Introduction

The advent and development of metallocene catalysts for olefin polymerization has been extensively reviewed in recent years¹⁻³. Metallocene catalysts and related soluble transition metal catalysts are finding increasing use in commercial applications, even though the amounts remain low w.r.t. world production of polyolefins. Some of the earliest commercial applications of metallocene catalysts were in the production of polyethylenes, for example the range of plastomers and linear low density polyethylene (LLDPE) produced by Dow and Du Pont⁴.

The commercialization of these catalysts has been slow due in part to the lack of processability of these polymers compared to LLDPE prepared by Ziegler-Natta catalysts. Amongst the possible solutions to the processing problems of metallocene LLDPE is the inclusion of long-chain branching in the polymer chain, a broader or bimodal molecular weight distribution, and postproduction blending⁵. Metallocene catalysts are also capable of synthesizing oligomers from the α -olefins, at conditions that differ from those used during polymerization.

The α -olefin oligomers (and polymers) prepared by metallocene catalysts usually have vinyl or vinylidene end-groups. These functional groups allow further polymerization, or functionalization reactions (for example the formation of functional groups such as esters and amines). Furthermore the oligomers or higher α -olefins can be converted to plasticizer alcohols, additives for lubricants, amine oxides and amines, detergent alcohols and nonionics, lubrication oil additives and surfactants, or oil field chemicals and wax replacements⁶.

Oligomerization of the ethylene to yield higher, linear α -olefins have traditionally been achieved by the use of late transition metal compounds (for example the Shell Higher Olefin Process (SHOP)⁶). The chain lengths of these α -olefins vary from four carbons (1-butene) to more than thirty (C_{30+}). 1-Butene is a gas at room temperature and C_6 - C_{18} are clear colorless liquids, whereas C_{20+} are waxy solids.

Propylene oligomers with vinyl and vinylidene end groups have been synthesized using the metallocene catalysts activated with methyl alumoxane (MAO) at higher temperature^{7,8}.

The copolymerization of ethylene with various higher α -olefins such as 1-pentene, 1-hexene, and 1-octene, using metallocene catalysts, have been reported in numerous studies to give polymers with even short chain distributions^{5,6,9-12}. The presence of these other olefins in the polymer chain results in decreased crystallinity, melting temperature and (in some cases) a reduction in molecular weight of the polymers^{6,12-15}.

Several metallocene catalysts are capable of incorporating long chain oligomers that resulted from chain termination, back into the growing polymer chain thus yielding polyolefins with long chain-branching¹⁶⁻¹⁸.

Although the metallocene catalysts are effective in the polymerizations of α -olefins, they suffer from poor activity in the polymerization of functional monomers. There has been limited effort in the synthesis of block copolymers of olefins with other functional group monomers such as methyl methacrylate^{19,20}.

1.2. Objectives

1.2.1. Synthesis of propene oligomers

It is with the understanding of the above applications that the project was focussed on synthesizing propylene oligomers of varying molecular weight, with vinylidene (Figure 1) or vinyl end groups, using metallocene catalysts activated with MAO. The oligomers will be synthesized at high temperatures, while varying the conditions such as oligomerization time and the ratios of cocatalysts to the catalysts.

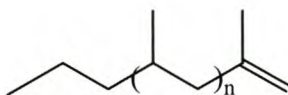


Figure 1: Propylene oligomer with vinylidene end-group.

Analysis of the oligomers will be made with regards to their molecular weight, presence of vinyl and vinylidene group and microstructure using Size Exclusion Chromatography and ^1H and ^{13}C NMR spectroscopy respectively.

1.2.2. Copolymerization of the propene oligomers

Copolymerization of the synthesized oligomers or macromers with ethylene will be attempted. Selected metallocene catalysts activated with MAO will be used while varying polymerization conditions such as temperature and monomer concentration. It is expected that the presence of the oligomers will offer long-chain branching in the polymer chain, or result in a decrease in molecular weight and broaden molecular weight distribution. This is based on the premise that some vinyl-terminated oligomers (rather than just the vinylidene-terminated species shown in Figure 1 above) will also be synthesized.

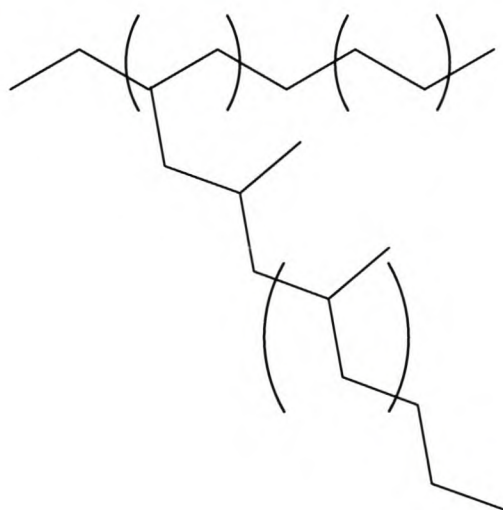


Figure 2: Proposed structure of ethylene and propylene oligomer copolymer.

The synthesized polymers will be analyzed with ^{13}C NMR to confirm the presence of the comonomer (macromer), and the effect of the macromer on the thermal

1.3. References.

1. K. Y. Mashima, Y. Nakayama, A. Nakamura; *Adv. Polym. Sci.*, **133**, **1997**, 1.
2. W. Kaminsky, M. Arndt; *Adv. Polym. Sci.*, **127**, **1996**, 143.
3. H. H. Brintzinger, D. Fischer, R. Mulhaupt, B. Rieger, R. M. Waymouth; *Angew. Chem. Int. Ed. Eng.*, **34**, **1995**, 1143.
4. A. M. Thayer; *Chemical and Engineering News*, **73**, **1995**, 16.
5. L. Buckalew and J. Schumacher, *Chemicals Economics Handbook, Marketing Research Report, Linear Low-Density Polyethylene (LLDPE) Resins*, August **2000**.
6. R. Modler, F. Dubois, M. Yamaki; *Chemicals Economics Handbook Marketing Research Report, Linear Alpha Olefins*, September **2000**.
7. W. Weng, A. Dekmezian, E. J. Markel, A. Gadkari, D. L. Peters; US Patent PCT, 6 117 962, Sept. **2000**.
8. P. F. Fu, S. Glover, R. K. King, C. Lee, M. R. Pretzer, M. K. Tomalia; *Polymer Preprints*, **41**, **2000**, 1903.
9. V. M. Litvinov, V. B. F. Mathot; *Solid State Nuclear Magnetic Resonance*, **22**, **2002**, 218.
10. K. Michiue, R. F. Jordan; *Macromol.*, **36**, **2003**, 9707.
11. R. Mulhaupt; *Macromol. Chem. Phys.*, **204**, **2003**, 289.
12. I. Kim, S. Y. Kim, M. H. Lee, Y. Do, M. S. Won; *J. Polym. Sci. Part A: Chem.*, **37**, **1999**, 2763.
13. C. L. P. Shan, J. B. P. Soares, A. Penlidis; *Polymer*, **43**, **2002**, 767.
14. K. J. Chung, T. H. Park; *Materials Letters*, **31**, **1997**, 11.
15. W. J. Wang, E. Kolodka, S. Zhu, Y. Hu, A. E. Hamielec; *J. Polym. Sci. Part A: Chem.*, **37**, **1999**, 2949.
16. D. Harrison, I. M. Coulter, S. Wang, S. Nistala, B. A. Kuntz, M. Pigeon, J. Tian, S. Collins; *J. Mol. Cat. A: Chem.*, **128**, **1998**, 65.
17. E. Kolodka, W. J. Wang, P. A. Charpentier, S. Zhu, A. E. Hamielec; *Polymer*, **41**, **2000**, 3985.
18. D. Beigzadeh, J. B. P. Soares, T. A. Duever; *Macromol. Rapid Commun.*, **20**, **1999**, 541.
19. T. C. Chung, G. Xu; Y. Lu, Y. Hu; *Macromolecules*, **34**, **2001**, 8040.

20. T. C. Chung, H. L. Lu; Y. Lu, Y. Hu; *J. Mol. Cat. A: Chem.* **115**, **1997**, 115.

Chapter 2

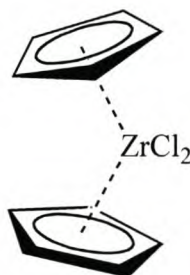
Background and Theory

2.1 *Metallocenes in General*

2.1.1 Introduction

Metallocene catalysts activated with methylalumoxane have been used to synthesize highly stereoregular polyolefins. The ability of these catalysts to display high catalytic activity, producing polymers with narrow molecular weight distribution and high molecular weight, has over the past decade attracted great interest both industrially and academically^{1,2}. These metallocene catalysts were initially thought to function in a “living” fashion, owing to their high activity and ability to resume polymerization again after monomer withdrawal³.

Metallocenes derive their name from Ferrocene with which they share a structural similarity^{4,5}. Nominally, the metallocenes comprise a central transition metal atom (normally Group IV) π -bonded to 2 cyclopentadienyl ligands and σ -bonded to 2 other ligands, normally halogen or hydrocarbyl. Thus a simple metallocene would be $(\eta^5\text{-Cp})_2\text{ZrCl}_2$:



Due to the fact that all the catalytic sites have the same electronic and steric structure, metallocene catalysts are commonly considered to be single site catalysts, although single-centre might be a better description⁶. These catalysts can have bridges between the Cp ligands or not; the bridged catalysts are commonly used for the polymerization of propylene and other higher α -olefins whereas the non-bridged catalysts are used mostly for ethylene polymerization⁴. The mechanism of polymerization with the metallocene catalysts will be discussed under propylene polymerization section below.

The ligands around the transition metal creates a symmetry which plays a pivotal role in determining the stereocontrol in olefin polymerization.

2.1.2 Tacticity and catalyst symmetry

Propylene can be polymerized with varying degrees of stereocontrol (see Figure 1). Atactic polypropylene (aPP) has a random orientation of methyl groups along the chain, it lacks crystallinity and is usually an oil or wax. In isotactic polypropylene (iPP) all methyl groups show the same orientation so that the polymer strands can align themselves to give crystalline domains. In hemiisotactic PP the orientation of every second methyl group is random, while in syndiotactic PP (sPP) the methyl orientations alternate.

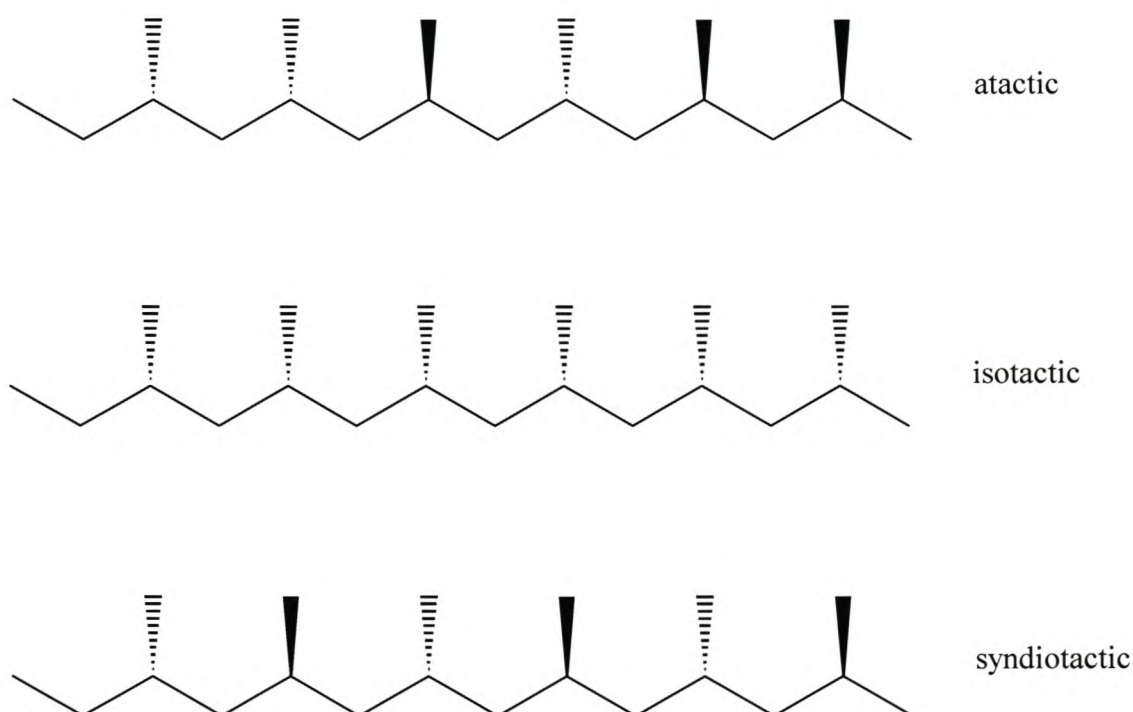


Figure 1: Different configurations of polypropylene.

The symmetry of the metallocene catalysts was described by Ewen and can be depicted as in Figure 2.

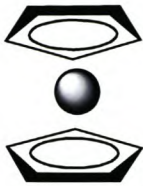
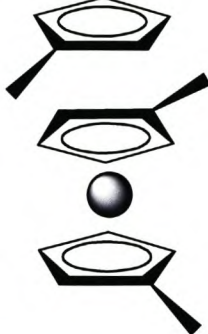
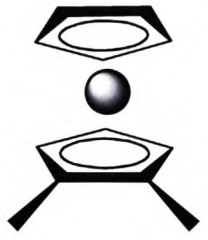
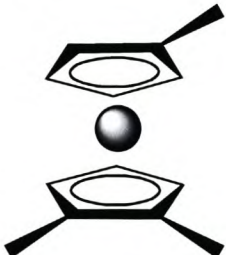
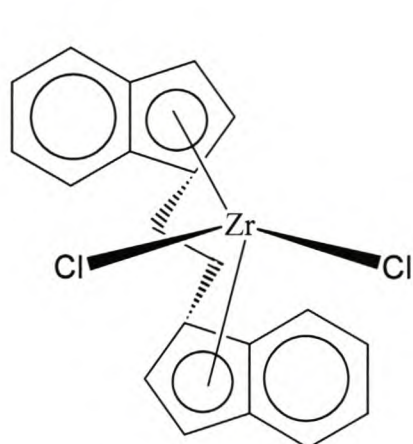
Symmetry		Sites	Polymer
C_{2v} , achiral		A,A, homotopic	Atactic
C_2 , chiral		E,E, homotopic	Isotactic
C_s , achiral		A,A diastereotopic	Atactic
C_s , prochiral		E,-E, Enantiotopic	Syndiotactic
C_1 , Chiral		E,A, Diastereotopic	Hemi-isotactic

Figure 2: The symmetry arrangements of metallocene catalysts, with description of the coordination sites and tacticities of the polymers formed by these symmetries.

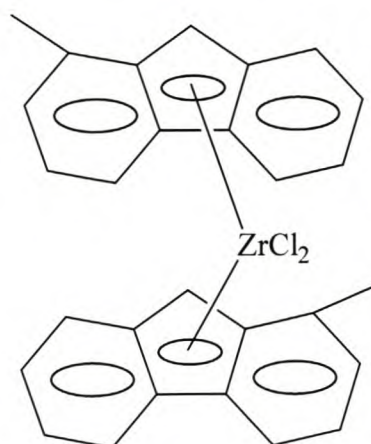
These metallocenes for stereospecific polymerization of propylene can be generalized into three main categories according to their symmetries: the C_2 -symmetric metallocenes give **isotactic** polypropylene, the C_s -symmetric metallocenes for **syndiotactic** polypropylene and the C_1 -symmetric metallocenes give **hemiisotactic to isotactic** polypropylene.

The isospecific catalysts can be further divided into three classes, the *ansa*- C_2 -symmetric (class I), the nonbridged, fluxional but chiral (class II), and the *ansa*- C_1 -symmetric (class III)⁶. Chiral, C_2 -symmetric *ansa*-zirconocenes can produce polypropylenes with a variety of different microstructures. These range from practically atactic to almost perfectly isotactic. These polymers will in most cases also contain regioirregularities due to 2,1- and 3,1-insertions⁶. The symmetry of an *ansa*-metallocene is maintained by the bridge linking the two cyclopentadienyl ligands, thus preventing rotation of the ligands. Thus C_2 -symmetric zirconocene catalysts produce isotactic polypropylene as a result of a site controlled mechanism (discussed in Section 2.2). This group of C_2 -symmetric catalysts can be further subdivided into three subdivisions based on ligands, being cyclopentadienyl, indenyls and fluorenyls.

The subdivision comprising the catalysts with cyclopentadienyl (Cp) ligands usually show low catalytic activity and poor enantioselectivity, which, however, is improved by the presence of the substituents on the Cp ring. The bisindenyl ligands (second subdivision) (Figure 3) show improved enantioselectivity (over the catalysts with Cp ligands). Resconi *et al*⁶ report that substituents in 2-position (which is α to the bridge), the 3-position (β to the bridge) and the 4-position (on the condensed benzene ring) are the most important with respect to the effects on stereoselectivity and molecular weight variation. The presence of substituents in the 3-position of the ligand improves enantioselectivity. The stereoselectivity of these catalysts is affected by the nature of the bridge and increase in the order $H_2C < Me_2C < C_2H_4 < Me_2Si$.



$rac\text{-}C_2H_4(1\text{-Ind})_2ZrCl_2$
isospecific C_2 -symmetric catalyst



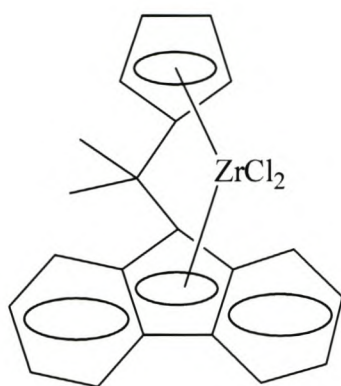
$bis(1\text{-methyl-Flu})ZrCl_2$
unbridged C_2 -symmetric catalyst

Figure 3: Examples of C_2 -symmetric metallocenes.

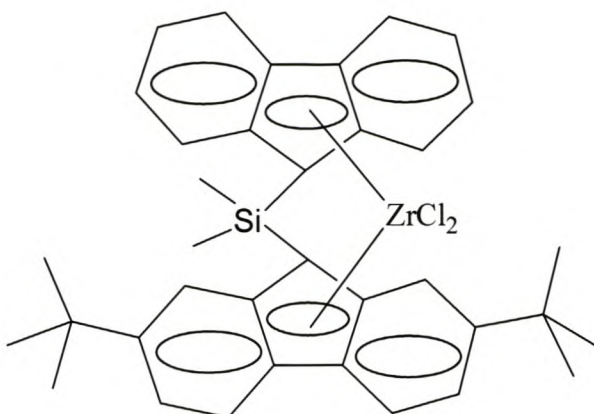
The introduction of an alkyl substituent in the 2-position of *ansa*-bisindenyl zirconium complexes increases both stereoregularity and molecular weight of the polypropylene produced and reduces the amount of regioirregularities in comparison to the unsubstituted analogue. The stereoselectivity is increased further by a combination of substituents on 2- and 4-positions on the indenyl ligands⁶.

The final subdivision of these C_2 *ansa* metallocenes is the one based on bisfluorenyl ligands. The unbridged, substituted bis(fluorenyl) complex shown in Figure 3 produces polypropylene with low tacticity, while similar, but unsubstituted catalysts produce polymers which are atactic. The substituted, unbridged bisfluorenyl catalysts show more stereoselectivity than the unbridged bisindenyl and bisindenyl complexes.

The C_s -symmetric catalysts which are represented by a catalyst of the formula $Me_2C(Cp)(9\text{-Flu})\text{-}ZrCl_2$ (Figure 4) produces highly syndiotactic polypropylene. With these catalysts the available coordination sites are enantiotopic (see Figure 2). The stereospecificity of the polypropylenes produced by this class of catalysts is affected by the bridging group and it decreases in the order $Me_2C > Ph_2C > PhP > CH_2CH_2 > Ph_2Si > Me_2Si$



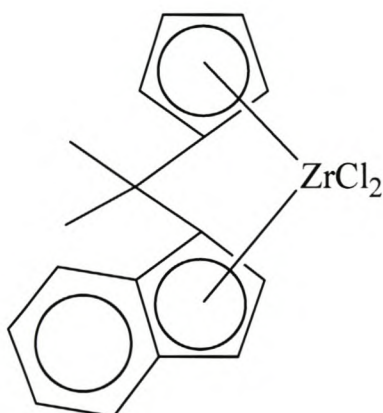
$\text{Me}_2\text{C}(\text{Cp})(9\text{-Flu})\text{-ZrCl}_2$
 C_s -symmetric catalyst



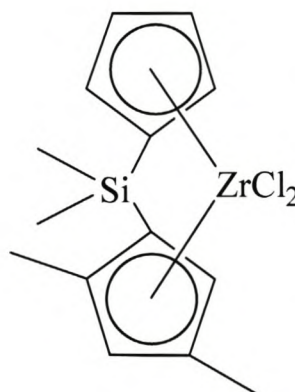
$\text{Me}_2\text{Si}(9\text{-Flu})(2',7'\text{-}^t\text{Bu}_2\text{-9'-Flu})\text{ZrCl}_2$
 C_s -symmetric catalyst

Figure 4: Examples of C_s -symmetric catalysts.

The final group of symmetric catalysts in the polymerization of propylene that are of interest are the C_1 -symmetric metallocenes. Generally these catalysts lack a symmetry element. The coordination sites for these catalysts are diastereotopic (that is the coordination sites are nonequivalent).



$\text{Me}_2\text{C}(\text{Cp})(1\text{-Ind})\text{ZrCl}_2$
 C_1 -symmetric catalyst



$\text{Me}_2\text{Si}(\text{Cp})(2',4'\text{-Me}_2\text{-Cp})\text{ZrCl}_2$
 C_1 -symmetric catalyst

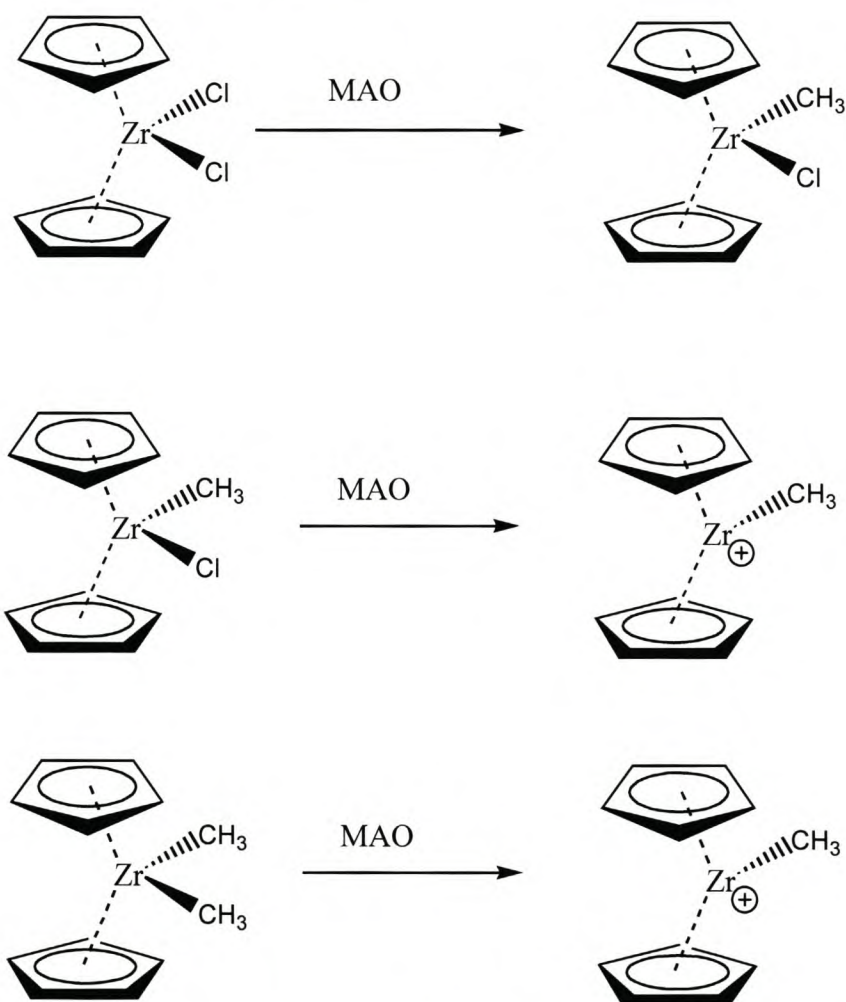
Figure 5: Examples of C_1 -symmetric catalysts.

2.2 Polypropylene by metallocene catalyzed polymerization

2.2.1 Mechanism of polymerization

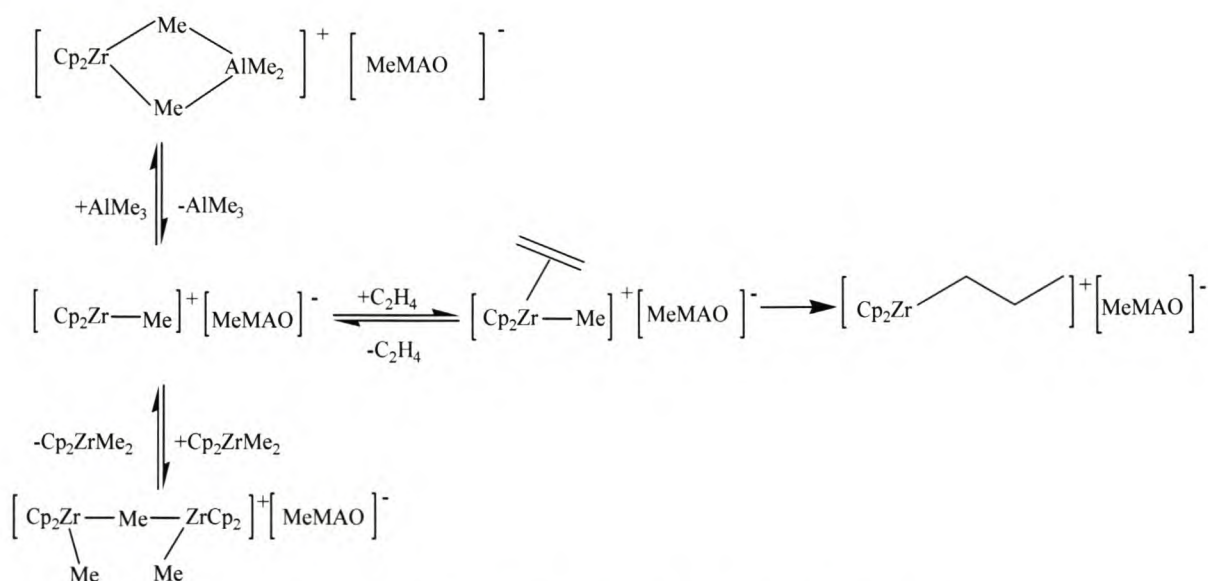
2.2.1.1 Formation of the active species

The active species in the olefin polymerization by metallocene catalysts is thought to be a cation-like, alkyl zirconocene which is created through the alkylation of transition metallocene by the cocatalyst MAO⁷. This is followed by further abstraction of chloride or another leaving group in the transition metal complex by the cocatalyst leaving a vacant coordination site. The types of cocatalysts are discussed later, suffice to say that the most common cocatalyst used is an oligomeric compound derived by the partial hydration of trimethyl aluminium (TMA), called methylalumoxane (or methylaluminooxane) (MAO). Some perfluorinated phenyl boranes and borates can also be used.



The formation of monomeric $[\text{Cp}_2\text{Zr}(\text{Me})^+][\text{Me.MAO}]^-$ and dimeric $[(\text{Cp}_2\text{ZrMe})_2(\mu\text{-Me})]^+[\text{MeMAO}]^-$ species has been evidenced through NMR studies⁸.

Reactivity of $(C_5Me_5)(\eta^5-C_2B_9H_{11})TiCH_3$ with ethylene has been probed⁹. Ethylene insertion of β -agostic Ti-Et species $(Cp^*)(\eta^5-C_2B_9H_{11})Ti(CH_2CH_3)$ is much slower than for Ti-Me species $(Cp^*)(\eta^5-C_2B_9H_{11})TiCH_3$. Metallocene catalysts form methyl-bridged binuclear complexes such as $[(Cp_2Zr(CH_3)_2)(\mu Me)]^+[MeB(C_6F_5)_3]^-$ and $[(Cp_2Zr(\mu-Me)_2AlMe_2)]^+[MeB(C_6F_5)_3]^-$. These ion pairs are possible dormant states for active sites for olefin polymerization and are also possibly responsible for catalyst deactivation reactions as outlined in Scheme 1:

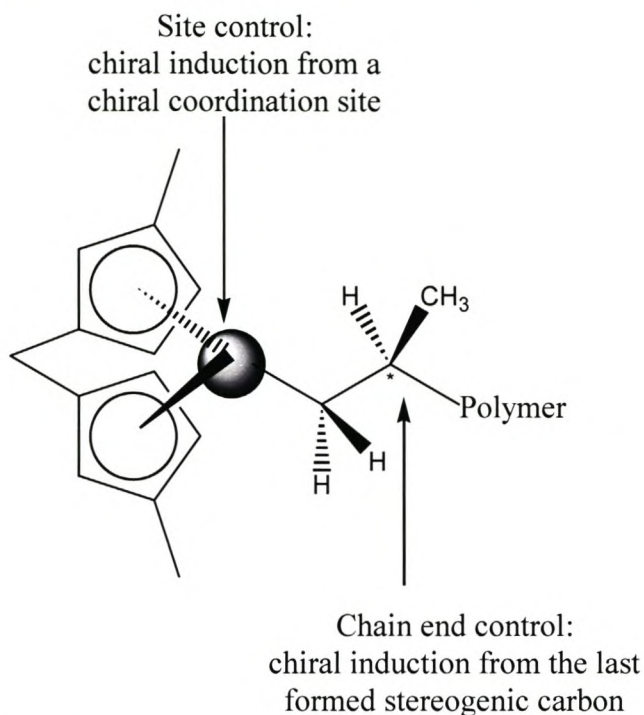


Scheme 1: Reactivation of the dormant site⁸

2.2.1.2 Olefin coordination

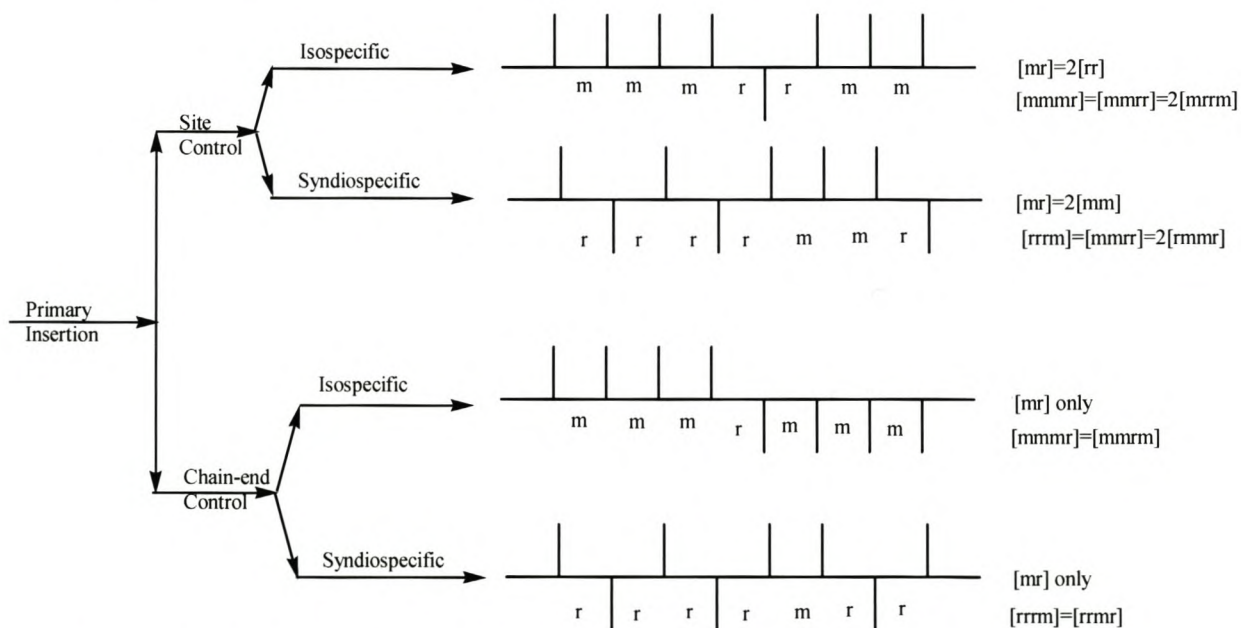
Olefins can coordinate on the available sites on the central metal atom in one of 4 ways⁶. The olefin can coordinate in such a way that insertion will occur in a 1,2-fashion with respect to the last inserted monomer unit (head-to-tail) or in a 2,1-fashion (head-to-head). In addition, the arrangement of the pendant group of the coordinating olefin can be arranged in one of two ways with respect to the arrangement of the polymer chain attached to the central metal atom, designated *re* or *si*. The choice of method of coordination (1,2 *re*, 1,2 *si*, 2,1 *re* or 2,1 *si*) will be guided by energy considerations, which in turn will be determined by the ligand structure and chain conformation. A detailed description of these factors can be found in a comprehensive review by Resconi *et al.*⁶. The deviation from the energetically preferred method of coordination could, amongst other factors, lead to the formation of stereoerrors.

Stereoerrors are caused, inter alia, by monomers coordinating on the “wrong” enantioface. The control of monomer coordination can be either by control of the catalyst or by control of the last inserted monomer unit (Scheme 2):



Scheme 2: Control of monomer coordination.

The type of stereoerror is determined by the type of stereocontrol (Scheme 3):

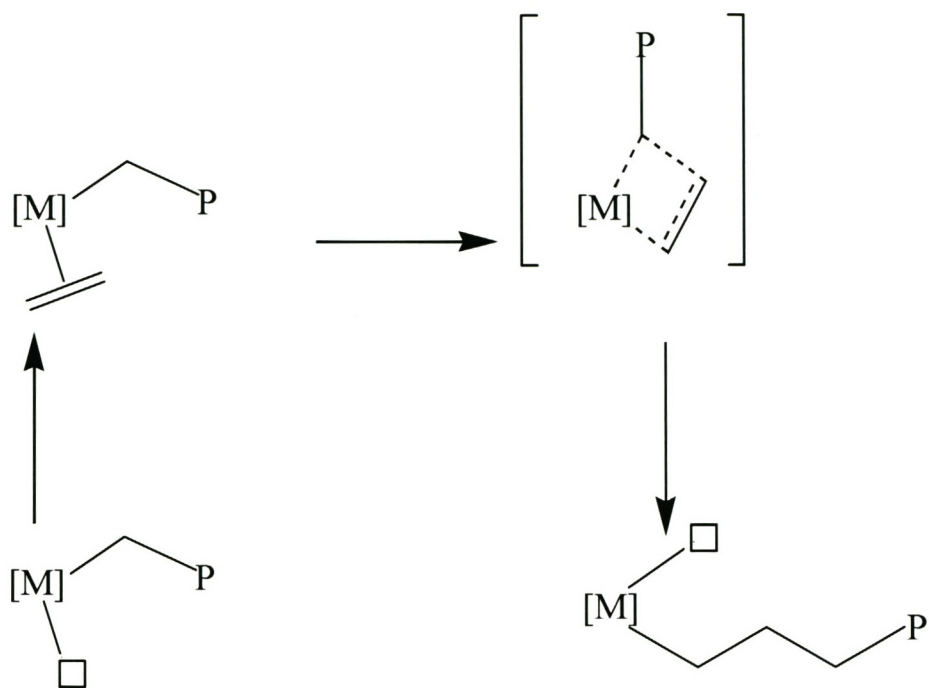


Scheme 3: Types of stereoerrors determined by stereocontrol mechanism.

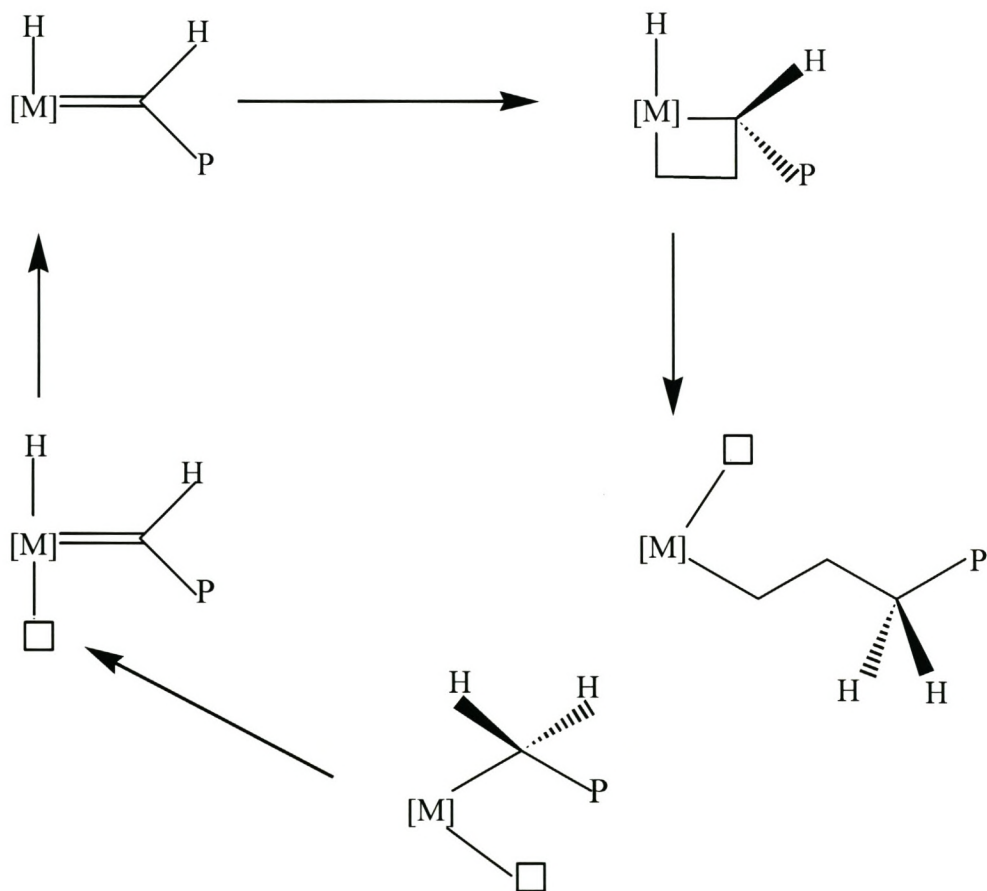
In isospecific site control a misinsertion leads to an isolated *mrrm* sequence, while chain end control shows no *rr* sequences (*mr* diads only, no *rr*). Similarly, the stereoerrors in syndiospecific polymerization are different for chain end control and site control mechanisms. Stereoerrors are not due only to enantioface selections, but could be due to other factors, like chain epimerization (isospecific polymerization) and skipped insertions (syndiospecific polymerization).

2.2.1.3 Olefin insertion

There are two leading mechanisms of olefin insertion in d^0 -metallocene polymerization catalysts, which are (1) direct insertion of the coordinated olefin [Cossee-Arlman mechanism] and (2) the α -agostic assisted olefin insertion [Green-Rooney, hydride mechanism]. The α -agostic interaction is of particular interest, since such an interaction might lower the activation barrier to olefin insertion and influence the stereochemical outcome of the olefin insertion step. Using isotope labeling to probe the nature of the olefin insertion, α -isotope effects were in some instances observed, which is strong evidence that α -C-H bonds are involved in the transition state of the insertion step. However, in other related systems, no isotope-effect were found¹⁸. Specifically, the α -agostic interaction firmly orients the polymer chain into the open sector of the catalyst structure to minimize interactions between the alkyl substituent of the monomer and the ligand/ polymer array during olefin insertion.



Scheme 4: Cossee-Alrman mechanism for olefin insertion¹⁸.

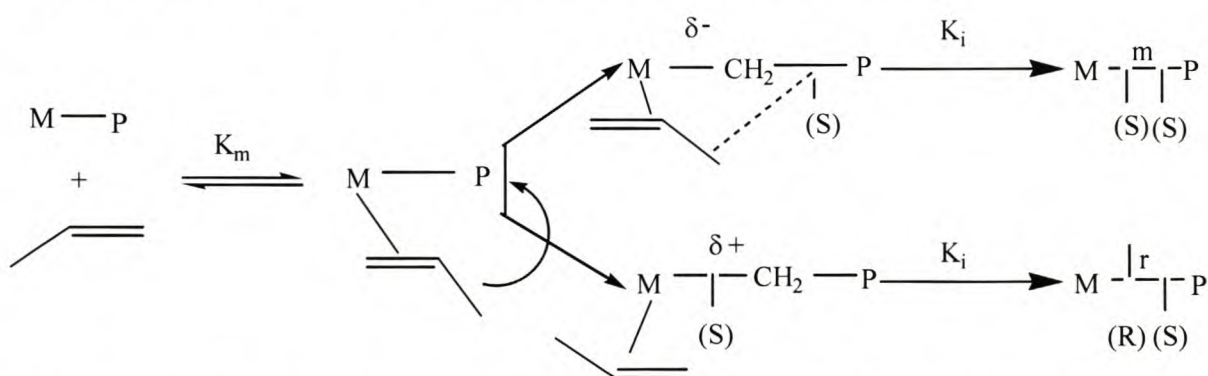


Scheme 5: Green-Rooney mechanism for olefin polymerization¹⁸.

2.2.1.4 Stereocontrol

Isotactic polymer is produced when the monomer molecules in successive insertion steps, bind to the metal via the same enantioface (either *re*, *re* or *si*, *si*), while coordination to the opposite enantioface in every second insertion step leads to the syndiotactic polymer¹⁰. When the propene monomer binds to the metal in a random fashion, then atactic polypropylene is produced. Two mechanisms are used in the stereocontrol chemistry by metallocene catalysts. The first one is the chain-end stereochemical control process where the configuration of the inserting monomer is determined by the configuration of the chain ends, whereas in second one, the enantiomeric site control process the configuration of the inserting monomer is influenced by the configuration at the catalyst site¹⁵.

In the mid 80's Ewen¹⁴ reported on the use of $\text{Cp}_2\text{Ti}(\text{Ph})_2$ activated by MAO at low polymerization temperatures (-45°C) to synthesize isotactic PP having novel stereoblock microstructure which was consistent with a chain-end stereochemical control mechanism. This leads to a polymer in which a stereoerror is perpetuated and not corrected. The isotactic content of the polymers produced with this catalyst was dependent on polymerization temperatures, with the polymer becoming more atactic at 25°C . C_2 -symmetric catalysts *rac*- $\text{Et}(\text{Ind})_2\text{TiCl}_2$ and *rac*- $\text{Et}(\text{Ind})_2\text{ZrCl}_2$ produced isotactic PP using an enantiomeric site control model.



Scheme 6: Mechanism of stereoregulation for both syndiotactic and isotactic chain-end controlled propylene polymerization¹⁴.

Scheme 6 shows the mode of monomer coordination (2,1- or 1,2-insertions) which results in production of either syndiotactic or isotactic polypropylenes in $\text{Cp}_2\text{TiPh}_2/\text{MAO}$ system.

During isospecific polymerization of propylene, the growing chain isomerizes resulting in formation of stereoerrors in the polymer chain. There are two mechanisms to explain these isomerization processes. The first one is a direct transfer of a hydrogen atom of the γ -methyl group to the α -carbon, with simultaneous Zr-C $_{\gamma}$ bond formation and Zr-C $_{\alpha}$ bond cleavage. The H-transfer suffers from strain energy due to the presence of a small ring in the transition state. Another mechanism is via β -elimination, reorientation, and reinsertion that leads to the same product, but a scrambling of the stereogenic centre¹³.

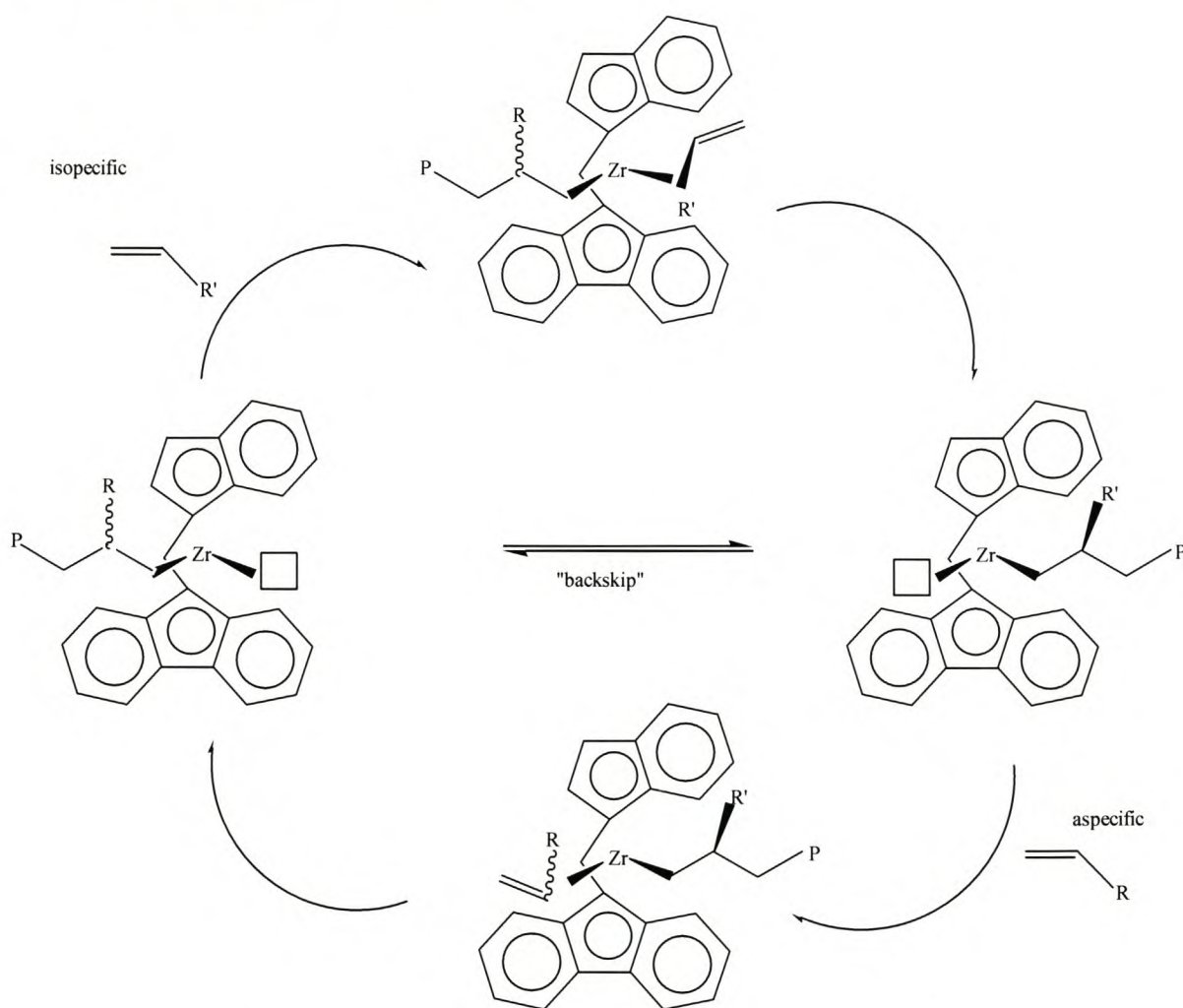
At low monomer concentration the olefin insertion rates are decreased with the consequence of increased isomerization reactions causing more intrinsic stereoerrors^{19,20}. The isotactic content of polypropylenes produced by C₂-symmetric catalysts *rac*-C₂H₄ (H₄-Ind)₂ZrCl₂, *rac*-C₂H₄(Ind)₂ZrCl₂, *rac*-Me₂Si(Ind)₂ZrCl₂, and *rac*-Me₂Si(1-Benz-Ind)₂ZrCl₂ was reported to be dependent on monomer concentration^{21b}. This observed decrease in stereoregularity is a result of the slow reaction of epimerization of the last-inserted monomeric unit which competes with that of chain polymerization. This effect was found to be of less importance in substituted *rac*-Me₂Si(2-Me-4-Ph-1-Ind)₂ZrCl₂/MAO compared to its homologue *rac*-Me₂Si(Ind)₂ZrCl₂/MAO.

The isomerization processes were initially reported by Busico and Cipullo²¹ using *rac*-C₂H₄(H₄-Ind)₂ZrCl₂. They observed that widening the gap aperture angle of the metallocene tends to release the steric constraints to chain propagation after a regioirregular (2,1)-inserted propene unit; this makes the isomerization of the latter into a 3,1 unit a less convenient alternative. For C₂-symmetric zirconocenes the decrease in propylene insertion rate after regioirregularity is lower the higher the value of the aperture angle; consequently, the ratio of 2,1 to 3,1 units in propylene polymers produced at a given temperature and monomer concentration increases in the same direction. The chain isomerizations misinsertion in propylene polymerization has been found to be more prominent when the aperture angle is greater.

Addition of substituents especially on 3,3'-positions of the C₂-symmetric catalyst increases the enantioselectivity, and the effect is further enhanced in the presence of the bigger substituents⁶. This effect becomes stronger on the indenyl systems than

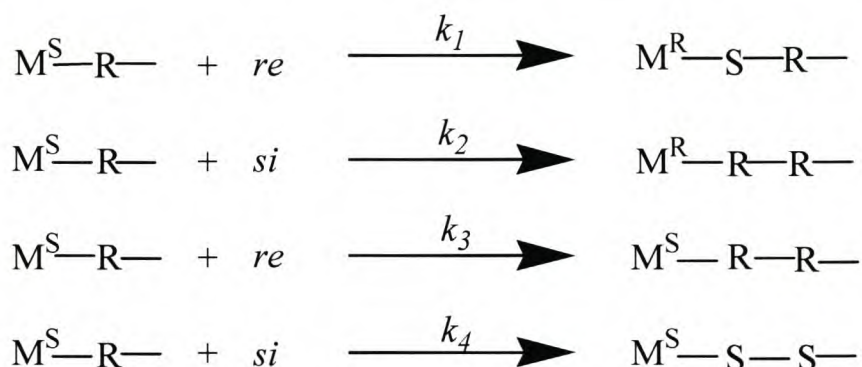
in the cyclopentadienyl systems. In a review by Busico and Cupillo, they stressed that substitution on the Cp rings, which results in a chiral C_2 -symmetric coordination environment of the transition metal, as the most successful strategy towards obtaining isotactic-selective catalysts. Furthermore, introduction of a bridge in a ligand helps prevent the rotation of Cp ligands, thus locking them in a chiral configuration.

The stereoerrors observed in the synthesis of iPP using C_1 -symmetric catalyst, can be explained by the chain backskipping method as shown in Scheme 7. It can be stated that this is due to catalysts switching between stereoselective and nonstereoselective coordination sites.



Scheme 7: Enantiomorphic site control mechanism¹⁷.

Syndiotactic polypropylene is produced by metallocene catalysts with C_s -symmetry, which implies site enantiotopicity (i.e. the preference for opposite propene enantiofaces)²². The first highly syndiotactic polypropylene was reported in 1988 by Ewen using the catalyst $\text{Me}_2\text{C}(\text{Cp})(9\text{-Flu})\text{ZrCl}_2/\text{MAO}$ ¹⁶. Like in cases of C_2 -symmetric catalysts, the stereocontrol of these catalysts is also dependent on propylene concentration²². Asanuma *et al.*, proposed the following mechanism for syndiospecific polymerization¹¹:



wherein M represents the catalyst with catalyst site S in superscript, and chain ends R, and the monomer chirality are denoted by italics *re* and *si*. It is proposed that when the chain-end catalyst site does not migrate, the chain end changes to the site and adds to the monomer coordinated to the opposite site. For propylene polymerization, the 1,2 – *re* insertion is most favourable with a low activation barrier (7.5 kcal/mol) compared to the 1,2 – *si* and 2,1-*re* which have similar activation barriers (12.1 and 12.3 kcal/mol respectively)¹².

The origins of stereoerrors in the production of sPP using C_s -symmetric catalyst $[\text{Me}_2\text{C}(\text{Cp})(9\text{-Flu})\text{ZrCl}_2/\text{MAO}]$ were investigated by Busico *et al.*²³. The site epimerizations accounted for much of the stereoerrors observed, and it is a result of the loosening of ion couple in the catalyst/ cocatalyst pair. It is highlighted that the proximity of the counterion to the active cation is mandatory for a regular chain migratory insertion mechanism.

The influence of the bridge in C_s -symmetric catalysts is different from the one observed in C_2 -symmetric catalysts. The syndiotacticity increases in the order $\text{Me}_2\text{C} > \text{Ph}_2\text{C} > \text{PhP} \sim \text{Me}_2 > \text{Ph}_2\text{Si}$ ⁶.

2.3 Effect of cocatalysts: The alumoxanes

Methylalumoxane is the mostly used alumoxane cocatalyst with metallocene catalysts. Other alumoxanes such as ethyl and butyl alumoxanes have also been used in the polymerization processes. Methylalumoxane is a compound in which aluminum and oxygen atoms are arranged alternatively and free valences are saturated by methyl substituents. It is gained by partial hydrolysis of trimethylaluminium^{10,24,25}. The resulting product is a complex structure, and the structure of MAO and nature of its reaction centers and unique ability to activate metallocene catalysts still remain unclear.

Panchenko and co workers modeled the three dimensional structure of MAO using density functional theory quantum-chemical method²⁶ (Figure 6).

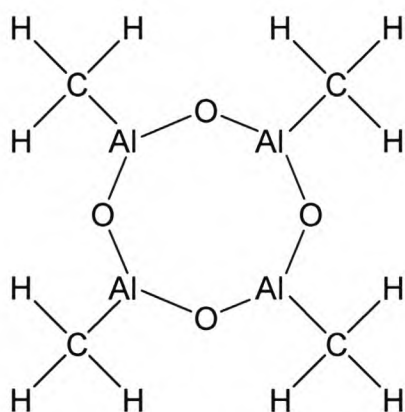


Figure 6: Inner layer of triple-layer cage structure of MAO²².

MAO has the following roles during olefin polymerization^{10,24,25,27}:

1. Fast ligand exchange reaction with metallocene dichloride, abstracting the halogen from the metallocene by Al center in MAO thus rendering the metallocene methyl and dimethyl compounds.
2. Formation of a metallocene cation and MAO anion, creating a vacant coordination site.
3. Provides counteranions, acting as a stabilizer of the active species.
4. Acts as a Lewis acid.
5. Scavenges impurities such as O₂ and H₂O in the polymerization medium.

The alkylated metallocene cation represents the active center.

The concentration of MAO in metallocene catalyzed polymerizations influences the catalytic activity. However it was established that the microstructure of the PP produced by $\text{Me}_2\text{Si}(\text{Benz}[\text{e}]\text{Ind})_2\text{ZrCl}_2$ was not influenced by the MAO concentration while the microstructure of the polymer produced by $\text{Me}_2\text{Si}(2\text{-Me-Benz}[\text{e}]\text{Ind})_2\text{ZrCl}_2$ was influenced by the MAO concentration²⁸.

The zirconocene-trialkylaluminium systems have been reported to be inactive (or having low activity) towards ethylene polymerization²⁹. The TMA which is freely available in MAO solution, acts as chain transfer agent in olefin polymerization which results in formation of Al-C bond which cleaves to generate polymers with saturated end groups. It has been shown that removal of the TMA leaves a solid MAO²⁶, which gives polymers with unsaturated end groups when activated with metallocene catalysts³⁰. This TMA, when added to MAO, decreases the catalyst activity in olefin polymerizations^{24,31}. TMA, when used alone or in excess with MAO, can be considered as an inhibiting agent. On the other hand, when used in combination with MAO, its presence is essential to obtain MAO with an active oligomeric structure.

Wang *et al*³². reported on low activity of Cp_2ZrCl_2 when activated with ethylalumoxane, butylalumoxane and ethyl-butylalumoxane (EBAO) for ethylene polymerization. The polymers produced by these alumoxanes had low Mw and broader MWD, suggesting that these alumoxanes activate catalysts with multiple reactive sites. In a separate study, catalytic activity decreased when isobutylalumoxane was used as cocatalyst or when added to MAO solution, this however does not affect the Mw and the polydispersities of the polymers produced³¹.

Tetra-iso-octylalumoxane (TIOAO) and poly-iso-octylalumoxanes (TAO) were synthesized from the hydrolysis of tri-iso-octyl aluminum (TIOA)³³. Attempts to copolymerize ethylene and propylene using the *rac*-Et(IndH₄)₂ZrCl₂ activated by TAO and TIOA were ineffective while TIOAO was much more active in comparison. It is assumed that the TIOAO contains both TAO and TIOA in its composition. The failure of TAO and TIOA to show activity could be explained in the following way: TIOA can act as an alkylating agent generating the cationic metallocene alkyl species but it lacks the species which generates the ionic pair function whereas TAO could

generate the ionic pair alkyl metallocene/ alumoxane but lacks the alkylating agent. This was supported when TAO showed activity when combined with $\text{rac-Et(IndH}_4)_2\text{ZrMe}_2$, which already has the alkyl group as a ligand.

Methylalumoxanes have been synthesized in situ on heteropoly acids, (phosphotungstic, silicotungstic, and phosphomolybdic acid) to form alumoxo-heteropoly compounds for use as weakly coordinating anions for metallocenes in the oligomerization of alkenes^{34,35}. When $\text{Et(Ind)}_2\text{ZrCl}_2$ was activated using alumoxo-phosphotungstate it formed a thermally more stable compound than its phosphomolybdate analog. However, for this catalyst system the activity loss was more pronounced than for $(\text{CH}_3)_2\text{Si(Ind)}_2\text{ZrCl}_2$ at higher temperatures. The metallocene $\text{Cp}_2\text{Zr(CH}_3)_2$, when activated with alumoxo-silicotungstate had higher activity in oligomerization of propene as compared to the one activated with pure MAO. Branched oligomers could also be prepared using the latter heteropoly acid. The effect of various alkyl aluminiums on distribution of comonomer (1-hexene) short chains in PE resin has been investigated using CRYSTAF. It was observed that copolymers produced with catalyst activated with TMA and TEA had distinctive bimodal crystallinity distributions³⁶.

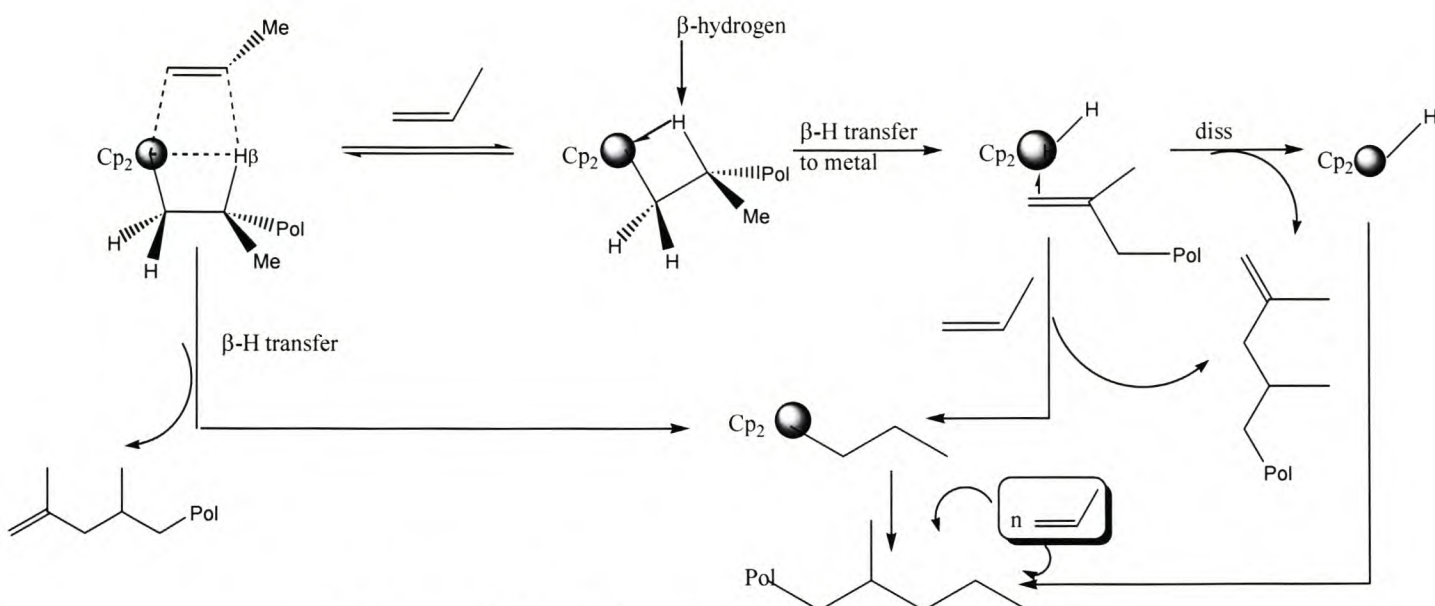
2.3.1 Other cocatalysts

Highly electrophilic borane compounds, such as $\text{B(C}_6\text{F}_5)_3$, are also used as cocatalysts in the absence or in conjunction with MAO. These borane containing compounds can ionize the neutral metallocene to generate an active species³⁷. Complexes such as Cp^*TiMe_3 can be activated by counteranions such as $\text{B(C}_6\text{F}_5)_3$ to form the active species $\text{Cp}^*\text{TiMe}_2(\mu\text{-Me)B(C}_6\text{F}_5)_3$. This system has been used to polymerize monomers such as isobutylene and isoprene to give polymer of low to high molecular weight depending on the catalyst concentration. However it was pointed out that these systems need high amount of catalyst as compared to those ones activated by MAO. The borates cocatalysts $[\text{Ph}_3]^+[\text{B(C}_6\text{F}_5)_4]^-$ on the other hand had proved to be more successful in activating metallocenes in conjunction with alkyl aluminiums. The draw back with these cocatalysts is that they suffer from poor solubility in hydrocarbons and poor thermal stability resulting in short catalytic life time. These problems are alleviated when the fluoroarylborate salt is functionalized by groups such as $^t\text{BuMe}_2\text{Si}$ ³⁸.

2.4 Chain transfer reactions

During polymerization, there is a double catalytic cycle:

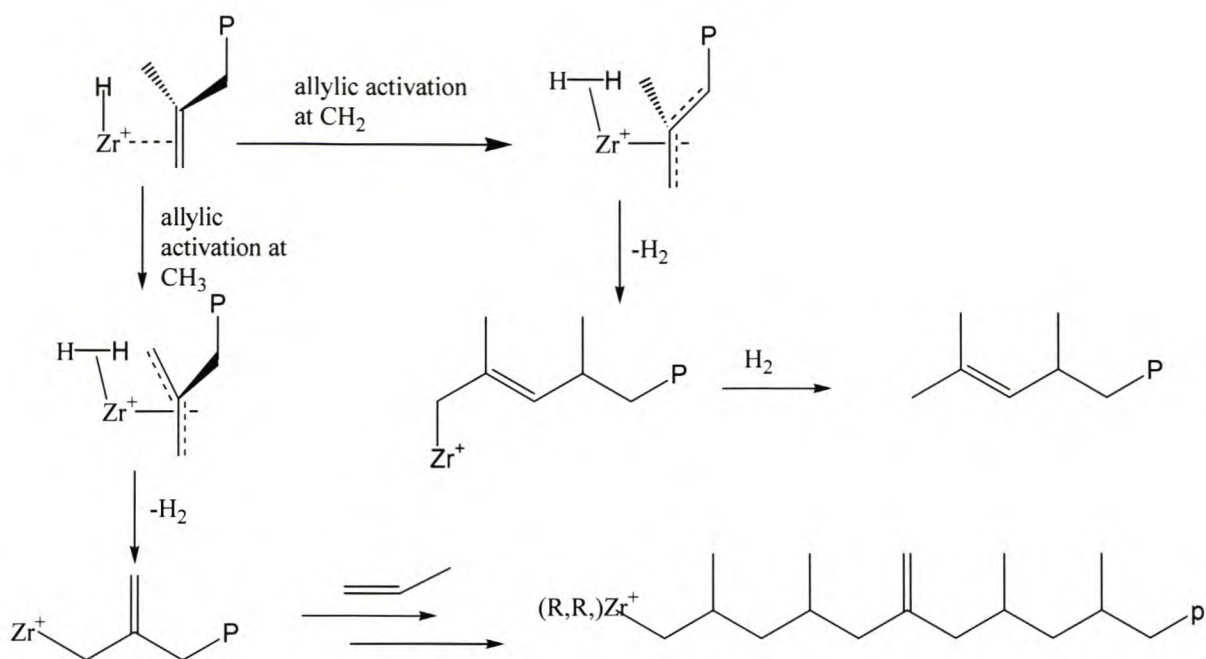
- Multiple insertion of monomer at a given metal center.
- Production of multiple chains at the same catalytic center. These two cycles are connected by a set of reactions that liberate a polymer chain from the catalytic center and form an active metal-hydride complex.



Scheme 8: Depiction of β -hydride transfer reactions.

In the above cycle (Scheme 8), a number of β -hydride transfer reactions are shown, which essentially all lead to vinylidene-terminated polymer chains and the reformation of the catalytically active metal hydride species. During propylene polymerization using $\text{Cp}^*_2\text{ZrCl}_2/\text{MAO}$, β -methyl abstraction is the dominant form of chain termination while $\text{Cp}_2\text{ZrCl}_2/\text{MAO}$ has β -H abstraction as most important form of chain termination⁴⁰. The formation of vinyl-terminated polypropylenes as a result of β -methyl transfer reactions when using isospecific C_2 -symmetric catalyst is illustrated in Scheme 10.

During the polymerization stages, the growing polymer chains undergo different chain transfer reactions, which in some instances result in chain termination. Molecular hydrogen is usually introduced during the polymerization with heterogeneous catalysts to lower the polymer molecular weight and increase the catalyst activity by



Scheme 11: Formation of internal vinylidene⁴².

On the other hand introduction of hydrogen in the polymerization process minimizes the occurrence of this internal vinylidene group. Scheme 11 outlines the formation of the internal vinylidene bond in the presence of hydrogen.

2.5 Effect of the transition metal on catalyst productivity

The transition metal in metallocenes for olefin polymerization plays a significant role in determining the activity of the catalyst, and the resultant molecular weight, polydispersity and microstructure of the synthesized polymers. The commonly used transition metals are zirconium, titanium and hafnium, with zirconium being the most commonly used metal^{2,43,44}. Rieger *et al.*⁴⁵, used the Hf metal in the presence of borates as cocatalyst in the catalysts systems *rac*-[1-(9- η^5 -Flu)-2-(5,6-cyclopentyl-2-methyl-Ind)EtMX₂, (with M being Hf or Zr and X being chloride or methyl groups), ultra high molecular weight *i*PP was produced when Hf is used as the transition metal than when Zr is used as the transition metal in the catalyst complex. Polymerizations in liquid propene resulted in increased molecular weight which was inversely proportional to polymerization temperature.

Elastomeric polypropylenes (elpp) synthesized using (2-Ph-Ind)₂ZrCl₂ and (2-Ph-Ind)₂HfCl₂, catalysts had similar molecular weight although the Hf based catalyst produced elpp with low polydispersities and lower tacticity in comparison with

the Zr based catalyst (28-36%). The product produced by the Hf-based system was tacky with no melting temperature⁴⁶. Amongst possible explanations for the discrepancies observed between these two metals is the slow rate of propagation at the isospecific site for Hf.

However, for C_s symmetric metallocenes, highly syndiotactic polymers are produced by Zr or Hf based catalysts, in contrast to stereoirregular polymers obtained when using Ti as the transition metal⁴⁷. Furthermore, under these conditions isotactic PP was obtained using a C_2 -symmetric catalyst with Ti, which could be explained by small metal radii and co-operative non-bonded repulsion of the methyl of the incoming monomer.

Low activity was observed when $[M(\eta^5\text{-}\eta^1\text{-C}^5\text{Me}_5\text{SiMe}_2\text{NCH}_2\text{CH}_2\text{OCH}_3)\text{R}_2$, $M = \text{Zr, Hf}$, $\text{R} = \text{Me, } ^n\text{Bu}]$ were used for the polymerization of ethylene⁴⁸. The Hf metal had very low activity in comparison to the Zr metal at various polymerization temperatures. However, it has been demonstrated that the insertion barriers in these types of catalysts increase in the order of $\text{Ti} < \text{Zr} \approx \text{Hf}$. The Ti catalysts easily suffer decomposition at temperatures above 50°C, compared to the Zr-based catalysts⁴⁹.

2.6 Effect of the ligand

The stereoregularity of the polyolefins, in particular polypropylene, synthesized using metallocene catalysts depends largely on the ligands around the transition metal complex. Highly isotactic (91%) polypropylene has been synthesized using $\text{Et}(\text{IndH}_4)_2\text{ZrCl}_2$ activated with MAO¹. Although the synthesis of the ligand 2-Me-Benz(Ind) (See Figure 7) appeared as if it was the end of the ligand development⁵, Brintzinger *et al.*⁵⁰ in 1994 found that $(\text{CH}_3)_2\text{Si}(\text{Benz}[\text{e}])(\text{Ind})_2\text{ZrCl}_2$ and $(\text{CH}_3)_2\text{Si}(2\text{-Me-Benz}[\text{e}]\text{Ind})_2\text{ZrCl}_2$ when activated with MAO are much more active than their bis indenyl analogues in the polymerization of propylene. The benzindenyl catalyst produce polymers of low molecular weight, which results from chain transfer to monomer following 2,1-insertion.

Metallocene catalysts rely on a high Al:Zr ratio to obtain polymers of high molecular weight, as at low concentrations bimetallic reactions result in low molecular weight polymers. The introduction of substituents on cyclopentadienyl or indenyl ligands can decrease these bimetallic reactions, which, as a consequence could result in high

molecular weight polymers^{42,51}. When the isopropyl substituent on the 4,4'-positions of the indenyl ligands were substituted for benzannelated and phenyl groups, high Mw *i*PP was produced. The high molecular weight was affordable by replacing the hydrogen in 2-position of the indenyl for methyl to create the synergistic effect⁵¹. High molecular weight *i*PP was synthesized using *rac*-Me₂Si-(2-Me-Ind)₂ZrCl₂ and its tetrahydroindenyl derivative⁵². This is possibly due to electronic effects created by introduction of the methyl group next to the silyl bridge, resulting in a decrease of the local Lewis acidity at the cationic Zr atom of the active species which lowers its tendency to abstract a β-H atom. On further investigation of these silyl bridged complexes, Spaleck⁵³ and co-workers in 1995 reported higher activity for the *racemic* stereoisomer of Me₂Si(Ind)₂ZrCl₂ as compared to its *meso* stereoisomer.

Regioirregular insertions were observed for ethylene and silyl bridged zirconocenes in propene polymerizations⁵⁵. It was observed that for Et(Ind)₂ZrCl₂ and Me₂Si(Ind)₂ZrCl₂, 2,1-misinsertions were observed but there were no 1,3-misinsertions observed at temperatures of 0-60°C, whereas for their tetrahydroindenyl analogues the misinsertions increase with the temperature. The 2,1-misinsertion leaves the catalyst site in a deactivated state for further olefin insertion and is a preferred mode for chain termination by β-H elimination.

In comparison to the bulkiness of the ligand, it was found that the silyl bridged indenyl ligand showed more enantioselectivity than its benzannelated indenyl and methyl benzannelated ligand in the polymerization of 3-methyl-1-pentene⁵⁴.

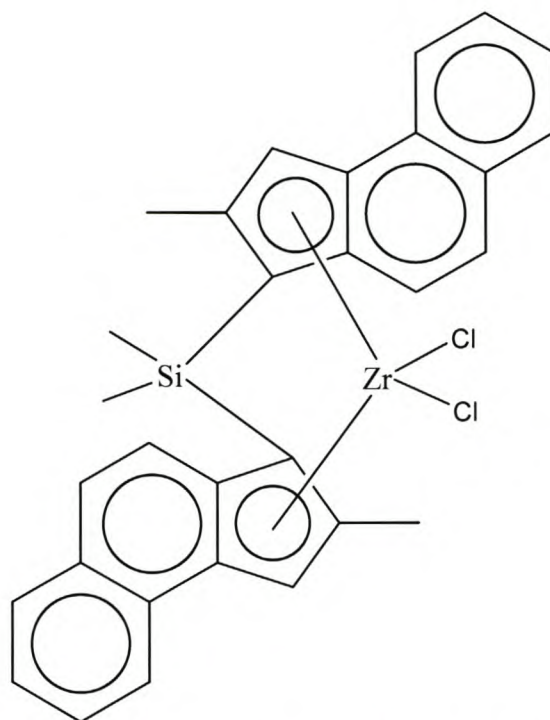


Figure 7: Structure of silyl bridged metallocene with benzindenyl ligands.

The silyl bridged methyl benzannelated zirconocene produced polymers with molecular weights of about 4 times higher than the former one. It is thought that the α -methyl substituents of the methyl-benzannelated indenyl blocks the chain terminations which arise from β -H transfer directly to a coordinated monomer molecule. The α -methyl substituents on the metallocene catalyst reduces the amount of 2,1-misinsertions compared to the unsubstituted ones.

A C_2 -symmetric catalyst rac -[CH₂(3-*t*-Bu-1-Ind)₂]ZrMe₂ was found to produce isotactic PP which has a higher molecular weight⁵⁶, tacticity as compared to the rac -[Me₂C(3-*t*-Bu-1-Ind)₂]ZrMe₂. The former complex was found to be more regiospecific with no 2,1- or 3,1-misinsertions.

Polo and co-workers³³ found that replacing the chloride ligands of rac -Et(Ind)₂ZrCl₂, with binaphtholate (BNP) resulted in reduced catalyst activity. The bulky naphtholate ligands hinder formation of the active species and the nature of the Zr-O bond (for the naphtholate) was more difficult to cleave in comparison with Zr-Cl bond. This problem could be alleviated by ageing the catalyst/alumoxane solution for 2 hrs, resulting in improved activity.

Formation of polyolefin stereoblocks arises due to occurrence of stereoerrors in the catalyst active site during the polymerization process. Lieber and Brintzinger⁵⁷ observed that the polymeryl exchange of polymer chain from the crowded Zr active center to the free Al is predominantly observed in the highly substituted isospecific metallocene and it occurs less in the less substituted isospecific, and syndiospecific metallocenes.

C₁-symmetric zirconocenes with an isopropylidene bridge and substituted cyclopentadienyl and fluorenyl ligands are of large interest as catalysts for the polymerization of propylene, leading to syndiotactic and hemiisotactic polymers^{25,58}. Fan and Waymouth¹⁷ synthesized alternating ethylene/propylene copolymers using Me₂Si(Ind)(Flu)ZrCl₂ and Me₂C(Ind)(Flu)ZrCl₂. The activity of the latter was poor, producing oligomeric products (M_w ~ 1 500) compared to those of the silyl bridged catalyst (M_w ~ 20 000). The highly alternating sequence distribution for the copolymers can be ascribed to an alternating-site mechanism where propylene inserts at the stereoselective site and ethylene inserts at the nonstereoselective site. In another investigation, Bercaw *et al.*⁵⁹ reported that for Me₂C(Me-Cp)(Flu)ZrCl₂/MAO, the tacticity of the PP is largely influenced by the ligand substituents.

Hydrogenation of the fluorenyl ligands in C₁-symmetric metallocene catalysts does not influence the catalytic activity, but the tacticities of the PP produced are negatively affected⁶⁰. The M_w of the polymers produced by these complexes were lower than those of the non-hydrogenated catalysts. The less stereorigid geometry of the partially and fully hydrogenated fluorenyl ligand allows for easier β-H elimination.

It was observed that in C₁-bridged fluorenylidene cyclopentadienyliidene zirconocenes, a *t*-Bu in position 3 of the cyclopentadienyl leads to highly isotactic polypropylene^{61,62}. The *t*-Bu group sterically blocks one side of the catalysts, restricting the movement of the growing chain, thus allowing insertion of propylene monomers at one side only. Substituting the methyl for *t*-Bu showed the same effect. However, the tacticities decreased when allyldimethyl and trimethylsilyl groups were placed on the 3-position of the Cp.

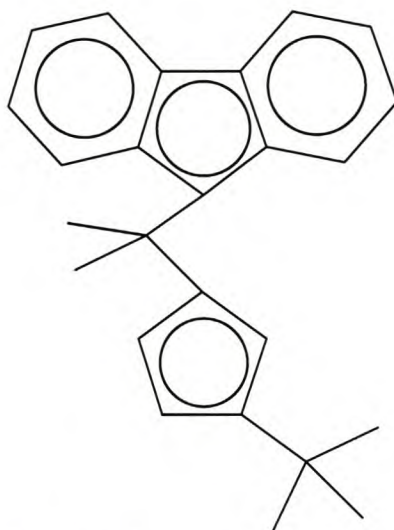


Figure 8: Substituted ligands for C_1 bridged catalysts⁵⁴.

In comparison of the bridging group in constrained geometry (CG) catalysts, van Leusen *et al.*⁶³ reported high activity of the catalyst $[C_5Me_4(CH_2)_2N-t-BuTiCl_2]$ as compared to its silyl bridged analogue in ethylene homopolymerization. However, this ethylene bridged catalyst, was found to be inactive in propylene polymerization which is different to what is observed in $[C_5Me_4(SiMe_2)N-t-Bu]TiCl_2$. The activity was restored when the *tert*-butyl was replaced by a methyl group. The silyl bridged CG metallocenes have been found to be active in the polymerization of propylene. The only ethylene bridged catalyst capable of polymerizing propylene was $[C_5Me_4(CH_2)_2NCH_3]TiCl_2$.

Metallocenes with double bridges in their ligand have been synthesized for ethylene polymerization. The activity of $[\mu,\mu-(Me_2SiOSiMe_2)_2(C_5H_3)_2]ZrMe_2$ was found to be similar to those complexes having single bridge⁶⁴. These catalysts were observed to control chain configuration by enantiomorphic site control in the polymerization of propylene⁵⁹. At lower T_p and higher propylene concentration, highly syndiotactic PP with less stereoerrors was obtained. This implies that as stereoselectivity increases with propylene concentration, enantiofacial misinsertion is not the major stereoerror mechanism, but site epimerization and olefin insertion occur at competitive rates, resulting in epimerization being the major cause for stereoerrors.

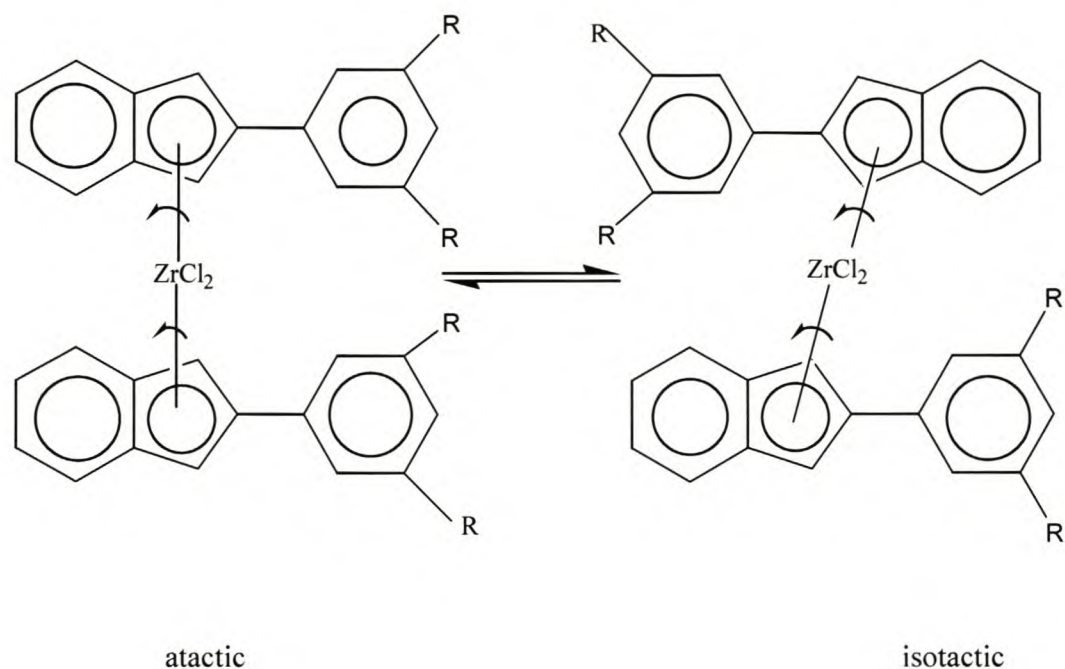
Half-sandwich titanocenes and zirconocenes produce olefin polymers when activated with MAO or with $B(C_6F_5)_3$. The effect of the pendant phenyl group in half-sandwich

complexes of $(C_5H_4CMe_2CH_2Ph)TiMe$ has been investigated in propylene polymerization⁶⁵. When this complex is activated with $B(C_6F_5)_3$, atactic low Mw propylene polymers were produced, with broader MWD (5 – 14). The broad polydispersities could be the result of either catalyst decomposition or of slow equilibrium between dormant and active states.

2.5.1 Ligands for elastomeric PP

Elastomeric polypropylene forms an integral part of the thermoplastic rubber industry owing to its excellence in elastic recovery which is insensitive to elongation up to 500%⁶⁶. The first homogeneous catalyst that generated elastomeric polypropylene (elpp) was a C_1 -symmetric bridged titanocene⁶⁷. Investigations were carried out to produce elpp using titanium based nonsymmetric *ansa*-metallocene catalysts. The presence of two isomeric propagating stages was highlighted using these catalysts⁶⁸. Later Waymouth⁶⁹⁻⁷¹ and his group reported synthesis of the catalyst $(2-PhInd)_2ZrCl_2$ which is able to isomerize between achiral and chiral coordination geometries in order to produce atactic-isotactic stereoblock poly- α -olefins. With this catalyst, it was thought that the distribution of isotactic and atactic stereosequences could be controlled by varying polymerization conditions to produce polymers with a range of elastomeric properties. This rotation of the ligands can be explained by using the effect of the solvent, in particular polar solvents such as dichlorobenzene and cocatalyst tetrakis(perfluorophenyl)borate/ $Al(isobutyl)_3$. In polar solvent, there is less interlocking of cation/anion which results in the ligand being locked in one position for a shorter period before it rotates to the other position resulting in overall non-crystallizable polymer⁷².

Introduction of phenyl substituents on the indenyl ligand is supposed to inhibit the rotation of the ligand such that it would be slower than that of monomer insertion yet faster than the time required to construct one polymer chain in order to produce the atactic-isotactic stereoblocks^{67,73}. Studies have shown that *rac*-isomer is favoured in the isomerization equilibrium for these $(2-PhInd)_2ZrCl_2$ catalyst during elpp synthesis. The larger fraction of atactic polymer in the elpp is a consequence of higher rate of polymerization of the *meso*- isomer⁷⁴.



R = H, Me, Et

Figure 9: The Wymouth compounds and their rotation to synthesize elastomeric PP⁷³.

The complex *rac*-(1-Me-2-PhInd)₂ZrCl₂ was used in the polymerization of propylene and showed low activity; producing polymer with low isotactic pentads as compared to the (2-PhInd)₂ZrCl₂. The Mw of the polymers were low and they had low MWD⁷³. To investigate effect of fluxional metallocene on production of elastomeric PP, Cp*(2-PhInd)IndZrCl₂, Cp*(1-Me-2-PhInd)IndZrCl₂ and Cp(2-PhInd)ZrCl₂ were compared against bis(2-PhInd)ZrCl₂⁷⁵. Although the activity of Cp(2-PhInd)ZrCl₂ was slightly higher it suffered from low tacticity (% *mmmm* = 8) compared to Cp*(2-PhInd)ZrCl₂ which had tacticity of 30%, similar to that of bis(2-PhInd)ZrCl₂.

To evaluate the effect of the chirality of metallocene complexes, bis(neomenthylindenyl)zirconium dichloride and bis(neoisomenthylindenyl)zirconium dichloride and their tetrahydroindenyl derivatives, have been investigated in propylene polymerization⁷⁶. Enantiomorphic site control was dominant in both catalysts, although the bis(neoisomenthylindenyl) zirconocene had higher stereo control. This led to polymers with high amounts of isotactic pentads.

Metallocene with indenyl ligands having methyl, *i*-pr, benzyl and cyclohexyl substituents were activated with MAO to produce thermoplastic PP⁷⁷. The isotactic

pentads increased in the order $i\text{-Pr} < \text{Me} < \text{Cy} < n\text{-Bu} < \text{Benz}$. The metallocenes with methyl and $n\text{-Bu}$ substituted indenyls had high catalytic activity in both polymerization of ethylene and propylene, and they produced polymers with high Mw and broader MWD. Surprisingly the benzyl substituent had lower activity in both situations, which can chiefly be explained by its electron withdrawing power. The catalysts having alkenyl substituted cyclopentadienyl ligands with more linear substituents had lesser activity than the branched ones in the polymerization of ethylene⁷⁸ (Figure 10). The complexation of the alkene group of the ligand at the vacant polymerization site and the blocking of the inserting monomer caused by rotation of the long chain in the ligand probably influenced the catalyst activity.

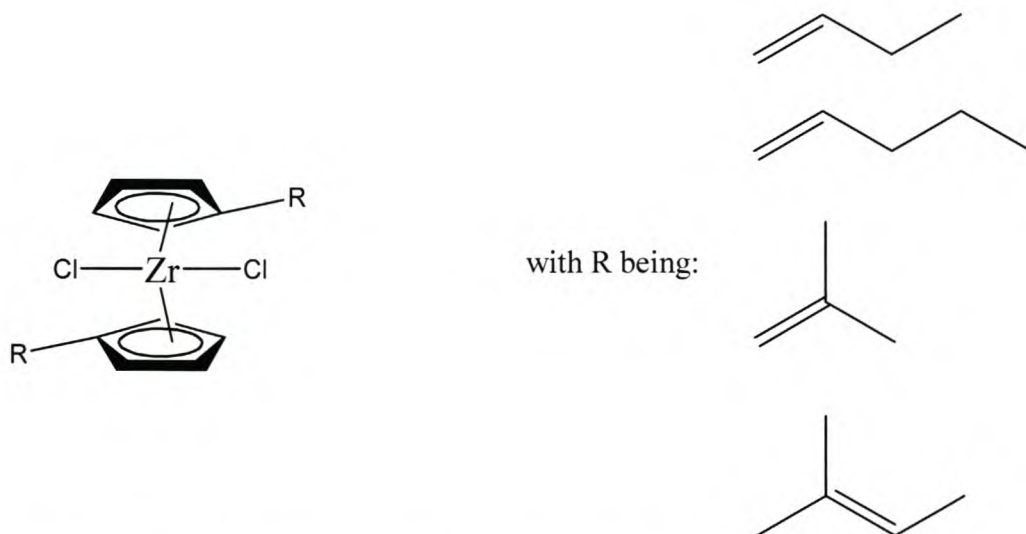


Figure 10: Cyclopentadienyl zirconocene with alkenyl substituents⁷⁸.

Biscyclopentadienyl zirconocenes with phenyl rings as substituents on the Cp rings were investigated for ethylene and propylene polymerization⁷⁹. The activities of $(\text{Ph}_3\text{Cp})_2\text{ZrCl}_2$ and $(\text{CyPh}_2\text{-Cp})_2\text{ZrCl}_2$ (Figure 11) in ethylene polymerization were found to decrease slightly with a decrease in Al:Zr ratio as compared to that of Cp_2ZrCl_2 . These compounds when activated with MAO were only able to produce oily propylene oligomers, which lacked stereospecificity suggesting that the presence of the bulky ligands was not good enough to restrict the rotation of the Cp ligand about the Zr atom. These oily propylene oligomers had vinylidene end-groups indicating $\beta\text{-H}$ elimination as the main chain termination process. Replacing one of

the Ph substituents by a cyclohexyl only lowered the catalytic activity, which was probably due to steric hindrance in the front side of the Zr atom which is larger and the coordination gap aperture for the monomer is smaller.

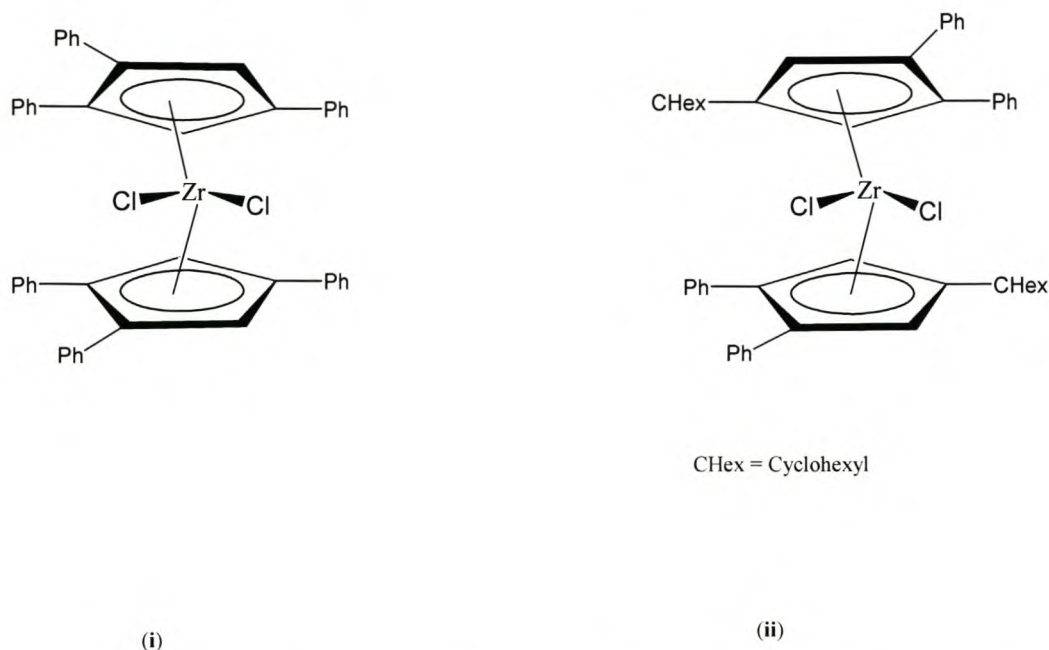


Figure 11: Phenyl substituted biscyclopentadienyl zirconocenes⁷⁹.

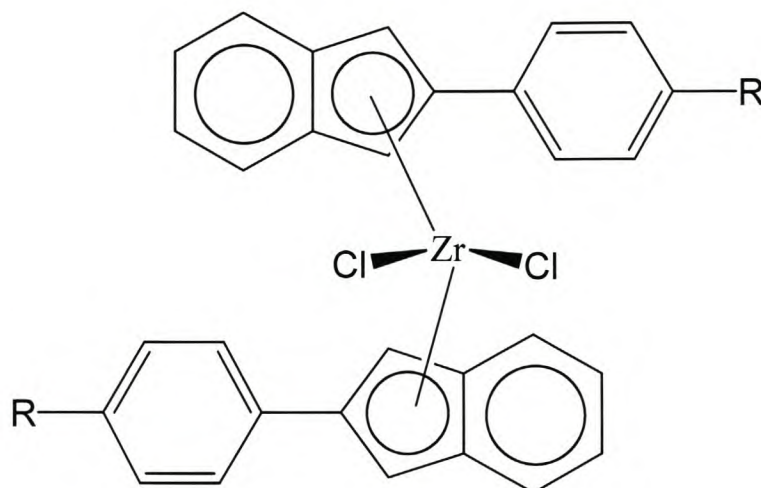
Brintzinger *et al.*⁸⁰ found that the 2-methyl substituted cyclopenta(l) phenanthracene zirconocene was more active than the $(\text{Ph-Ind})_2\text{ZrCl}_2$ when activated with MAO. However the tacticity of the polymers produced using the methyl substituted complex was very poor.

2.5.2 Halogenated ligands

Several reports have highlighted how the activity of the metallocene catalysts decreases when halogens are placed in the ligand around the transition metal^{70,81,82}.

In the mid 90's Waymouth *et al.*⁷⁰ compared the activity of the arylindenyl zirconocenes $(2\text{-PhInd})_2\text{ZrCl}_2$, $[2\text{-(3,5-Me}_2\text{Ph)Ind}]_2\text{ZrCl}_2$ and $[2\text{-(3,5-CF}_3\text{-PhInd})_2\text{ZrCl}_2$ in the presence of MAO in the polymerization of propylene. The microstructure of PP produced by the methyl substituted aryl was found to be much less (15% isotactic) in comparison to those of the unsubstituted and trifluoromethyl substituted aryl. The CF_3 substituted arylindene zirconocene produced the polymers having the highest

isotactic pentads (45-73%). A similar trend is observed in Hf catalyst, though the Zr metal has a larger effect on stereospecificity⁸¹.



R = CF₃, Cl, SiMe₃, H, t-Bu

Figure 12: Zirconocene with substituted ligands.

It was observed that the activity of the methyl substituted arylindene was much lower than that of the other two complexes which had no substituent or had CF₃ as substituent on the arylindene, and the molecular weight of the polymers was also lower in comparison.

The effect of steric and electronic substituents on the *p*-position of the aryl in [2-(4-R-Ph)Ind]₂ZrCl₂ for propylene polymerization was studied by Lin *et al.*⁸¹. The %*mmm* pentads were slightly influenced by electron withdrawing groups, but when Cl and CF₃ were used, the activity of the catalyst decreased. Substituting the chlorine atoms by bromine did not affect the microstructure of the polymers produced by (2-ArInd)₂ZrCl₂ and (2-ArInd)₂ZrBr₂ in the presence of MAO⁸². However the polydispersities of the polymers produced by the dichloride analogues were broader than that of the dibromide catalysts. For catalysts having mixed ligand systems the microstructure of the PP ranged from 21% for [2-(3,5-Me₂-Ph)Ind](2-PhInd)ZrBr₂ to 54% for the [2-(3,5-Me₂-Ph)Ind]₂ZrBr₂.

2.5.3 Other functional ligands

A series of unbridged bis(2-R-Ind) zirconocenes were activated with MAO to polymerize propylene, with R being phenyl, 3,5-dimethoxyphenyl, 4-methylamino, 3,5-ditert-butyl-4-methoxyphenyl and adamantanyl substituents. The complexes with dimethoxy substituents and *tert*-Bu-methoxy had polymers with much more isotactic pentads⁸³. All of these metallocenes had electron donating substituents with varying steric demands. The catalysts with dimethoxy substituents had lower activity as compared to the *p*-methoxy-substituent, which can be explained by the shielding effect of the adjacent *tert*-butyl groups.

Ansa-metallocenes containing amide ligands displayed lower activities in propylene polymerization in comparison to their chlorine and methyl counterparts^{84,85}. Pretreatment of these catalysts with AlR_3 before activation with MAO resulted in high catalytic activity. The isotacticity does not increase in these systems, instead atactic material is produced. This could be the result of propylene being more sensitive to the amine substituents, or that the substituent blocks the monomer from reaching the coordination center.

For ethylene polymerization, Janiak *et al.*⁸⁶ observed a decrease in catalytic activity in the following order: $\text{Cp}_2\text{ZrCl}_2 > (\text{CH}_3)_4\text{CpCp}^*\text{ZrCl}_2 > (\text{Cp}^*)_2\text{ZrCl}_2 > (\text{CH}_3)_4\text{C}_4\text{P}(\text{Cp}^*)\text{ZrCl}_2 > [(\text{CH}_3)_4\text{Cp}]_2\text{ZrCl}_2 \gg (\text{Cp}^*)_2\text{ZrCl}_2 > [(\text{CH}_3)_4\text{C}_4\text{P}]_2\text{ZrCl}_2$. The lower activities of the phosphoryl as compared to the tetra- and penta-methylcyclopentadienyl could be the result of the electron withdrawing effect of the phosphorus substituent.

2.7 Copolymerization of higher α -olefins

The polymerization of higher α -olefins has been done using silyl bridged Benz(e)indenyl complexes activated with MAO^{50,87-90}. Addition of a comonomer in the polymerization system generally resulted in increased catalytic activity. The molecular weight of the copolymers tend to be higher than that of the corresponding homopolymers.

The incorporation of 1-hexene comonomer decreased with increase in the 1-hexene in the feed for ethylene copolymerizations with the aspecific metallocenes $(n\text{-BuCp})_2\text{ZrCl}_2$ while the opposite was true for $(\text{Ind})_2\text{ZrCl}_2$ ⁹¹. The former catalyst is

weaker in activity towards 1-hexene insertion. Propylene and hexadecene comonomers showed an increase in comonomer incorporation with increase in the feed under similar conditions using both catalysts. These catalysts behaved as single site species at low comonomer concentrations. The melting temperatures of the copolymers decreased as large percentages of the comonomers was incorporated in the polymer chains^{89,91}.

C_s-symmetric catalysts have been used to produce poly-1-hexene, which increase in molecular weight with a decrease in the reaction pressure⁹².

Ethylene-propylene copolymers are of industrial importance, in particular in the production of elastomers⁹³. It has been found that the reactivity ratio for ethylene in propylene copolymerization decreased in the order (2-PhInd)₂ZrCl₂ > [(CF₃)₂PhInd]₂ZrCl₂ > Et(Ind)₂ZrCl₂ whereas the reactivity for the propylene was in the order Et(Ind)₂ZrCl₂ < (2-PhInd)₂ZrCl₂ < [(CF₃)₂PhInd]ZrCl₂. The molecular weight of the polymers produced using arylindenyl and fluorinated arylindenyl catalysts increased with the increase of ethylene in the reaction feed.

When 1-octene was used as a comonomer in ethylene copolymerization using [C₅Me₄(SiMe₂N-*tert*-Bu)]TiMe₂/TPFPB/MMAO, the activity of the catalyst decreased with increasing 1-octene mole feed. As the amount of the comonomer increased, the molecular weight distribution increased whereas the molecular weight decreased. The crystallinity of the copolymers was also reduced with increased 1-octene content⁹⁴.

Van Reenen *et al.*⁸⁹ reported the copolymerization of propylene with higher α -olefins such as 1-octene, 1-decene, tetradecene, and octadecene, using Me₂Si(2-Me-Benz[e]Ind)₂ZrCl₂/MAO. Copolymerization of propylene with other higher α -olefins results in increased catalytic activity, with little change to the molecular weight of the copolymers produced⁹⁵. Graef *et al.*⁹⁶ reported a decrease in the *rrrr* % when copolymerizing propylene with higher α -olefins using the syndiospecific catalysts.

The effect of the bridge in Me₂C(Cp)(Flu)ZrMe₂ and Et(Cp)(Flu)ZrMe₂ has been studied for ethylene/1-hexene copolymerization activated with the non-coordinating cocatalyst [Ph₃C][B(C₆F₅)₄]. It was found that the syndiospecific catalysts bridged with ethylene had a smaller dihedral angle which limits the amount of 1-hexene to be incorporated into the polymer chain⁹⁷. The catalysts with only one carbon in the

bridge easily insert 1-hexene in the polymer chain compared to the ethylene bridged catalyst. The ethylene bridged catalysts showed higher activity in ethylene homo- and copolymerization. Syndiotactic homopolyolefins (1-butene, 4-methyl-1-pentene, 1-pentene, 1-hexene and 1-octene) were synthesized using 1-Me-1-ethylidene-(Cp-1'-Flu)ZrCl₂, activated with MAO⁹⁹. Of these polymers, crystalline products were obtained from 1-butene and 4-methyl-1-pentene.

Harrison *et al.*⁹⁸ synthesized polyethylene with long-chain branching using Et(Ind)₂ZrCl₂ supported on alumina at elevated temperatures, with the long-chain branching confirmed by ¹³C NMR. The above polymerization system afforded more long-chain branching using slurry phase polymerization than in gas phase. These supported systems produced copolymers with less comonomer (1-hexene and 1-octene) content compared to their soluble counterparts. Although the activity of these catalysts increased in the presence of the comonomer, the molecular weight decreased due to facile chain transfer to the metal or to comonomer⁸⁷.

2.8 Long-chain branching in polyolefins

Long-chain branching in polyethylenes were earlier reported by Malpass¹⁰⁰ (Exxon) using the Ziegler-Natta catalysts. In α -olefin polymerization, long chain branches are observed as a result of β -CH₃ or β -H transfer reactions, which result in macromonomers capable of being incorporated into the polymer chain. The concentration of macromonomer in the reaction and its rate of insertion relative to olefin (propylene in this case) determines the branching level in the polyolefin¹⁰¹. Preferably the metallocenes which are capable of making vinyl terminated end-groups are used in the making of *in-situ* long-chain branching in polyolefins. Long-chain branched polypropylenes were prepared using Me₂Si(2-Me,4-Ph-Ind)₂ZrCl₂/MAO.

Incorporation of ethylene-propylene macromonomer in ethylene polymerization depends on the polymerization temperature and ethylene pressure. The macromonomer content in the polymer increases with temperature, but it decreases with ethylene pressure^{102,103}. Long-chain branching in ethylene polymerization using Cp₂ZrCl₂/MAO in slurry phase was observed after copolymerization of ethylene macromonomer formed as a result of β -H elimination¹⁰³. This catalyst produced only short-branching in a continuous stirred reactor, owing to chain isomerization. The

macromonomer has easier diffusion to the catalyst active site at higher temperatures than at lower temperatures. The molecular weight of the polymers produced increased with a reduction in polymerization temperature, due to increased monomer solubility. The density of the long chain branching increased with decreasing the Al/Zr ratio. However at higher Al/Zr ratio, chain transfer to MAO is supposed to be high resulting in reduced numbers of macromers with terminal double bonds.

Homogeneous incorporation of the propylene macromonomer in propylene polymerizations has been reported by Shiono *et al*¹⁰⁴. The presence of the macromonomer in the reaction resulted in decreased catalyst productivity, which is a contrast to the enhanced productivity observed when the macromonomer was copolymerized with ethylene using CG catalysts combined with MAO¹⁰⁵.

Using a combination of metallocene catalysts, polyolefins with long-chain branching have been synthesized¹⁰⁶. Hence using a borato complex, $(C_5H_5B-OEt)_2ZrCl_2$, and a constrained geometry catalyst, $[(\eta^5-C_5Me_4)SiMe_2(\eta^1-NCMe_3)TiCl_2]$, activated with MAO, branched polyolefins with reduced melting temperatures (91°C) have been synthesized. The former catalyst is capable of producing ethylene oligomers with unsaturated chain ends, and the latter catalyst incorporates the oligomers into the ethylene polymer chain resulting in a polymer with long side chain branches.

Beigzadeh *et al.*¹⁰⁷ showed that, the frequency of long-chain branching in polyethylenes can be increased by combining an ethylene bridged catalysts capable of producing macromonomers via β -H elimination and a CG catalyst capable of incorporating higher olefins or macromonomers into the polymer chain. $Et(Ind)_2ZrCl_2$ could not produce long-chain branches by itself. The CG catalyst produced high molecular weight polymers with broader or bimodal distribution as a results of inclusion of the macromonomers.

It has been stated that the presence of comonomers in olefin copolymerization results in chain disorder and irregular crystal structure. This causes a decrease in melting temperatures of the copolymers synthesized. Chu and Park¹⁰⁸ observed that copolymerizing ethylene with comonomers (1-butene, 1-hexene and 1-octene) using the symmetric catalyst Cp_2ZrCl_2 resulted in copolymers with longer side chains with much decreased melting temperatures.

2.9 Temperature

The problem facing metallocene catalysts by increasing polymerization temperature is the possibility of catalyst decomposition^{8,39,59,87,88,109}. Metallocene catalysts show increased catalytic activity at high polymerization temperatures ($T_p > 50^\circ\text{C}$), while the molecular weights of the synthesized polyolefins decrease.

For the unbridged mono-substituted indenyl metallocenes Schmidt and Alt¹¹⁰ found a decrease in catalysts activity with increasing polymerization temperature. This decrease in polymerization activity resulted in a lower M_n and M_w which could have been caused by accelerated β -H elimination.

The polymers synthesized at high T_p using homogeneous catalysts tend to have lower melting temperature, which is not surprising as crystallinity and stereoregularity of these polymers decrease at elevated temperatures. On a contrary note, when these catalysts are supported (e.g. on silica) the stereoselectivity and regioselectivity increase with temperature yielding polymers of high T_m ⁸⁷.

Thomas *et al.*⁶⁰ found that in the octahydro and tetrahydro-fluorenyl C_1 symmetric zirconocenes, the stereoregularity of the PP decreased with increase in T_p in contrast to the fluorenyl analogue which showed similar tacticities at low and high temperatures. This could be due to the hydrogenated rings of the fluorenyl moieties that can "ring flip" and are therefore less stereorigid than the fluorenyl itself. The ring flip can occur more rapidly, therefore reducing the steric directing effect on both the polymer configuration and the incoming monomer leading to more random chain propagation.

Grisi *et al.*⁴⁷ demonstrated that highly syndiotactic PP with T_m of 170°C is produced by metallocene catalysts with C_s -symmetry at temperatures as low as -60°C . Furthermore under identical conditions, C_2 -symmetric catalysts produced isotactic polymers.

2.10 Dimerization and oligomerization of olefins

In the dimerization and oligomerization of olefins, one of the crucial factors, which determine the success of the process, is the rate of chain transfer versus chain propagation. For effective oligomerization, the rate of chain transfer has to be faster than the chain propagation rate¹¹¹.

Earlier on, propylene oligomers were synthesized using the catalyst $(Cp^*)_2MCl_2$ (with M being Zr or Hf) activated with MAO at $50^\circ C$ ^{40,112}. These catalysts were able to produce oligomers with vinyl and vinylidene end-groups, with β -Me abstraction being the main form of chain termination. Analysis of the oligomers using GC showed one carbon decrement confirming the involvement of β -Me abstraction. The interaction of the β -Me with the transition metal appeared to be more favourable than that of β -H since mutual repulsion between the β -Me group on growing carbon chain and methyl substituents on Cp ring becomes enormous. When Cp_2ZrCl_2 was used, oligomers with vinylidene end-groups were exclusively produced.

Michelotti *et al.*¹¹³ found that raising the temperature from 20-80°C during the oligomerization of ethylene resulted in a decrease of Mw from 50 000 to 6 000 when using Cp_2ZrMe_2 catalyst. However when using $Et(Ind)_2ZrCl_2$ for propylene oligomerization, highly isotactic polypropylene was obtained and limited amount of oligomers were formed. Cp_2ZrMe_2 produced low molecular weight propylene oligomers which could be separated using the GC-MS. The cooligomerization of ethylene and propylene promoted chain transfer to the propylene monomer, which resulted in the vinylidenic and vinyl end-group in the oligomer formed from Cp_2ZrMe_2 and $Cp_2^*ZrCl_2$ respectively. The latter type of chain end-group results from β -CH₃ elimination.

In a patented report, chiral silyl bridged metallocenes supported on alumina or silica were activated with MAO or other alkyl aluminiums and non-coordinating anion precursors such as dimethylanilinium tetrakis(perfluoroaryl)borate $[DMAH]^+ [(C_6F_5)_4B]^-$ at high temperatures (90-120°) to obtain stereospecific polypropylene macromonomers with vinyl end-groups⁴³. The obtained macromonomers had low molecular weight, ranging from 2 000 – 50 000. The preferred Al:Zr ratio ranged between 20 and 175, with 40 being the most preferred one.

Ethylene/propylene oligomers have been synthesized using the metallocenes $Me_2Si(Ind)(9-Flu)ZrCl_2$ and $Me_2C(Ind)(9-Flu)ZrCl_2$ activated with MAO at low temperatures ($0^\circ C$)¹⁷. The silyl bridged metallocene produced highly alternating oligomers in comparison to the carbonyl bridged catalysts. Highly active catalysts for propylene oligomerization were obtained by anchoring MAO on a molecular sieve

support via *in situ* hydrolysis of TMA¹¹⁴. The catalyst Cp₂ZrCl₂ produced mainly dimers and trimers.

Van Lookeren *et al.*³⁵ used Et(Ind)₂ZrCl₂, Me₂Si(Ind)₂ZrCl₂ and Cp₂ZrMe₂ in the presence of alumoxo-heteropoly compounds to synthesize propylene oligomers. It was observed by Bazan and Rogers¹¹⁵ that Cp*CrMe₂(PMe₃)/MAO produce low molecular weight straight chain alkane oligomers from reactions with ethylene.

Propene and 1-hexene oligomers with vinylidene and vinyl end-groups have been synthesized using a series of symmetrical and unsymmetrical zirconocenes¹¹⁶. Catalysts of the type (C₄Me₄P)(C₅H₅)ZrCl₂ and (C₄Me₄P)₂ZrCl₂ showed low activities compared to non-phosphoryl catalysts, which is partially due to the steric hindrance of the ligand.

Higher α -olefins such as 1-butene, 1-pentene, 1-hexene, and 1-heptene, were dimerized using different metallocenes at various Al/Zr ratios^{117,118}. However branched olefins such as 3-methyl-1-butene and 4-methyl-1-pentene tend to isomerize giving low yield of dimeric products.

2.11 Polymerization of functionalized monomers

The metallocene catalyst systems are poor in polymerization of functionalized monomers due to lack of activity arising from the complexation of the transition metal with electron donating groups such as oxygen and nitrogen¹¹⁹. The polymerization activity of functionalized monomers is dependent on a number of factors such as the functionality itself, the steric nature of the functional group, metallocene, and cocatalyst, and the length of the methylene spacer between the double bond and the functional group.

In the early 90's Waymouth and his group¹²⁰ reported the polymerization of 1-pentene containing silyl-protected alcohols and tertiary amines using catalysts such as Cp*₂ZrMe₂ activated with B(C₆F₅)₃ or [N,N-dimethylanilinium][B(C₆F₅)₄]. The catalyst activity was higher for 1-hexene than for the functionalized 1-pentenes. On this account amino-olefins were polymerized using Cp*₂ZrMe₂ activated with [HNMe₂Ph]⁺[B(C₆F₅)₄]⁻ to generate the active species [Cp*₂ZrMe]⁺[B(C₆F₅)₄]⁻. The activity of the catalyst system was very low yielding oily oligomers from these aminoolefins¹¹⁹. High molecular weight polymers were obtained in the polymerization of [5-(N,N-(*i*-Pr)₂N-1-C₅H₉)] using the Ziegler-Natta as compared to the

homogeneous systems. The decrease in activity in aminopentene could arise from either intermolecular inhibitive interaction or an intramolecular inhibition of the last inserted monomer in a “back-biting” manner. On the contrary MAO activated catalysts displayed poor activity in the polymerization of these functionalized monomers. This can be explained by the fact that the anionic borate is unlikely to coordinate to the Lewis basic functional monomers.

Helaja *et al.*¹²¹ demonstrated the decomposition of alkoxide compounds formed from the reactions of alcohols, MAO and Cp_2ZrCl_2 . α - and β - positioned hydroxyl groups were more likely to decompose than the tertiary ones which are sterically hindered. Attempts to copolymerize monomers with carbonyl groups (methyl decenoate) resulted in complete deactivation of the catalyst system due to the interaction of the CO_2R or $\text{C}=\text{O}$ group with the catalyst system.

Galimberti *et al.*¹²² using the Ziegler-Natta catalyst $[\text{V}(\text{acac})_3/\text{AlEt}_2\text{I}]$ prepared copolymers of ethylene/propylene and 1-iodo-3-butene. The presence of the halogenated monomer decreased the activity of the catalysts, which resulted in gradual decrease with increasing halogenated monomer concentration.

2.11.1 Functionalized polyolefins

Functional polyolefins are a class of polymers which have new properties due to the presence of functional polar groups attached to the backbone but also maintain, to a large extent, the original properties of the polyolefins¹²³. The synthesis of polyolefins with functional groups using the metallocene catalysts has not attracted much attention owing to the poisoning of the catalysts by the polar monomers. Polyolefins with blocks containing functional groups have been synthesized using methods such as grafting polar monomers to polyolefin chains¹²⁴. While synthesis of graft copolymers can be relatively simple, the preparation of block copolymers requires special polymerization techniques.

In 1997 Chung and Lu¹²⁵ copolymerized ethylene and 5-hexenyl-9-BBN (9-borabicyclo[3.3.1] nonane) using $\text{Et}(\text{Ind})_2\text{ZrCl}_2$ and Cp_2ZrCl_2 both activated with MAO to obtain borane containing polyethylene. The available borane functional groups were easily converted to hydroxyl groups through the ionic process of $\text{NaOH}/\text{H}_2\text{O}_2$. Propylene was also polymerized with $\text{Et}(\text{Ind})_2\text{ZrCl}_2/\text{MAO}$ to obtain polymers with vinylidene end groups which were converted to the borane end groups by reacting

with 9-borabicyclononane. These 9-BBN terminated polyolefins were subjected to oxidation reactions by molecular oxygen in the presence of methyl methacrylate and other free radical polymerizable acrylates to obtain PP-b-PMMA, PP-b-PVA, and PP-b-PS diblock copolymers.

In the olefin polymerization using the metallocene catalysts, the boranes act as chain transfer agents. The effects of the boranes in olefin polymerization were later investigated with regard to their reactivity toward amido ligands of the metallocene catalysts. Thus 9-BBN, dimesitylborane $[\text{HB}(\text{Mes})_2]$, and bis(2,4,6-triisopropylphenyl)borane $[\text{HB}(\text{Trip})_2]$ were used as chain transfer agents in the polymerization of ethylene using $[\text{Cp}^*_2\text{ZrMe}]^+[\text{MeB}(\text{C}_6\text{F}_5)_3]^-$. The catalytic activity was found to be dependent on the borane concentration. However for the $\text{HB}(\text{Trip})_2$ no polymer was observed suggesting a formation of a monomeric species by this monomer and ethylene. The hydroboration reaction which takes place between the ethylene and borane has a significant negative effect on the polymerization of ethylene¹²⁶. The effect of chain transfer was clearly observed with a decrease in Mw, and the narrow MWD shows single site polymerization with a single chain transfer reaction. When the constrained geometry catalyst $[\text{C}_5\text{Me}_4(\text{SiMe}_2\text{N}^i\text{Bu})\text{TiMe}]^+[\text{MeB}(\text{C}_6\text{F}_5)_3]^-$ was used for ethylene polymerization in the presence of these chain transfer agents, there was no evidence of interaction between the borane and the amido group.

Later on an alkene substituted with an alkoxyamine group was copolymerized with propene and 4-methyl-1-pentene using the *rac*-Et(THInd)₂ZrMe₂ and *N,N*- $[\text{HNMe}_2(\text{C}_6\text{H}_5)]^+[\text{B}(\text{C}_6\text{F}_5)_4]^-$. The presence of the alkoxyamine initiating groups allowed grafting of vinyl polymer chains to be grown from the polyolefin backbone¹²⁷.

2.12 Mechanical properties

Unbridged metallocene catalysts $(2\text{-PhInd})_2\text{ZrCl}_2$ produce polypropylenes with stereoblocks of atactic and isotactic fractions. The melting temperatures of the polymers produced by these catalysts, increase with increasing the *mmmm* %, and for fractions of polymers which are ether soluble, no melting peaks are observed¹²⁸. The polymers where hydrogen was introduced to control the molecular weight, they showed higher crystallinity than the polymers with higher molecular weight as revealed by X-ray diffraction and DSC measurements. The ether soluble fraction of

these polymers suggested smectic phase. The degree of crystallinity in these polymers decreases with increasing the polymerization temperature. The crystallinity values estimated by XRD at room temperature was similar to those estimated from the DSC.

Ethylene/1-hexene copolymers showed bimodal crystallinity distributions, which increased to lower crystallization temperature with increasing amount of 1-hexene in the copolymer³⁶. These copolymers showed similar Mw with different polydispersities due to tailing at high molecular weight region, which arises because of a drift in comonomer concentration during polymerization. Furthermore, with this varying comonomer incorporation the crystallinity of the resins as observed via the DSC was found to be low in comparison to that of perfectly crystalline PE, which also concurs with the results from the CRYSTAF. The melting temperatures of these copolymers decreased with the amount of 1-hexene incorporated into the copolymer. The longer side chain in ethylene copolymers could cause disordered and irregular crystal structure¹⁰⁸.

Owing to low side chain branching, narrow polydispersities and higher molecular weight, high-density polyolefins synthesized using metallocene catalysts have higher melt viscosities than the polyolefins from the Ziegler-Natta catalysts¹²⁹. The effect of the long branching on rheological properties of polyethylene has been studied. It was observed that the melt flow index decreases with the increase of long chain branching in the polymer chain, (0.44 branch per 1000 carbons)¹²⁶. However for those polymer chains with less long chain branching content there was hardly a change in the melt flow index. The storage modulus increases with increasing long chain branching content in the polymer chain.

2.13 References

1. W. Kaminsky, K. Kulper, H. H. Brintzinger, F. R. W. P. Wild; *Angew. Chem. Int. Ed. Eng.*, **24**, **1995**, 507.
2. V. K. Gupta, S. Satish, I. S. Bhardwaj; *J. Mol. Sci. Rev. Macromol. Chem. Phys.*, **C34**, **1994**, 439.
3. H. Sinn, W. Kaminsky, H. J. Vollmer, R. Woldt; *Angew. Chem. Int. Ed. Eng.*, **19**, **1980**, 390.
4. L. Garbassi, L. Gilla, A. Proto, *Polymer News*, **19**, **1994**, 367.
5. G. W. Coates, *Chem. Rev.*, **100**, **2000**, 1223.
6. L. Resconi, L. Cavallo, A. Fait, F. Piemontesi; *Chem. Rev.*, **100**, **2000**, 1253.
7. C. Sishta, R. M. Hathorn, T. J. Marks; *J. Am. Chem. Soc.*, **114**, **1992**, 1112.
8. I. Tritto, R. Donetti, M. C. Sacchi, P. Locatelli, G. Zannoni; *Macromolecules*, **30**, **1997**, 1247.
9. C. Kreuder, R. F. Jordan, H. Zhang; *Organomet.*, **14**, **1995**, 2993.
10. M. Bochmann; *J. Chem. Soc. Dalton. Trans.*, **1996**, 255.
11. T. Asanuma, Y. Nishimori, M. Ito, T. Shiomura, *Makromol. Chem. Rapid Commun.*, **14**, **1993**, 315.
12. L. Petitjean, D. Pattou, M. F. Ruiz-Lopez; *J. Mol. Structure (Theochem)*, **541**, **2001**, 227.
13. J. C. W. Lohrenz, M. Buhl, M. Weber, W. Thiel; *J. Organomet. Chem.*, **592**, **1999**, 11.
14. J. A. Ewen; *J. Am. Chem. Soc.*, **106**, **1984**, 6355.
15. T. M. Madkour, A. Soldera; *Eur. Polym. J.*, **37**, **2001**, 1105.
16. J. A. Ewen, R. L. Jones, A. Razavi; *J. Am. Chem. Soc.*, **110**, **1988**, 6255.
17. W. Fan, R. M. Waymouth; *Macromolecules*, **34**, **2001**, 8619.
18. R. H. Grubbs, G. W. Coates; *Acc. Chem. Res.*, **29**, **1996**, 85.
19. M. K. Leclerc, H. H. Brintzinger; *J. Am. Chem. Soc.*, **117**, **1995**, 1651.
20. M. K. Leclerc, H. H. Brintzinger; *J. Am. Chem. Soc.*, **118**, **1996**, 9024.
21. V. Busico, R. Cipullo; *J. Organomet. Chem.*, **497**, **1995**, 113.
22. V. Busico, R. Cipullo; *Prog. Polym. Sci.*, **26**, **2001**, 443.

23. V. Busico, R. Cipullo, F. Cutillo, M. Vacatello, V. V. A. Castelli; *Macromol.*, **36**, **2003**, 4258.
24. L. Resconi, S. Bossi, L. Abis; *Macromolecules*, **23**, **1990**, 4489.
25. W. Kaminsky; *Catalysis Today*, **62**, **2000**, 23.
26. V. N. Panchenko, V. A. Zakharov, I. G. Danilova, E. A. Paukshtis, I. I. Zakharov, V. G. Goncharov, A. P. Suknev; *J. Mol. Cat. A: Chem.*, **174**, **2001**, 107.
27. D. Coevoet, H. Cramail, A. Deffieux, C. Mladenov, J. N. Pedeutour, F. Peruch; *Polym. Int.*, **48**, **1999**, 257.
28. S. Koltzenburg, *J. Mol. Cat. A: Chem.*, **116**, **1997**, 355.
29. H. Sinn, *Adv. Organomet. Chem.*, **18**, **1980**, 99.
30. P. F. Fu, S. Glover, R. K. King, C. Lee, M. R. Pretzer, M. K. Toamli; *Polymer Preprints*, **41**, **2000**, 1903.
31. P. A. Charpentier, S. Zhu, A. E. Hamielec, M. A. Brook; *Polymer*, **39**, **1998**, 6501.
32. Q. Wang, J. Weng, Z. Fan, L. Feng; *Eur. Polym. J.*, **36**, **2000**, 1265.
33. E. Polo, M. Galimberti, N. Mascellani, O. Fusco, G. Muller, S. Sostero; *J. Mol. Cat. A: Chem.*, **160**, **2000**, 229.
34. K. Soga, T. Uozomi, N. Kishi, *Macromol. Rapid. Commun.*, **16**, **1995**, 793.
35. L. K. M. Van Looveren, I. F. J. Vankelecom, D. E. De Vos, B. H. J. Wouters, P. J. Grobet, P. A. Jacobs; *Appl. Catal. A: Gen.*, **180**, **1999**, L5.
36. C. L. P. Shan, J. B. P. Soares, A. Penlidis; *Polymer*, **43**, **2002**, 767.
37. F. Barsan, A. Karam, *Macromolecules*, **31**, **1998**, 839.
38. E. Y. X. Chen, T. J. Marks; *Chem. Rev.*, **100**, **2000**, 1391.
39. G. Moscardi, F. Piemontesi, L. Resconi; *Organomet.*, **18**, **1999**, 5275.
40. L. Resconi, F. Piemontesi, G. Franciscano, L. Abis, T. Fiorani; *J. Am. Chem. Soc.*, **114**, **1992**, 1025.
41. V. Busico, R. Cipullo; *Makromol. Chem. Rapid. Commun.*, **13**, **1992**, 15.
42. L. Resconi; *J. Mol. Cat. A: Chem.*, **146**, **1999**, 167.
43. W. Weng, A. Dekmezian, E. J. Markel, A. Gadkari, D. L. Peters; US Patent, 6 117 962, Sept. **2000**.
44. S. S. Reddy, S. Sivaram; *Prog. Polym. Sci.*, **20**, **1995**, 309.
45. B. Rieger, C. Troll, J Preuschen; *Macromol.*, **35**, **2002**, 5742.

46. M. D. Bruce, G. W. Coates, E. Hauptman, R. M. Waymouth, J. W. Ziller; *J. Am. Chem. Soc.*, **119**, **1997**, 11174.
47. F. Grisi, P. Longo, A. Zambelli, J. Ewen; *J. Mol. Cat. A: Chemical*, **140**, **1999**, 225.
48. H. Juvaste, T. T. Pakkanen, E. I. Iiskola; *J. Organomet. Chem.*, **606**, **2000**, 169.
49. W. Kaminsky; *Macromol. Symp.*, **97**, **1995**, 79.
50. U. Stehling, J. Diebold, R. Kirsten, W. Roll, H. H. Brintzinger, S. Jungling, R. Mulhaupt, F. Langhauser; *Organomet.*, **13**, **1994**, 964.
51. W. Spaleck, F. Kueber, A. Winter, J. Rohrmann, B. Bachmann, M. Antberg, V. Dolle, E. F. Paulus; *Organomet.*, **13**, **1994**, 954.
52. W. Spaleck, M. Antberg, J. Rohrman, A. Winter, B. Bachmann, O. Kiprof, J. Behm, W. Herrmann; *Angew. Chem. Int. Ed. Engl.*, **31**, **1992**, 1347.
53. W. Spaleck, M. Aulbach, B. Bachmann, F. Kuber, A. Winter; *Macromol. Symp.*, **89**, **1995**, 954.
54. M. C. Sacchi, E. Barsties, I. Tritto, P. Locatelli, H. H. Brintzinger, U. Stehling; *Macromolecules*, **30**, **1997**, 1267.
55. G. Schupfner, W. Kaminsky; *J. Mol. Cat. A: Chem.*, **102**, **1995**, 59.
56. L. Resconi, D. Balboni, G. Baruzzi, C. Fiori, S. Guidotti; *Organomet.*, **19**, **2000**, 420.
57. S. Lieber, H. H. Brintzinger; *Macromolecules*, **33**, **2000**, 9192.
58. J. Ewen; *Makromol. Chem. Macromol. Symp.*, **48/49**, **1991**, 253.
59. D. Veghini, L. M. Henling, T. Burkhardt, J. E. Bercaw; *J. Am. Chem. Soc.*, **121**, **1999**, 564.
60. E. J. Thomas, M. D. Rausch, J. C. W. Chien; *J. Organomet. Chem.*, **631**, **2001**, 29.
61. H. G. Alt, E. Samuel, *Chem. Soc. Rev.*, **27**, **1998**, 323.
62. H. G. Alt, M. Jung; *J. Organomet. Chem.*, **568**, **1998**, 87.
63. D. Van Leusen, D. J. Beetstra, B. Hessen, J. H. Teuben; *Organomet.* **19**, **2000**, 4084.
64. J. Jung, S. K. Noh, D. Lee, S. K. Park, H. Kim; *J. Organomet. Chem.*, **595**, **2000**, 147.

65. J. Saßmannshausen, A. K. Powell, C. E. Anson, S. Wocadlo, M. Bochmann; *J. Organomet. Chem.*, **592**, **1999**, 84.
66. J. C. W. Chien, Y. Iwamoto, M. D. Rausch, W. Wedler, H. H. Winter; *Macromolecules*, **30**, **1997**, 3447.
67. D. T. Mallin, M. D. Rausch, Y. G. Lin, D. Sizhong, J. C. W. Chien; *J. Am. Chem. Soc.*, **112**, **1990**, 2030.
68. G. H. Llinas, S. H. Dong, D. T. Mallin, M. D. Rausch, Y. G. Lin, H. H. Winter, J. C. W. Chien, *Macromolecules*, **25**, **1992**, 1242.
69. G. W. Coates, A. L. Mogstad, E. Hauptman, M. D. Bruce, R. M. Waymouth; *Polymer Preprints*, **36**, **1995**, 545.
70. E. Hauptman, R. M. Waymouth; *J. Am. Chem. Soc.*, **117**, **1995**, 11586.
71. G. W. Coates, R. M. Waymouth; *Science*, **267**, **1995**, 217.
72. V. Busico, R. Cipullo, W. P. Kretschmer, G. Talarico, M. Vacatello, V. V. A. Castelli; *Angew. Chem. Int. Ed.*, **41**, **2002**, 505.
73. R. Kravchenko, A. Masood, R. M. Waymouth; *Organomet.*, **16**, **1997**, 8636.
74. J. L. M. Petoff, T. Agoston, T. K. Lal, R. M. Waymouth; *J. Am. Chem. Soc.*, **120**, **1998**, 11317.
75. R. Kravchenko; *J. Am. Chem. Soc.*, **120**, **1998**, 2039.
76. G. Erker, M. Aulbach, M. Knickmeier, D. Wingsbermhühle, C. Kruger, M. Nolte, S. Werner; *J. Am. Chem. Soc.*, **115**, **1993**, 4590.
77. G. Y. Lee, M. Xue, M. S. Kang, O. C. Kwon, J. S. Yoon, Y. S. Lee, H. S. Kim, H. Lee, I. M. Lee; *J. Organomet. Chem.*, **558**, **1998**, 11.
78. L. Wang, Y. Wang, Y. Yuan, J. Pan, C. Ye, L. Feng, Y. Qian, J. Huang; *Eur. Polym. J.*, **37**, **2001**, 215.
79. F. Zhang, Y. Mu, J. Wang, Z. Shi, W. Bu, S. Hu, Y. Zhang, S. Fen; *Polyhedron*, **19**, **2000**, 1941.
80. N. Schneider, F. Schaper, K. Schmidt, R. Kirsten, A. Geyer, H. H. Brintzinger; *Organomet*, **19**, **2000**, 3597.
81. S. Lin, E. Hauptman, T. K. Lal, R. M. Waymouth, R. W. Quan, A. B. Ernst; *J. Mol. Cat. A: Chem.*, **136**, **1998**, 23.
82. C. D. Tagge, R. L. Kravencho, T. K. Lal, R. M. Waymouth; *Organomet.*, **18**, **1999**, 380.

83. P. Witte, T. K. Lal, R. M. Waymoth; *Organomet.*, **18**, **1999**, 4147.
84. I. Kim, R. F. Jordan; *Macromolecules*, **29**, **1996**, 489.
85. P. Jutzi, C. Muller, B. Neumann, H. G. Stamler; *J. Organomet. Chem.*, **625**, **2001**, 180.
86. C. Janiak, U. Versteeg, K. C. H. Lange, R. Weimann, E. Hahn; *J. Organomet. Chem.*, **501**, **1995**, 219.
87. S. Jungling, R. Mulhaupt, U. Stehling, H. H. Brintzinger, D. Fischer, F. Langhauser; *J. Polym. Sci. A: Chem.*, **33**, **1995**, 1305.
88. S. Jungling, S. Koltzenburg, R. Mulhaupt; *J. Polym. Sci. A: Chem.*, **35**, **1997**, 1.
89. A. J. Van Reenen, R. Brull, U. M. Wahner, H. G. Raubenheimer, R. D., Sanderson, H. Pasch; *J. Polym. Sci. A: Chem.* **38**, **2000**, 4110.
90. R. Brull, H. Pasch, H. G. Raubenheimer, R. Sanderson, U. M. Wahner; *J. Polym. Sci. A: Chem.*, **38**, **2000**, 2333.
91. C. Lehtinen, P. Starck, B. Lofgren; *J. Polym. Sci. A: Chem.*, **35**, **1997**, 307.
92. A. Fries, T. Mise, A. Matsumoto, H. Ohmori, Y. Wakatsuki; *Chem. Commun.*, **1996**, 783.
93. R. Kravechenko, R. M. Waymouth, *Macromolecules*, **31**, **1998**, 1.
94. W. J. Wang, E. Kolodka, S. Zhu, A. E. Hamielec; *J. Polym. Sci. Chem.*, **37**, **1999**, 2949.
95. M. L. Ferreira, G. B. Gallano, D. E. Damiani, M. A. Villar; *J. Polym. Sci. A: Chem.*, **39**, **2001**, 2005.
96. S. M. Graef, U. M. Wahner, A. J. van Reenen, R. Brull, R. D. Sanderson, H. Pasch; *J. Polym. Sci. A: Chem.*, **40**, **2002**, 128.
97. I. Kim, S. Y. Kim, M. H. Lee, Y. Do, M. S. Won; *J. Polym. Sci. A: Chem.*, **37**, **1999**, 2763.
98. D. Harrison, I. M. Coulter, S. Wang, S. Nistala, B. A. Kuntz, M. Pigeon, J. Tian, S. Collins; *J. Mol. Cat. A: Chem.*, **128**, **1998**, 128.
99. T. Asanuma, Y. Nishimori, M. Ito, N. Uchikawa, T. Shiomura; *Polymer Bull.*, **25**, **1991**, 567.
100. D. B. Malpass; U.S. Patent, 485 148 9, July 25 **1989**.
101. W. Weng, W. Hu, A. H. Dekmejian, C. J. Ruff; *Macromol*, **35**, **2002**, 3838.

102. E. Kolodka, W. J. Wang, S. Zhu, A. Hamielec; *Macromol. Rapid. Commun*, **24**, **2003**, 31.
103. E. Koldka, W. J. Wang, P. A. Charpentier, S. Zhu, A. E. Hamielec; *Polymer*, **41**, **2000**, 3985.
104. T. Shiono, S. M. Azad, T Ikeda; *Macromol.*, **32**, **1999**, 5723.
105. T. Shiono, Y. Moriki, T. Ikeda, K. Soga; *Macromol. Chem. Phys.*, **198**, **1997**, 3229.
106. R. W. Barnhart, G. C. Bazan; *J. Am. Chem. Soc.*, **128**, **1998**, 1082.
107. D. Beigzadeh, J. B. O. Soares, T. Duever; *Macrol. Rapid Commun.*, **20**, **1999**, 541.
108. K. J. Chu, T. H. Park; *Materials Lett.*, **31**, **1997**, 11.
109. M. Eskelinen, J. V. Seppala; *Eur. Polym. J.*, **32**, **1996**, 331.
110. R. Schmidt, H. G. Alt, *J. Organomet. Chem.*, **621**, **2001**, 304.
111. J. Skupinska; *Chem. Rev.*, **91**, **1991**, 613.
112. T. Mise, A. Kageyama, S. Miya, H. Yamakazi; *Chem. Letters*, **1991**, 1525.
113. M. Michelotti, A. Altomare, F. Ciardelli, P. Ferrarini; *Polymer*, **37**, **1996**, 5011.
114. L. K. van Looveren, D. E. De Vos, K. A. Vercruysse, D. F. Geysen, B. Janssen, P. A. Jacobs; *Catal. Letters*, **56**, **1998**, 53.
115. J. S. Rogers, G. C. Bazan; *Chem. Commun.*, **2000**, 1209.
116. C. Janiak, K. C. H. Lange, P. Marquardt; *J. Mol. Cat. A: Chem.* 3408, 2001, 1.
117. U. M. Wahner, R. Brull, H. Pasch, H. G. Raubenheimer, R. D. Sanderson; *Angew. Makromol. Chem.*, **270**, **1999**, 49.
118. J. Christoffers, R. G. Bergman; *Inorg. Chim. Acta*, **270**, **1998**, 20.
119. U. M. Stehling, K. M. Stein, M. R. Kesti, R. M. Waymouth; *Macromolecules*, **31**, **1998**, 2019.
120. M. R. Kesti, G. W. Coates, R. M. Waymouth; *J. Am. Chem. Soc.*, **114**, **1992**, 9679.
121. T. Helaja, K. Hakala, J. Helaja, B. Lofgren; *J. Organomet. Chem.*, **579**, **1999**, 164.
122. M. Galimberti, U. Giannini, E. Albizzati, S. Caldari, L. Abis; *J. Mol. Cat. A: Chem.*, **101**, **1995**, 1.

123. T. Simonazzi, A. D. Nicola, M. Aglietto, G. Ruggeri; *Comprehensive Polymer Science*; Pergamon Press: New York, 1992; 1st Supplement, Chapter 7; pp 133-158.
124. M. A. J. Schellekens, B. Klumperman, *J. M. S., Rev. Macromol. Chem. Phys.*, **C40**, **2000**, 167.
125. T. C. Chung, H. L. Lu; *J. Mol. Cat. A: Chem.*, **115**, **1997**, 115.
126. T. C. Chung, G. Xu, Y. Lu, Y. Hu; *Macromolecules*, **34**, **2001**, 8040.
127. U. M. Stehling, E. E. Malmstrom, R. M. Waymouth, C. J. Hawker; *Macromolecules*, **31**, **1998**, 4396.
128. Y. Hu, M. T. Krejchi, C. D. Shah, C. L. Myers, R. M. Waymouth; *Macromolecules*, **31**, **1998**, 6908.
129. J. F. Vega, A. Munoz-Escalona, A. Santamaria, M. E. Munoz, P. Lafuente; *Macromolecules* **29**, **1996**, 960.
130. D. Yan, W. J. Wang, S. Zhu; *Polymer*, **40**, **1999**, 1737.
131. J. S. Yoon, Y. S. Lee, E. S. Park, I. M. Lee, D. K. Park, S. O. Jung; *Eur. Pol. J.*, **36**, **2000**, 1271.
132. Y. Ju, E. D. Carlson, G. G. Fuller, R. M. Waymouth; *Macromolecules.*, **32**, **1999**, 3334.

Chapter 3

Experimental

All manipulations involving air sensitive materials were performed in a nitrogen environment, using Schlenk techniques or a glove box.

3.1 Oligomerization

3.1.1 Chemicals

Toluene (AR, Sigma Aldrich) was distilled over sodium metal before use, as was diethyl ether (AR, Merck)¹. Sodium metal (SaarChem) was used as received. Methanol (Merck) was used as received, as was benzophenone (Sigma Aldrich).

Nitrogen, (99%, Afrox) was passed over self-indicating silica gel (packed column) and 4 Å molecular sieves prior to use. Propylene (Messer Fedgas), was passed over molecular sieves 4 Å to remove moisture and a copper catalyst to remove air, before use.

Methylalumoxane (10% solution in toluene) (Sigma Aldrich) was used as received. The catalysts *rac*-ethylene bisindenyl zirconium dichloride (Strem Chemicals) and dimethylsilyl bis[2-methyl-4,5-benzoindenyl] zirconium dichloride (Boulder Scientific) was used as received.

3.1.2 Preparation of catalyst solutions (typical).

The procedure was carried out in a nitrogen filled glovebox. Schlenk tubes were dried overnight at 120°C in the oven and cooled under nitrogen gas flow. Into these Schlenk tubes were weighed, respectively, 1.248 mmol (0.522 g) *rac*-ethylene bisindenyl zirconium dichloride and 1.246 mmol (0.720 g) dimethylsilyl bis[2-methyl-4,5-benzoindenyl] zirconium dichloride. The Schlenk tubes were stoppered with rubber septa and removed from the glovebox. 10 ml of freshly distilled toluene was injected into each of the Schlenk tubes. Syringes were thoroughly flushed with nitrogen gas before injection. The catalyst solutions were aged for 6 hours before use.

3.2.3 Oligomerization procedure (typical).

The oligomerization reactions were carried out in a 450 ml Parr Autoclave equipped with ball-valve and needle-valve inlets, pressure gauge, a glass insert and a magnetic follower. The reactor, magnetic follower, and glass insert were washed and dried in the oven (120°C) for 18 hours prior to use. The reactor was assembled while hot and was allowed to cool under nitrogen atmosphere.

The reactor was subjected to three purging cycles comprising pressurization with nitrogen and subsequent removal of the gas under vacuum, and then filled with nitrogen. The reactor was then sequentially charged with 24.95 mmol catalyst (as toluene solution) (either $\text{Et}[\text{Ind}]_2\text{ZrCl}_2$ or $\text{SiMe}_2[2\text{-Me-4,5-BenzInd}]_2\text{ZrCl}_2$), 12.47 mmol (8.27 ml of a 10% toluene solution) methylalumoxane, and 30 ml toluene using glass Luer-lock syringes with stainless steel needles. The reactor was weighed and placed in a preheated oil bath. Temperature was controlled by a heater-stirrer unit. Temperature was set at the required reaction temperature (varied between 80 – 100°C), and the reactor allowed to equilibrate for 5 minutes before being charged with propylene gas for a period of 10 minutes.

After 10 minutes of oligomerization, the reactor was removed from the oil bath and weighed. The excess propylene was slowly discharged in a fume hood. The reactor was cooled before opening. The oligomers were isolated by adding methanol to the reaction medium. The resultant mixture was then stirred for 12 hours. The mixture was then extracted with diethyl ether and filtered under reduced pressure. The diethyl ether extract was isolated and the solvent mixture (ether/methanol) was removed in a rotary evaporator and the product was dried overnight in vacuum oven at 60°C, weighed to obtain the yield, and placed in sample holders for analysis and further use.

3.2 Copolymerization of oligomers with ethylene

3.2.1 Materials

The catalysts *i*-propylidene(cyclopentadienyl)(9-fluorenyl) zirconium dichloride and tetramethyl-cyclopentadienyl dimethyl silyl *t*-butylamido titanium dimethyl, both purchased from Strem chemicals, were used as received.

Ethylene (polymerization grade) was obtained from Afrox and used as received.

All the other chemicals used were described in Section 3.1.1.

3.2.2 Preparation of catalyst solutions

The procedure used here is similar to the one described in Section 3.1.2. The required amount of the catalysts used here were, 5.45 mmol (0.018 g) of tetramethylcyclopentadienyl dimethyl silyl *t*-butylamido titanium dimethyl and 4.20 mmol (0.018 g) of *i*-propylidene(cyclopentadienyl)(9-fluorenyl) zirconium dichloride, which were then dissolved in 10 ml toluene. The catalyst solutions were aged for 3 hours before use.

3.2.3 Copolymerization reactions

The reactor used for copolymerization reactions was the same as the one used in the synthesis of the oligomers. The reactor, glass insert and magnetic follower were washed and dried in the oven prior to use. The glass insert was removed from the oven and the required amount (3-7 g) of propylene oligomer was weighed into the glass insert, and then placed in a vacuum oven at 50°C for 3 hours prior to the copolymerization reaction.

Nitrogen gas was used to break vacuum in the oven and the glass insert was swiftly transferred into the reactor which had been dried in the oven. The reactor was immediately assembled, and then cooled under nitrogen.

The reactor was subjected to three purging cycles comprising pressurization with nitrogen and subsequent removal of gas under vacuum, and then filled with nitrogen. The reactor was sequentially charged with 5.6 μmol catalyst (as toluene solution) (either $\text{Me}_2\text{C}(\text{Cp}^*)\text{N}^t\text{BuTiMe}_2$ or $i\text{-Pr}(\text{Cp})(9\text{-Flu})\text{ZrCl}_2$), 0.016 mol methylalumoxane (10% solution in toluene), and 80 ml toluene. The reactor was weighed and placed in a preheated oil bath which was set at the required reaction temperature, followed by charging with the required amount of ethylene. The polymerization was allowed to continue for 6 hours. The reactor was removed from the oil bath, excess gaseous monomers was slowly vented in a fume hood, and the reactor allowed to cool to room temperature.

The reactor was opened and the dissolved polymer was precipitated by addition of methanol, and the mixture was allowed to stir overnight. The polymers were filtered under reduced pressure. The resultant polymers were dried overnight in vacuum oven at 60°C.

To remove the unreacted oligomers from the polymers, the polymers were subjected to Soxhlet extraction using diethyl ether as the solvent for 6 hours or until no more oligomers could be separated from the polymers. The polymers were once again dried in the vacuum oven for 6 hours at 60°C. The isolated polymers sealed in sample holders and stored in a dark area.

3.3 *Functionalization and block copolymerization reactions of propylene oligomers*

3.3.1 Materials

Mercuric acetate (AR), sodium borohydride (AR) and sodium hydroxide (Merck) were used as received. Diethyl ether (AR) and tetrahydrofuran (AR) (Merck) were stored in darkness and distilled over sodium prior to use¹.

Acryloyl chloride 99%, methacryloyl chloride 99%, methacrylic anhydride and triethylamine (Sigma Aldrich) were used as received.

3.3.1 Hydration reactions

A typical hydration reaction was as follows: Into a 2-litre Ehrlenmeyer flask was added 22.8 mmol (7.29 g) mercuric acetate, 700 ml water and 800 ml THF while stirring. This resulted in a yellow solution. Previously prepared oligomer, (8.00 g) dissolved in dry THF was added. The solution was allowed to continue stirring for 6 hrs. The reaction mixture was quenched by cooling in ice and 3.00 M aqueous NaOH was slowly added, followed by addition of 11.4 mmol (0.42g) NaBH₄ in 3.00 M NaOH and was allowed to stir for an additional 2 hours. Metallic mercury formed as a coagulate on in the bottom of the flask. The aqueous and organic phases were separated in a separation funnel, and the organic layer was retained for further work-up².

THF is hydrophilic in its nature, hence after separation it contained small fractions of water. This remaining water was removed by adding 30% (by volume) of diethyl ether. The remaining mercury was removed by filtration.

The solvent was removed under reduced pressure in a rotary evaporator, the product thus isolated was placed in a sample holder and stored for later use.

3.3.2 Synthesis of acryloyl esters of the propylene oligomers.

A typical acryloyl ester synthesis was as follows: Into a three neck 500 ml round bottom flask equipped with a magnetic follower was added 8.00 g of the hydrated oligomer, 300 ml freshly distilled diethyl ether, and 0.060 mol (7.26 g) triethylamine. The reaction mixture was chilled in an ice bath while stirring and 0.10 mol (11.0 g) acryloyl chloride was added dropwise using an addition funnel³. The reaction was allowed to proceed for 6 hrs, and was quenched by washing with water to remove the quaternary ammonium salt formed. A 5% solution of sodium hydroxide (100 ml) was used to wash the solution, which was later dried with anhydrous sodium sulphate and the acryloyl ester of the oligomer was recovered by removing the ether in a rotary evaporator. The product was weighed and placed in a sample holder and stored at 4°C.

3.3.3 Synthesis of methacryloyl esters of the propylene oligomers.

Typically, to a 500 ml three neck round bottom flask equipped with a magnetic follower and dropping funnel, was added 8.00 g of the hydrated oligomer followed by the addition of 200 ml of anhydrous distilled THF, 0.010 mol (1.16 g) of triethylamine, and 8.00 mmol (0.80 g) DMAP (4-dimethylaminopyridine) under nitrogen. The flask was chilled in an ice bath. Freshly distilled methacryloyl chloride, 0.050 mol (5.23 g) was added slowly by means of an addition funnel. The reaction mixture was stirred throughout.⁴ The solution was allowed to warm slowly to room temperature over a period of 2 hrs and then stirred for 18 hours.

The reaction mixture was diluted with 100 ml THF and insoluble salts were filtered off. The solvent was removed on a rotary evaporator. Diethyl ether was added to the remaining viscous solution, which was extracted, in succession, with 0.1 M HCl, 0.1 M NaOH, water and saturated NaCl solution. The organic phase was dried over anhydrous Na₂CO₃ and filtered, the ether was removed on a rotary evaporator to obtain the a viscous liquid. The product was weighed and placed in a sample holder and stored 4°C.

3.3.4 Polymerization of oligomer acryl ester by free radical initiators.

To a 50 ml Schlenk tube with a magnetic follower was added 1.5 g of a propylene oligomer ester of acrylic acid, followed by addition of 20 ml freshly distilled toluene. Initiator α -azo-*iso*-butyronitrile (AIBN) was added to the reaction mixture and the Schlenk tube was placed in a temperature controlled oil bath and the temperature was raised to 80°C. The reaction was allowed to proceed for 6 hours, and it was stopped by addition of methanol. The polymer solution precipitated out and was stirred for 3 hours, followed by several washings with methanol. The product was dried in a vacuum oven overnight at 50°C.

3.4 Characterization techniques

3.4.1 NMR spectroscopy

Nuclear magnetic spectra were recorded on either a 300 MHz Varian VXR spectrometer equipped with a Varian magnet (7.0 T) and a 5 mm switchable probe, or a 600 MHz Varian Unity Inova spectrometer equipped with an Oxford magnet (14.09 T) and a 5 mm inverse detection PFG probe. Standard pulse sequences were used for obtaining ^1H , ^{13}C and APT spectra.

3.4.1.1 Spectroscopy for room temperature samples

Approximately 70 mg of the oligomer or polymer was weighed into an NMR tube, followed by addition 0.7 ml of deuterated chloroform which contained TMS as internal reference standard. The spectra were measured in a 300 MHz Varian VXR NMR spectrometer at room temperature.

By using a pulse angle of 45 degrees and a relatively short repetition time of 0.82 seconds, good sensitivity could be obtained by accumulating 4 000 transients for each sample. Resolution and accuracy were improved by performing apodization and zero filling before the spectra were transformed.

3.4.1.2 Spectroscopy for high temperature samples

This procedure was used for polyolefin polymers owing to their insolubility at room temperature to most solvents. Approximately 90 mg of the polymer was weighed into an NMR tube, followed by addition of 0.08 ml deuterated

benzene and 0.9 ml of trichlorobenzene. The solution was heated in a temperature controlled oil bath to 120°C and was kept at that temperature for 90 minutes. The solution was then gradually cooled to room temperature.

If during the heating period, there were air bubbles present in the sample, the heating and cooling process was repeated until the bubbles disappeared. The spectra were recorded in 300 MHz Varian NMR spectrometer at 100°C.

To obtain better resolution in the spectra, baseline and phase correction were performed in the spectra.

Due to differences in the relaxation times as well as different Nuclear Overhauser Effect (NOE) being experienced by carbons in different chemical environments, the integrals obtained in the conditions above have to be corrected. A gated proton decoupling experiment (decoupler gated off for 4.2 seconds to allow the build-up in NOE to vanish as much as possible) and a longer repetition time 5.02 seconds (instead of 0.8 seconds) was performed. The integrals and integral ratios obtained under these conditions were used to correct the values obtained by means of normal (fast) conditions.

3.4.2 Infrared spectroscopy

Infrared spectroscopic analyses of the oligomer and polymer samples were performed on a Perkin-Elmer Paragon 1000 Fourier Transform Infrared Spectrometer. The samples were dissolved in dichloromethane (usually 1% v/v for liquid samples) and small droplets were placed on a NaBr disk. After evaporation of the solvent, spectra were recorded. The absorption of the sample was then subtracted from the NaBr background.

The number of scans taken ranged from 40 – 100, depending on the molecular weight of the sample. For samples which had high molecular weight, a higher number of scans was performed for better resolution.

3.4.3 DSC

Differential scanning calorimetric analyses of samples were carried out. Typically, approximately 4 mg of a polymer sample was weighed in an aluminium DSC pan, and the pan was then capped and crimped. The thermal analyses were done on a Mettler TA 4000, in a Mettler DSC 25, with a TC 11

TA processor, by heating the samples from room temperature to 180°C at a heating rate of 10°C/min under nitrogen at a flow rate of 100 ml/minute. The sample was then cooled to room temperature and a second heating scan was performed. The melting temperature taken was that obtained in the second heating scan.

3.4.4 Size exclusion chromatography

3.4.4.1 Size exclusion chromatography for room temperature samples

Into a 5 ml sample holder was added 40 mg of the sample and 4 ml of distilled THF (AR). The sample solutions were allowed to stand for 12 hours before being filtered into size exclusion sample vials. The measurements were performed in Waters 717plus Autosampler with a Waters 410 Differential Refractometer at 30°C, a Waters 600E System controller with 4 columns of Phenogel, length 300 mm by 7.80 mm internal diameter, and a pore sizes of 100 Å, 10³Å, 10⁴ Å, and 10⁵ Å, using HPLC-grade THF sparged with IR-grade Helium as eluent at a flow of 1 ml/minute.

3.4.4.2 High temperature size exclusion chromatography

Into a sample vial, 4 mg of the polymer was weighed; a small magnetic follower was placed into the sample vial, followed by addition of 2 ml distilled trichlorobenzene. The sample was then crimped and placed in a magnetically stirring heating block and heated to obtain a homogenous mixture. The measurements were performed in Polymer Laboratories GPC 220 High Temperature chromatograph, with 3 columns packed with a polystyrene / divinylbenzene copolymer (PL gel mixed B), length 300 mm and internal diameter of 7.5 mm, particle size 10 µm, using trichlorobenzene as the solvent at oven temperature of 160°C and flow rate of 1 ml/minute.

3.4.5 Crystallization analysis by fractionation

The samples for crystallization fraction were done on a Crystaf Model 200 with liquid nitrogen cooling unit obtained from Polymer Char (Valencia, Spain). The sample consisting of about 20 mg dissolved in 30 ml of trichlorobenzene, was placed in a reactor equipped with a magnetic follower and was heated to

160°C in a heating block with magnetic stirrer to obtain a homogeneous mixture.

The samples were placed in the reactor, heated again to 160° and kept at this temperature for 10 minutes before being cooled to room temperature at a cooling rate of 0.1°C/minute while sampling at each interval until 30°C.

3.5 References

1. B. S. Funnis, A. J. Hannaford, V. Rogers, P. W. G. Smith, A. R. Tatchel; *Vogel's Text Book of Practical Organic Chemistry*, 4th Edition, Longman Incorporation, New York,
2. H. C. Brown, P. J. Geoghegan; *J. Org. Chem.*, **35**, **1970**, 1844.
3. S. Balasubramanian, B. S. R. Reddy; *Eur. Polym. Journal*, **32**, **1996**, 1073.
4. H. Y. Acar, J. J. Jensen, K. Thigpen, J. A. McGowen, L. J. Mathias; *Macromolecules*, **33**, **2000**, 3855.

Chapter 4

Oligomerization

4.1 Solution Oligomerization

4.1.1 Oligomer Synthesis

The propylene oligomers were synthesized using catalysts $\text{Et}(\text{Ind})_2\text{ZrCl}_2$ (**1**) (EBI) and $(\text{CH}_3)_2\text{Si}(2\text{-Me-4,5-BenzoInd})_2\text{ZrCl}_2$ (**2**) (MBI), activated with MAO. These catalysts produced propylene oligomers of varying chain length at different catalyst concentrations and oligomerization temperatures.

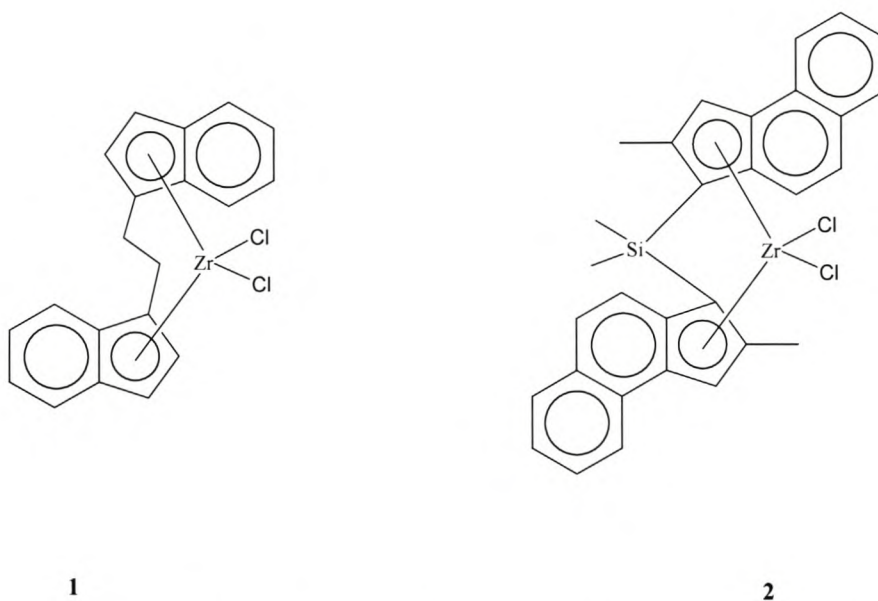
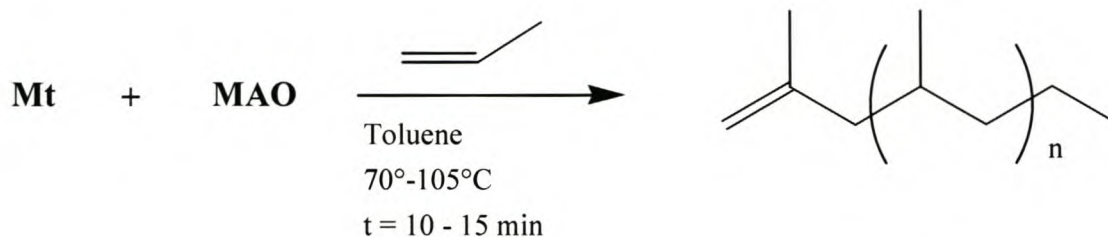


Figure 1: Metallocenes used for oligomerizations

The lower molecular weight ($M_w \geq 500 - 900$) oligomers appeared as viscous liquids which are soluble in most organic solvents, whereas the higher molecular weight oligomers appeared as sticky solids. The produced oligomers in some instances contained some crystalline material which was removed by dissolving the product in diethyl ether followed by filtration under reduced vacuum.



Mt = Complex 1 or 2

$n = 12 - 20$

Scheme 1: Oligomerization of propylene.

Table 1: Oligomerization of propylene: Representative results

Run	Catalyst (mmol)	T (°C)	Yield (g)	M _n	M _w /M _n	M _p	<i>mmmm</i> % ^{1,2}
1	1.1950	100	15	785	1.572	438	24.9
2	0.4780	100	14	794	1.600	460	26.8
3	0.2495	80	12	1278	1.989	1 601	17.8
4	0.2495	70	9.8	1358	1.914	1 615	35.2
5	0.2495	90	20	1043	1.600	1 033	23.6
6	0.2495	100	16	1234	1.921	1 461	29.7
7	0.0623	100	14	1697	2.471	2 554	36.9
8*	0.2495	100	9	1514	2.142	2 173	43.1
9*	0.3742	100	12	1159	2.236	1 010	40.2
10*	0.2495	90	11	1353	3.004	1 258	38.9
11*	0.2495	80	8	1756	3.014	3 444	41.8

Et(Ind)₂ZrCl₂ was used as the catalyst except for * where (CH₃)₂Si(2-Me-4,5-benzoInd)₂ZrCl₂ was used. The Al:Zr ratio was kept at 60, and the oligomerization time was kept at 10 minutes. M_p represents the peak molecular weight calculated by the instrument.

If we look at the EBI catalyst's products (runs 1 – 7) it can be seen that lowering the catalyst concentration resulted in increased oligomer molecular weight as well as their molecular weight distribution. In general, the temperature influenced the yields of the oligomers as well, thus oligomerizing at lower temperature resulted in low yields of THF or diethyl ether soluble oligomer.

The benzoindenyl (MBI) catalyst produced slightly lower yields, compared to the EBI catalyst, but at the same time yielded higher molecular weight materials when comparing runs done with similar catalyst concentrations and at the same temperature. In most cases the PDI was higher for the oligomers produced with this catalyst.

The molecular weight of the oligomers dropped to an extent; when the reaction was stopped and vented off immediately without cooling the reactor. This is due to the fact that at lower temperatures high molecular weight polymer will be formed during the cooling of the polymerizing system. The tacticities of the oligomers, as measured in the *mmm*% using NMR spectroscopy, seemed to be independent of the reaction temperature, or catalyst concentration. It is clear, however, that the isotacticity of the oligomers produced by the MBI catalysts are generally higher than that of the oligomers produced by the EBI catalyst. This aspect will be discussed in greater detail later on.

The yields given in Table 1 are approximate as the oligomer yields cannot be quantified to experimental conditions as only the recovered amount of oligomers which were soluble in diethyl ether, THF or pentane were given.

4.1.2. NMR Spectroscopy

4.1.2.1 ^1H NMR

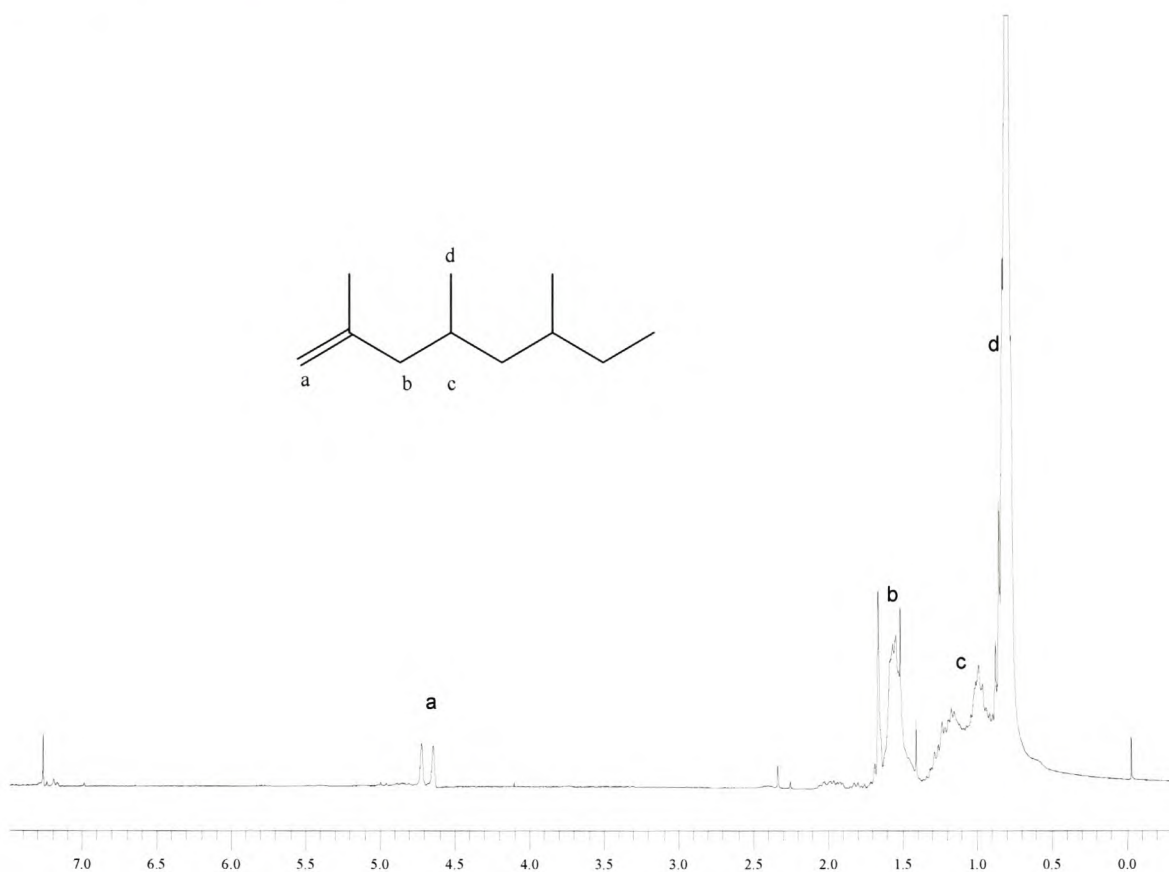


Figure 2: ^1H NMR of propene oligomer synthesized using $\text{et}(\text{Ind})_2\text{ZrCl}_2$ at 100°C .

The proton spectrum was obtained by dissolving the oligomers in deuterated chloroform, and measurements were taken at room temperature. The solvent peak can be identified at δ 7.26, and it was used as reference for other peaks. From the ^1H NMR two peaks of equal intensity at 4.75 ppm and 4.85 ppm are a characteristic of vinylidene end-group³. These two peaks represent the end group protons which was a result of β -H elimination. The ^1H NMR spectra hardly show the presence of vinyl end-groups, suggesting that these two catalysts don't really have β -methyl abstraction as way of chain termination. The oligomer backbone peaks can be observed at δ 0.7- 1.0 for the methyl protons and at δ 1.1-1.3 for the methine protons, and at δ 1.5-1.6 for the methylene protons.

4.1.2.2 ^{13}C NMR

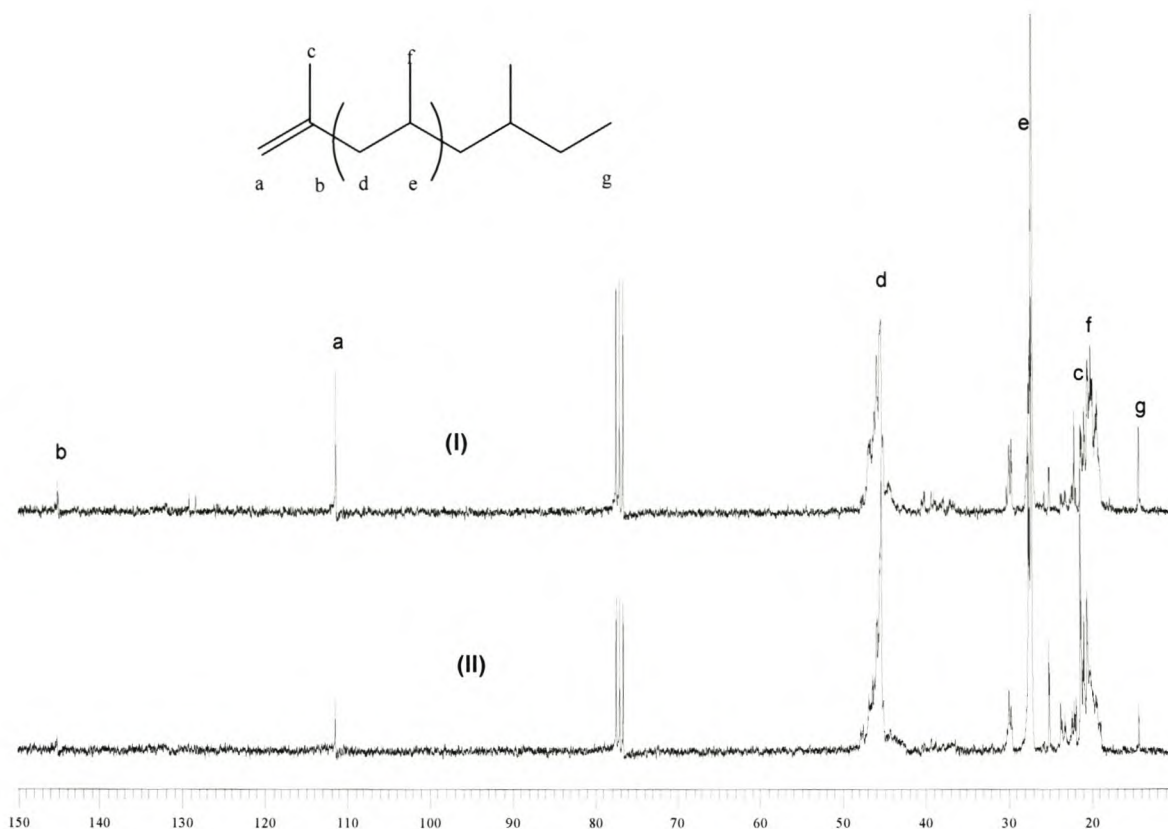


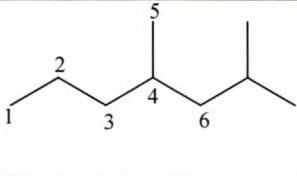
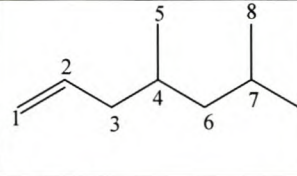
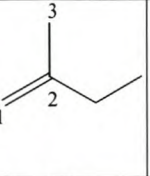
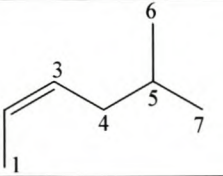
Figure 3: ^{13}C spectrum of propene oligomers: (I) synthesized using catalyst (1) and (II) synthesized using catalyst (2).

The oligomer was dissolved in deuterated chloroform and the spectrum was recorded at room temperature. From the above figure the peaks representing the vinylidene end-groups is observed at 110.9 ppm and 142 ppm. These peaks are characteristic of β -H elimination, which results in chain termination. The main chain oligomer backbone peaks can be identified at 45-46 ppm for the methylene carbons, 28-29 ppm for the methine carbons and at 19-21 ppm for the methyl carbons.

4.2 Microstructure of the Oligomers

The microstructure of the formed oligomers can quite clearly be deduced from the NMR spectra. Of particular interest are the stereoerrors evidenced, and the regioerrors and, of course, the endgroups. The following table lists the ^{13}C NMR shifts for the more common endgroups that we deal with here⁴:

Table 2: Common endgroups and ^{13}C NMR shifts for propylene polymers

C No				
1	14.47	115.57	111.38	12.91
2	20.12	137.67	142.87	124.48
3	39.68	41.38	22.60	129.66
4	30.50	30.80		34.37
5	20.81	20.64		31.37
6	45.98	45.33		
7				45.54
8		21.43		

What we would expect are the peaks for the n-propyl endgroups (one end of the chain following the normal insertion of propylene unit into a Zr-H bond). Two of the peaks (20.12 and 20.81) will show up in the region where we would normally see evidence of stereoerrors; something which needs to be borne in mind. Concerning the unsaturated endgroups; we wanted to see if we could find evidence of endgroups other than the expected vinylidene type which would arise from β -hydrogen abstraction. Shown below are three spectra which are typical of those which were obtained for 3 different catalysts.

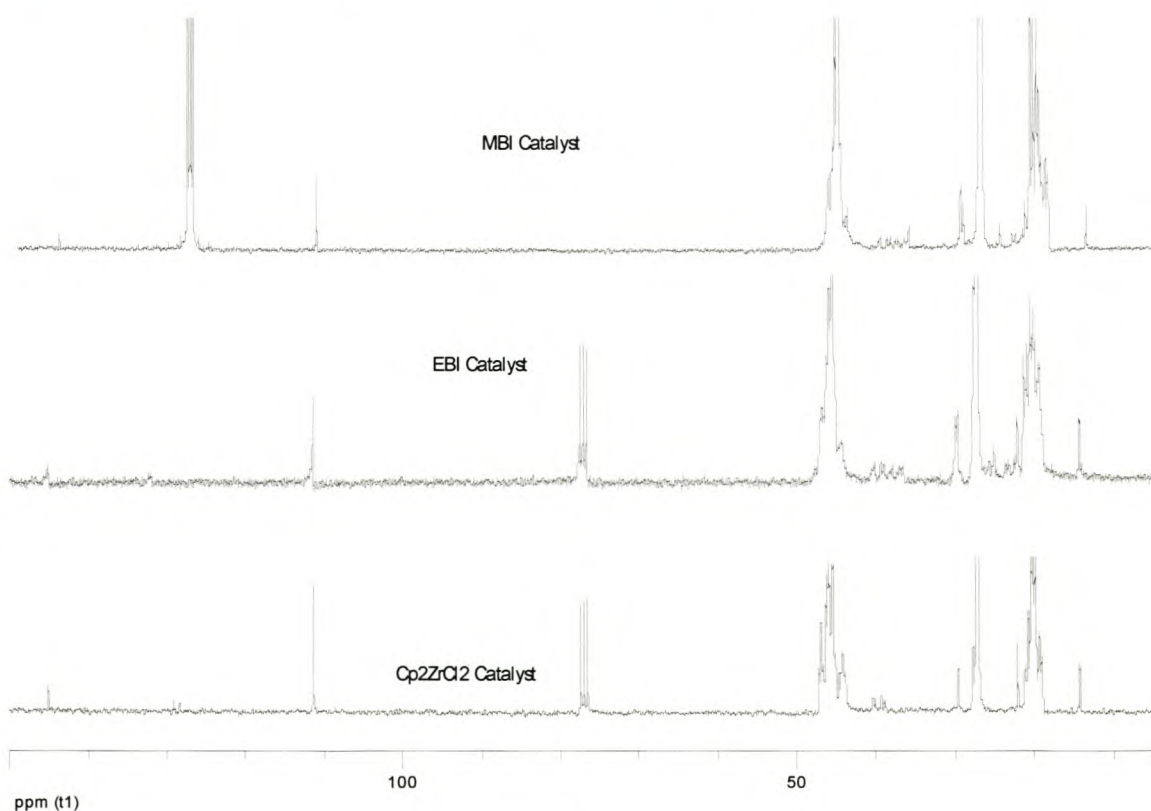


Figure 4: ^{13}C NMR spectra of oligomers prepared with 3 different catalysts.

In Figure 4, products from reactions using the C_2 -symmetric EBI and MBI catalysts as well as the C_{2v} symmetric catalyst; Cp_2ZrCl_2 are shown. What is clear here is that the products that were produced have only vinylidene endgroups (one end of the chain). There appears to be no evidence of vinyl endgroups, based on the evidence of the ^{13}C NMR spectra. In isolated spectra we see evidence of 2-butenyl endgroups, which is normally concomitant with an increase of 2,1-misinsertions.

If we look at the small peak at 22.6 ppm (which is due to the methyl on the vinylidene carbon 3 (Table 2)) and we compare this to the methyl endgroup arising from the n-propyl chain endgroup moiety, we see that in most cases these peaks are equivalent (1:1 ratio upon integration). This indicates that β -hydrogen abstraction is the primary mechanism of chain transfer during these oligomerization reactions. This is illustrated in Figure 5 below:

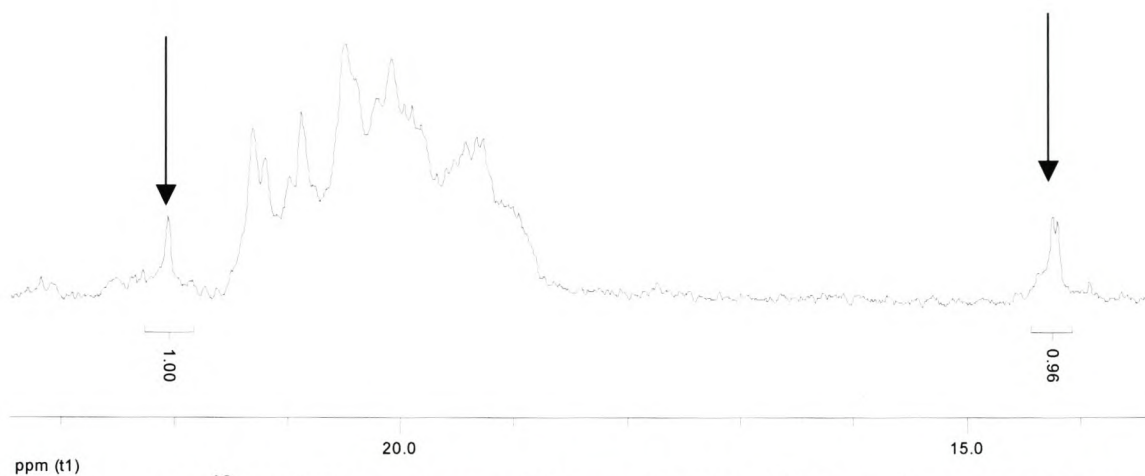
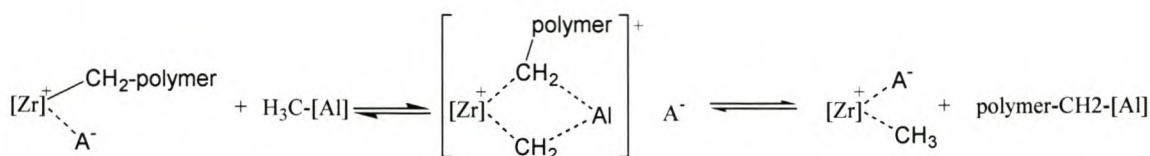


Figure 5: ^{13}C NMR spectrum of the region 14 – 23 ppm for a propylene oligomer prepared with the EBI catalyst. The arrows indicate the “vinylidene” and “n-propyl” methyls associated with the chain ends (refer to Table 5).

The commercial MAO being used in the polymerization process usually contains traces of TMA which helps to keep the MAO in solution^{5,6,7}. From end-group analysis, the intensity of the propyl end-groups was quantitative to that of the vinylidene end group, which could mean that the transfer of the polymer chain to the Al center, as shown in the scheme below is minimal or nonexistent⁹. Usually this transfer of the polymer chain is caused by the excess trimethyl aluminium (TMA) which is usually present in commercial MAO solutions.

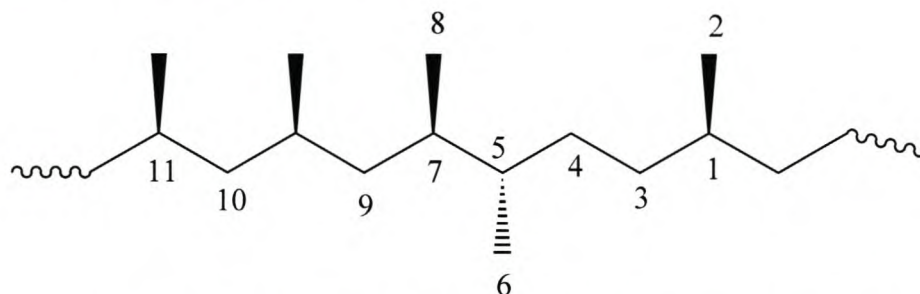


Scheme 2: The schematic representation of polymeryl transfer to the Al center⁸.

4.2.1 Regiochemistry.

If we study the regiochemistry or 2,1-misinsertion reactions that occur with each of the catalysts used we see that the levels of regioerrors differ from catalyst to catalyst.

It is important to note that the regioerrors are evidenced by the peaks appearing in the ¹³C NMR spectrum as assigned by Grassi *et al.* and Mizuno *et al.*^{11,12}. Take the following structure as example, assuming that the 2,1 misinsertion will be *threo* w.r.t the next propene insertion:



Scheme 3: Threo 2,1-insertion during propylene polymerization.

Of particular interest here are the carbons numbered 1, 3, 4, 5, 7 and 9. These main-chain carbons all fall between the peaks assigned to carbons 10 and 11 on the ¹³C NMR spectrum. As such this should allow us to calculate the level of 2,1-misinsertion, if we bear in mind that some carbons that are due to termination following a 2,1-misinsertion (2-butenyl endgroups) also fall in this region (Table 2). A Spectrum reproduced from a review article by Resoni *et al.*⁴ indicates the peaks assigned to the *threo*-2,1-misinsertions.

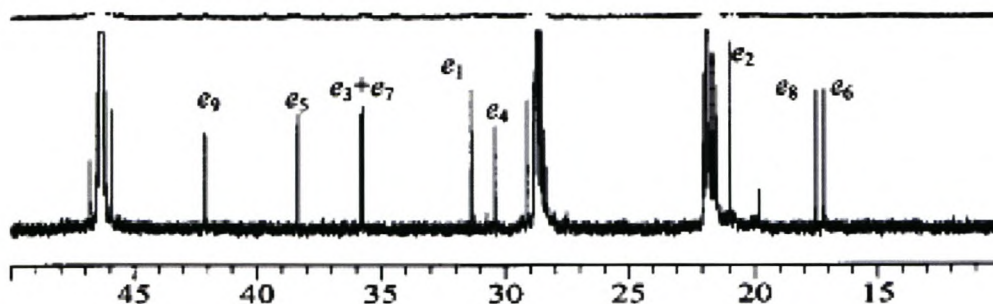


Figure 6: ^{13}C NMR spectrum illustrating the position of peaks arising from *threo*-2,1-misinsertions in polypropylene¹⁰. Refer to Scheme 3 for carbon numbering.

We can see, if we look at the “aliphatic” region of two ^{13}C NMR spectra of products produced by the EBI catalyst and the MBI catalyst that there are distinct differences in the levels of 2,1-misinsertions between the catalysts. (4.9% vs 4%).

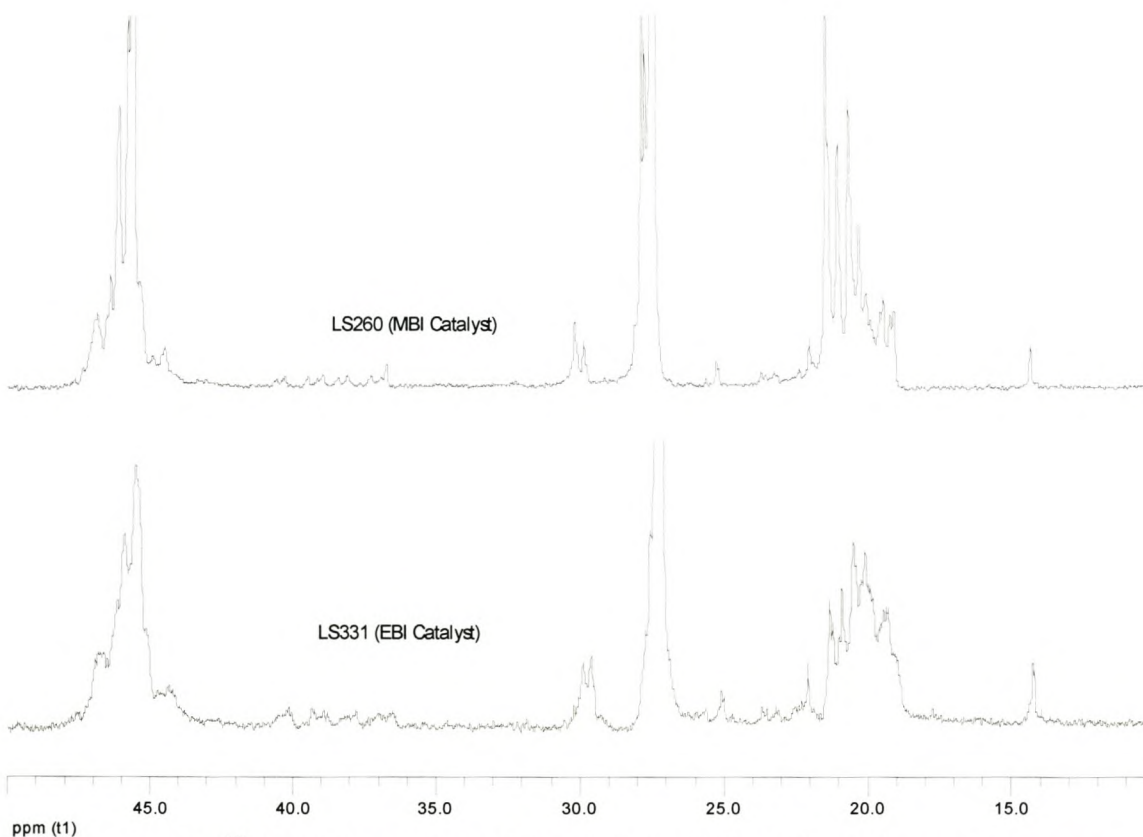


Figure 7: ^{13}C NMR spectra of the “aliphatic” region of two oligomers prepared by EBI catalyst (bottom trace) and MBI catalyst (top trace).

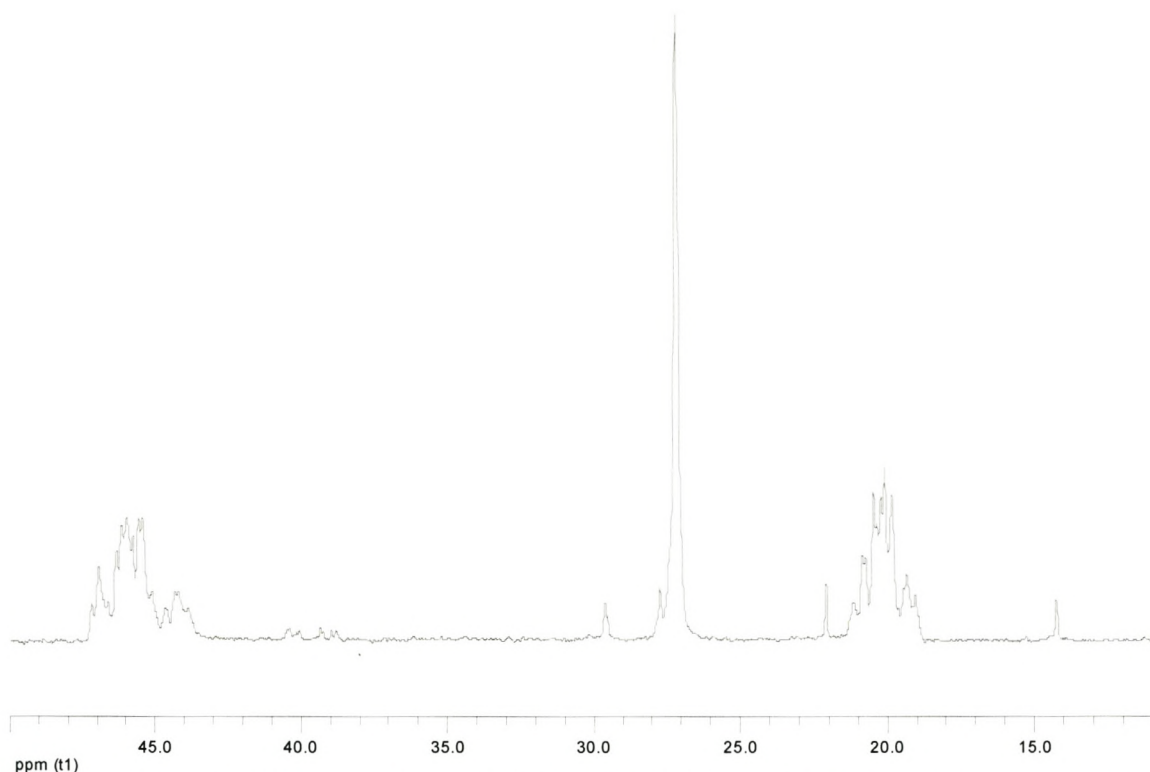


Figure 8: Oligomer prepared with a C_{2v} -symmetric metallocene catalyst.

In Figure 8 we see the ^{13}C NMR spectrum of an oligomer produced by the C_{2v} -symmetric catalyst Cp_2ZrCl_2 . The level of 2,1-misinsertions here are around 3%.

The effect of temperature on the microstructure of the oligomers produced by the EBI catalyst is particularly well illustrated by comparing the ^{13}C NMR spectra of 3 polymers made at 80, 90 and 100°C respectively.

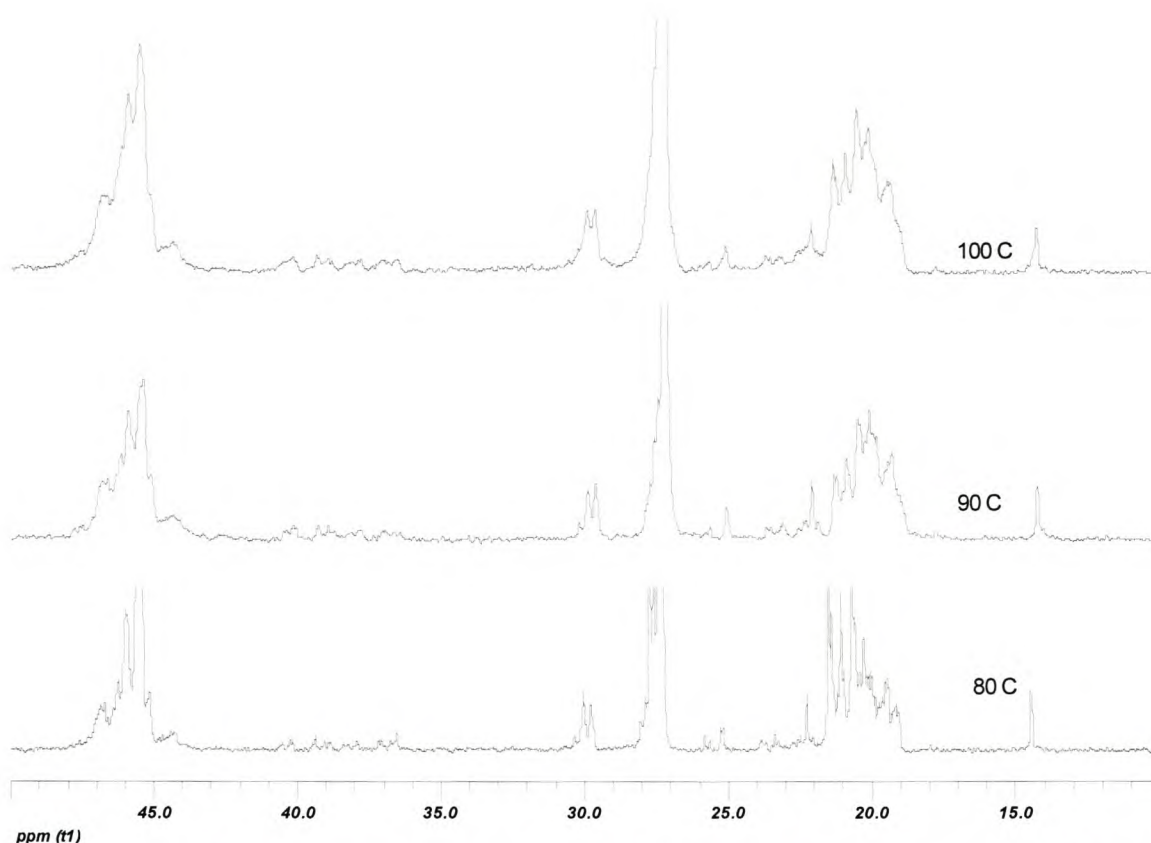


Figure 9: Microstructures of propylene oligomers prepared at different temperatures 80°C, 90°C and 100°C.

The above spectra show clearly that there are differences in the oligomers prepared at the different temperatures. The differences in the levels of 2,1-misinsertions can be quantified after integration of the relevant peaks. For the 80°C sample the level of 2,1-misinsertions is 4.9%, while it is 9.2% and 9.8% for the 90°C and 100°C samples, respectively. Similarly the tacticity seems to be dependent on temperature as well, although the dependency is not as clear-cut. The 80°C sample has a *mmmm*% of 35.3%, while the *mmmm*% for the 90°C and 100°C samples are 23 and 27.4 %, respectively. Careful perusal of the spectra indicates 2 small peaks at around 17.8 ppm, which could be attributed to the carbons numbered 6 and 8 in Scheme 3.

The fact that significant levels of 2,1-insertion are observed, and that very little evidence of β -hydrogen abstraction after 2,1-insertion is visible seems to indicate that even though 2,1-misinsertion reactions occur readily, the preferred mechanism of chain transfer reaction is β -hydrogen abstraction after 1,2-insertion.

4.2.2 The Development of stereoerrors.

One of the most interesting developments of the oligomerization study is the apparent change in the level of stereoerrors with the change in average molecular weight. If we take as example an oligomer produced with the MBI catalyst, with a molecular weight (M_n) of around 1 500 g/mol and a PDI of 2 (which would then give a M_w value of around 3 000 g/mole), we can calculate that we have chain lengths varying between 36 and 72 propylene units.

According to molecular modeling studies by Corradini *et al*⁹, the growing polymer chain is longer than one propylene unit (the first insertion is deemed to be non-stereospecific) in a C_2 -symmetric catalyst then subsequent insertion reactions should be stereospecific. In the Figure below, we show an oligomer as well as isotactic PP prepared by the same catalyst.

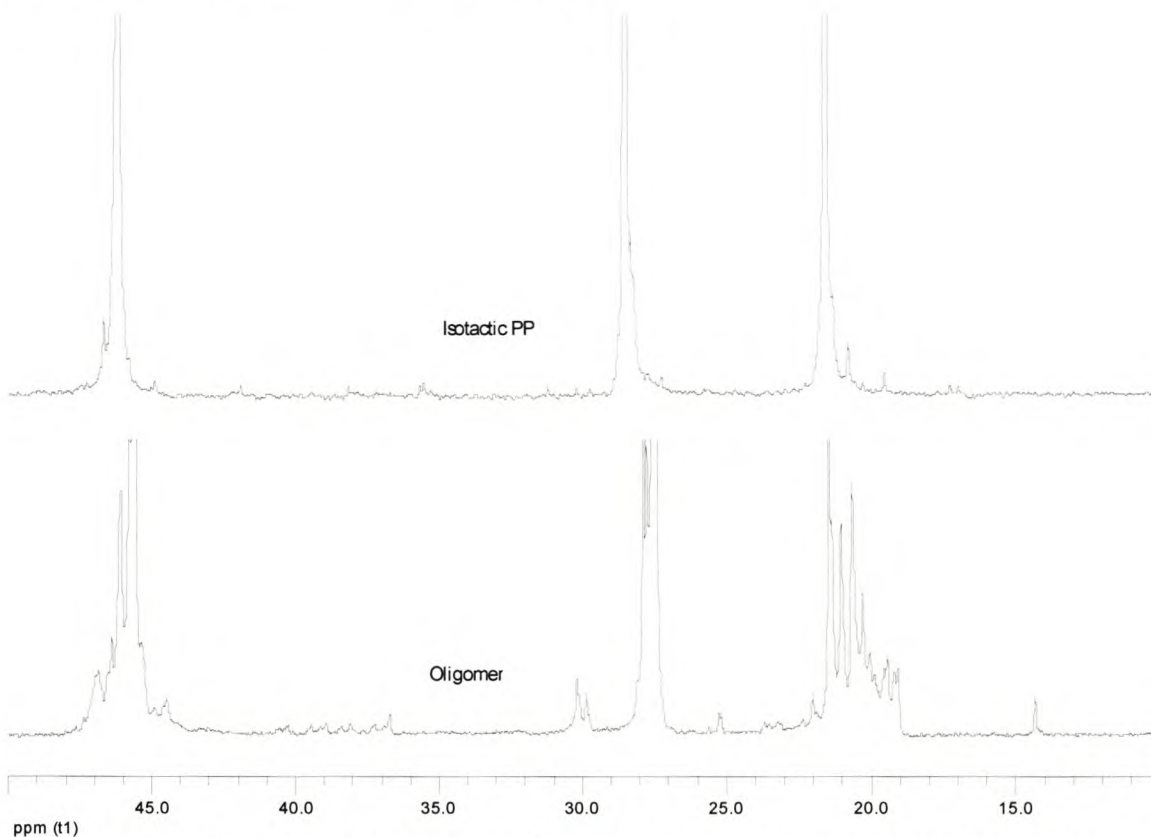


Figure 10: Spectra of polypropylene (top trace) and propylene oligomer (bottom trace) both prepared using C_2 -symmetric catalyst.

As there are some peaks in the region of the methyl carbon which are due to the presence of the n-propyl endgroups (20.81 and 20.64 according to Table 2), it is difficult to accurately calculate the tacticity of the oligomer, but it is obviously less than that of the polymer prepared by the same catalyst. The obvious reason

would be the elevated temperature of the reaction. In order to test this theory we carried out a polymerization reaction at 100°C as well and compared the ^{13}C NMR spectrum. This is shown in the Figure 11.

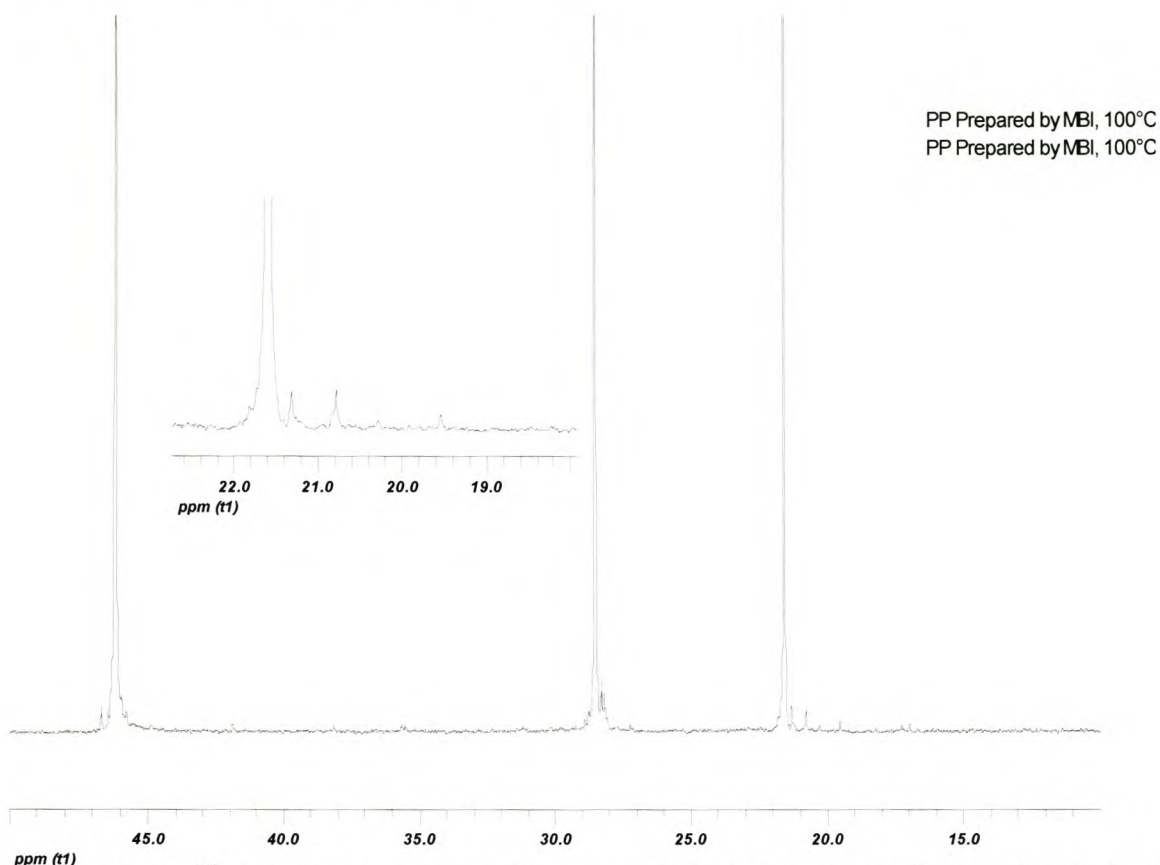


Figure 11: ^{13}C NMR of polypropylene prepared at 100°C using MBI catalyst.

The expansion shows the microstructure.

It is clear that even at 100°C the polymer still has a high tacticity. It seems clear that tacticity development is dependent on molecular weight. It seems that considerably more than just a few propylene units in the growing polymer chain is needed to direct the stereochemistry of propylene coordination and insertion into the catalytic centre.

This is further borne out by the fact that in the case of all the oligomers synthesized by C_2 -symmetric catalysts the stereoerrors that are present are representative of the whole range of possible stereoerrors. The ^{13}C NMR shifts of the whole range of possible stereoerrors as described by Busico *et al*². is shown in Table 3.

Table 3: Chemical shifts of different stereoerrors in polypropylene²

Region	Chemical Shift (ppm)	Stereoerrors
I	22.0 – 21.7	<i>mmmm</i>
II	21.7 – 21.4	<i>mmmr</i>
III	21.4 - 21.2	<i>rmmr</i>
IV	21.2 – 21.0	<i>mmrr</i>
V	21.0 – 20.7	<i>mrrm + rmrr</i>
VI	20.7 – 20.5	<i>rrmm</i>
VII	20.5 – 20.3	<i>rrrr</i>
VIII	20.3 – 20.0	<i>rrrm</i>
IX	20.0 – 19.7	<i>mrrm</i>

C_2 -symmetric catalysts are known to function by enantiomorphic site control, and thus allowing only *mmmr*, *mmrr* and *mrrm* errors. Isolated *r* errors arising from chain end control should not be present. Yet it is clear that all three major regions of stereoerrors (*mm*, *mr* and *rr*) are all present in the microstructure of all of the oligomers that were synthesized². Selected examples are shown in Figure 12.

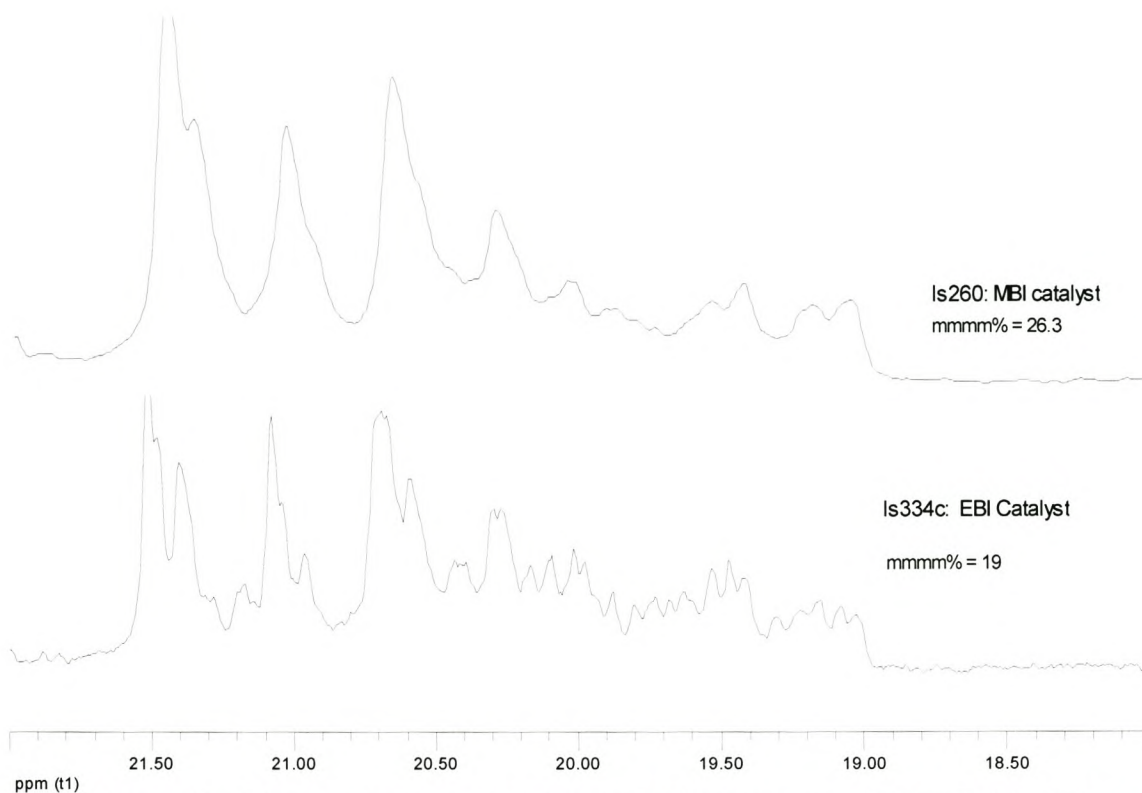


Figure 12: Stereoerrors present in two oligomers: refer to Table 3 for assignments.

It seems therefore, that enantiomorphic site control only really becomes effective when polymer chains become much longer than 20 or 30 units. The specimens of isotactic PP illustrated above have molecular weights in excess of 400 000 g/mol, which relates to 9 500 or more units per chain. In order to illustrate this further, we analyzed a product of an attempted oligomerization reaction which turned out to have a molecular weight of around 90 000 g/mole.

The microstructure of the low molecular weight polymer is shown in Figure 13.

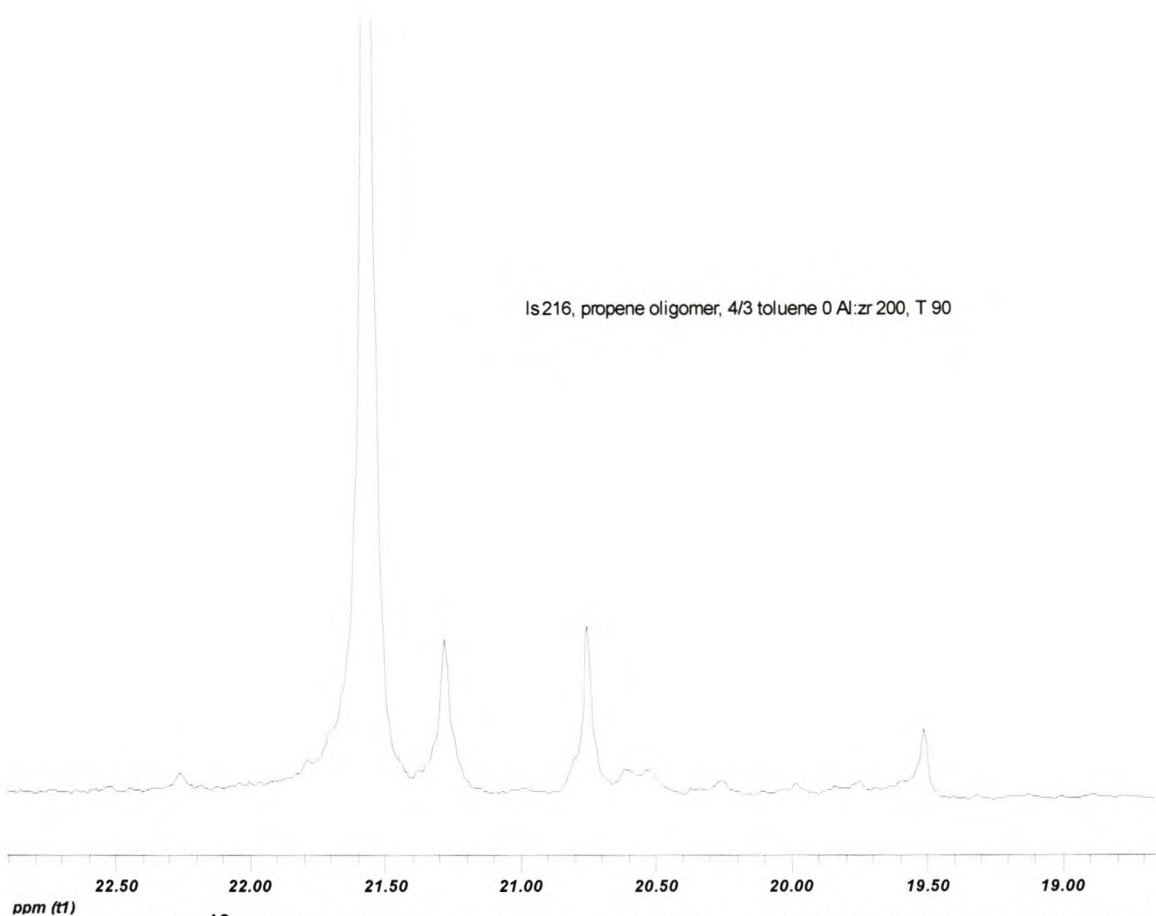


Figure 13: ^{13}C NMR of polypropylene with Mw of 90 000 prepared at 90°C using MBI as catalyst.

In this case, the majority of the stereoerrors that are shown are the “expected” errors (based on the theory of enantiomorphic site control), although there still appears to be some evidence of other errors (in the region between 19.50 and 20.70 ppm). The tacticity of this polymer (based on the *mmmm*%) is 77%.

From the above we can see that the tacticity of the same product prepared at the same temperature with the same catalyst is strongly dependant on the molecular weight of the product, increasing from around 30 – 35% for 60 – 80 repeat units, to 77% for 2 250 repeat units, to 92% for around 9 500 repeat units. A simplistic deduction from this would seem to be that a large proportion of stereoerrors in polypropylenes prepared by C_2 -symmetric catalysts are situated close to one of the chain ends.

4.2.3 Tacticity

Some results of tacticity measurements are shown in Table 4.

Table 4: Tacticity as measured by mmmm% of oligomers prepared with three different catalysts.

Run ID	Catalyst	<i>mmmm</i> %
LS 229	MBI	43
LS 230	MBI	58*
LS 231	MBI	42
LS 232	MBI	37***
LS 256	MBI	23
LS 257	MBI	38**
LS 258	MBI	23
LS 266	MBI	27
LS 268	MBI	39
LS 277	MBI	40
LS 292	MBI	26
LS 293	MBI	23
LS 325	EBI	12
LS 326	EBI	14
LS 327	EBI	15
LS 331	EBI	11
LS 334	EBI	19
LS 337	EBI	10
LS 338	EBI	15
LS 339	EBI	21
LS 356	MBI	27
<i>LS 362</i>	<i>Cp</i>	6
<i>LS 363</i>	<i>Cp</i>	5
LS 364	MBI	26
LS 368	MBI	22
LS 386	EBI	7
LS 403	EBI	17
LS 406	EBI	7

*Hexane extract of LS 229

**Pentane extract of LS 229

***Residue after ether extract of LS 229.

The oligomers that we had discussed until recently were all materials that had identifiable unsaturated endgroups, however if we look at all the oligomers made by the three catalysts (Table 4) we clearly see that the tacticity of the materials, as measured by ^{13}C NMR, is clearly influenced by the catalyst type. The C_{2v} symmetric catalyst produces, as expected, essentially amorphous oligo(propylene). The tacticity of the oligomers produced by the MBI catalyst

varies between $mmmm\% = 22$ and $mmmm\% = 58$. Typically the EBI catalyst produces materials that has an isotacticity varying between $mmmm\% = 7$ to $mmmm\% = 21$. This was, once again, not unexpected. Some thought was given to the possibility of getting crystallizable oligomers, which would be extremely useful materials for further reactions (see Chapter 6). From the Table above it is clear that the amount of tacticity attained with these oligomers precludes any crystallization of these materials. The reasons behind this were discussed in Section 4.2.2.

4.3 Attempted oligomerization reactions in bulk

Propylene was also reacted in bulk, using $(\text{CH}_3)_2\text{Si}[2\text{-CH}_3\text{-4,5-benzoInd}]_2\text{ZrCl}_2$ at temperatures ranging from $90^\circ - 100^\circ\text{C}$. In this situation the only solvent which as present was the toluene which is present in MAO. The polymers produced had higher crystallinity in comparison to other propene oligomers synthesized at high temperatures and low Al:Zr ratio³.

The molecular weights of the obtained materials which were in the range 80 000 - 90 000, were analyzed by high temperature GPC and these were lower than the usual high molecular weights of polypropylenes produced by this catalyst. This can be the result of low Al:Zr ratio, and higher polymerization temperatures. Of interest is the attainment of polymer rather than oligomer. A ^{13}C NMR spectrum of one of these materials was shown in Figure 13.

The materials obtained in the absence of solvent showed broad melting ranges, as evidenced by the DSC thermogram in Figure 14. These broad melting temperatures may be due to the low molecular weight of the materials, although the samples were crystalline. However these low melting temperatures are typical for all the materials synthesized at low Al:Zr ratios in the absence of solvent. The solution crystallization (Crystaf) peaks of these materials are represented in Figure 15.

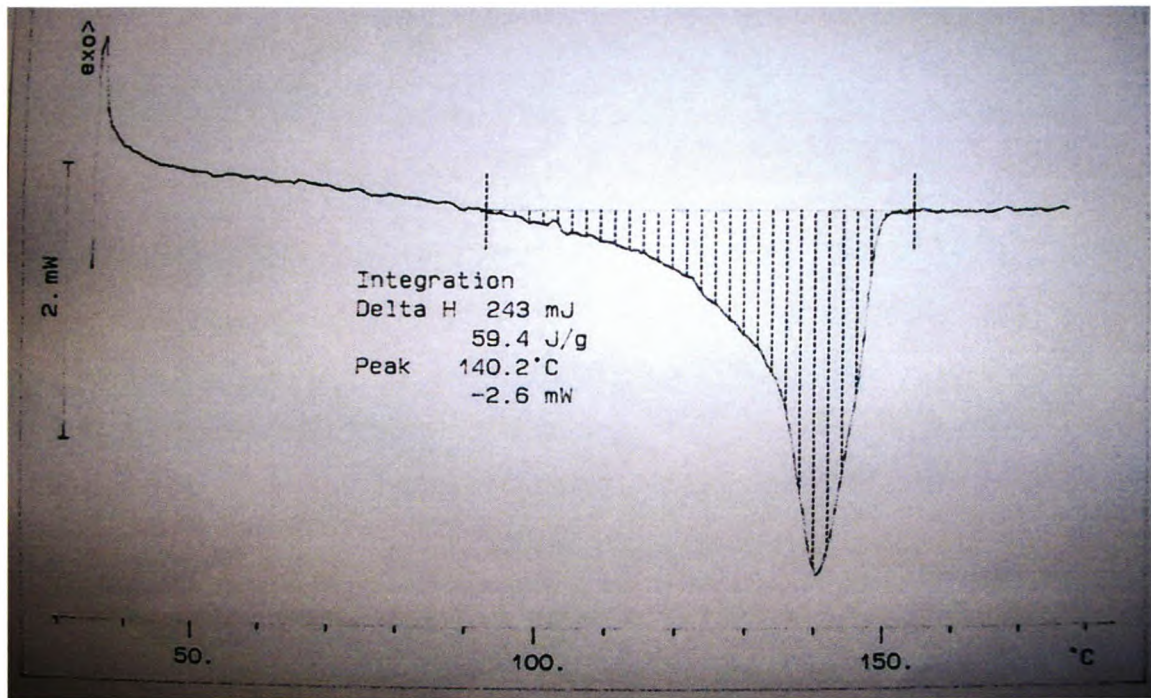


Figure 14: DSC thermogram of the oligomer.

The melting temperatures of the oligomers ranged in values from 138 – 144°C.

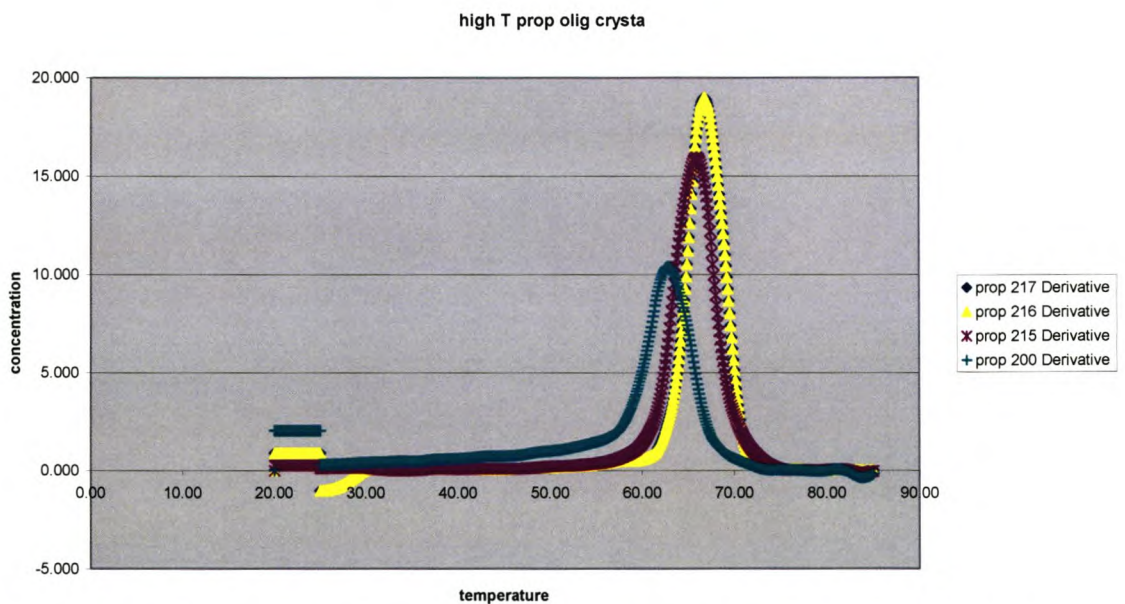


Figure 15: Crystallization curves of the materials synthesized in bulk.

These materials showed broad and low crystallization temperatures, 60° - 70°C which is unusual for isotactic PP. The concentration of the soluble noncrystalline

material was very low indicating the high crystallinity of the oligomers synthesized at these temperatures.

4.4 Conclusions

Successful oligomerization reactions were carried out at a range of temperatures. The use of the catalyst $\text{Et}(\text{Ind})_2\text{ZrCl}_2$ in conjunction with MAO lead to lower molecular weight oligomers than in the case of the the $\text{Me}_2\text{Si}(\text{2-Me-4,5-Benzolnd})_2\text{ZrCl}_2$ catalyst under similar conditions. Molecular weight could be controlled to be anywhere in the region of 500 to 1 500 g/mole. A high proportion of the endgroups were of the vinylidene type, and little evidence of transfer reactions to the cocatalyst was found.

Evidence of 2,1-misinsertions were found for all 3 catalysts that were tried, but very little evidence could be seen, in the ^{13}C NMR spectra, of 2-butenyl endgroups, which would result from β -hydride transfer after a 2,1-misinsertion. This indicates that the preferred method of termination was β -hydrogen abstraction after a normal 1,2-insertion.

Both catalysts yielded essentially oligomers with low isotacticity, although a slightly higher *mmmm*% (25 – 50%) was found for the oligomers prepared with the $\text{Me}_2\text{Si}(\text{2-Me-4,5-Benzolnd})_2\text{ZrCl}_2$ catalyst, than for the EBI catalyst (12 – 25%). Solvent-free oligomerization was attempted with the $\text{Me}_2\text{Si}(\text{2-Me,4,5-MeBenzolnd})_2\text{ZrCl}_2$ catalyst, but this yielded essentially isotactic polypropylene.

Most significantly, the stereoerrors present in the oligomers were an indication that the method of stereoregulation by the C_2 -symmetric metallocene catalysts is dependent on molecular weight. For the low molecular weight oligomers, the whole range of stereoerrors were found, while the same catalysts, when used to polymerize propylene, yield materials with (a) higher tacticity and (b) only the stereoerrors associated with enantiomorphic site control. Simplistic interpretation of this phenomenon indicates that most stereoerrors in polypropylenes synthesized by C_2 -symmetric catalysts are situated near the one chain end, and that stereoerrors arising from enantiomorphic site control only arises with the advent of significant molecular weight.

4.5 References

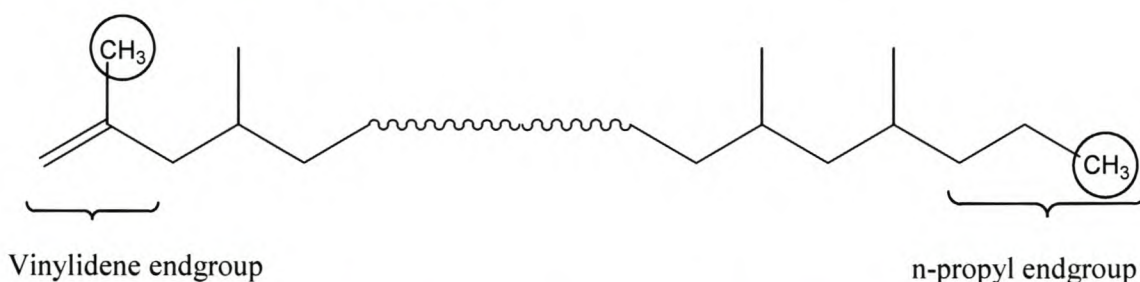
1. M. D. Bruce, R. M. Waymouth; *Macromolecules*, **31**, **1998**, 2707.
2. V. Busico, R. Cipullo; *Prog. Polym. Sci.*, **26**, **2001**, 443.
3. W. Weng, A. Dekmezian, E. J. Markel, A. Gadkari, D. L. Peters; US Patent, 6 117 962, September 2000.
4. P. F. Fu, S. Glover, R. K. King, C. Lee, M. R. Pretzer, M. K. Tomalia; *Polym. Preprints*, **41**, **2000**, 1903.
5. M. Michelotti, A. Atomare, F. Ciardellim, P. Ferrarini; *Polymer*, **37**, **1996**, 5011.
6. T. Mise, A. Kageyama, S. Miya, H. Yamakazi; *Chem. Lett.*, **1991**, 1525.
7. P. A. Charpentier, S. Zhu, A. E. Hamielec, M. A. Brok; *Polymer*, **39**, 1998, 6501.
8. L. Resconi, S. Bossi, L. Abis; *Macromolecules*, **23**, **1990**, 4489.
9. S. Lieber and H. H. Brintzinger; *Macromolecules*, **33**, **2000**, 9192.
10. L. Resconi, L. Cavallo, A. Fait, F. Piomentesi; *Chem. Rev.*, **100**, **2000**, 1253.
11. A. Grassi, A. Zambelli, L. Resconi, E. Albizzati, R. Mazzocchi; *Macromolecule*, **31**, **1998**, 2707.
12. A. Mizuno, T. Tsutsui, N. Kashiwa; *Polymer*, **33**, **1992**, 254.

Chapter 5

Reactions of the propene oligomers.

5.1 Copolymerization

From the results that were obtained during the oligomerization of propylene (see Chapter 4), it seemed that **virtually** no endgroups other than vinylidene groups were found. In some of the oligomers there seemed to be evidence of 2-butenyl endgroups (based on ^{13}C NMR). Careful study of the ^1H NMR spectra of some of the oligomers produced seemed to indicate a very low concentration of possible vinyl endgroups, which are evidenced by a “bump” at around 5 ppm on the ^1H NMR spectra. In particular, those materials which did not exhibit a clear-cut 1:1 ratio of the “vinylidene” methyl group to the n-propyl methyl group (see Scheme 1) as evidenced by the ^{13}C NMR spectra (peaks at 22.6 ppm and 14.3 ppm) may possibly have some vinyl endgroups.



Scheme 1: A schematic representation of a propylene oligomer with vinylidene and n-propyl endgroups. The methyls discussed in the text are circled.

An example is shown in Figure 1 below. Also visible in some of the ^1H NMR spectra is the presence of 2-butenyl endgroups at around 5.5 ppm.

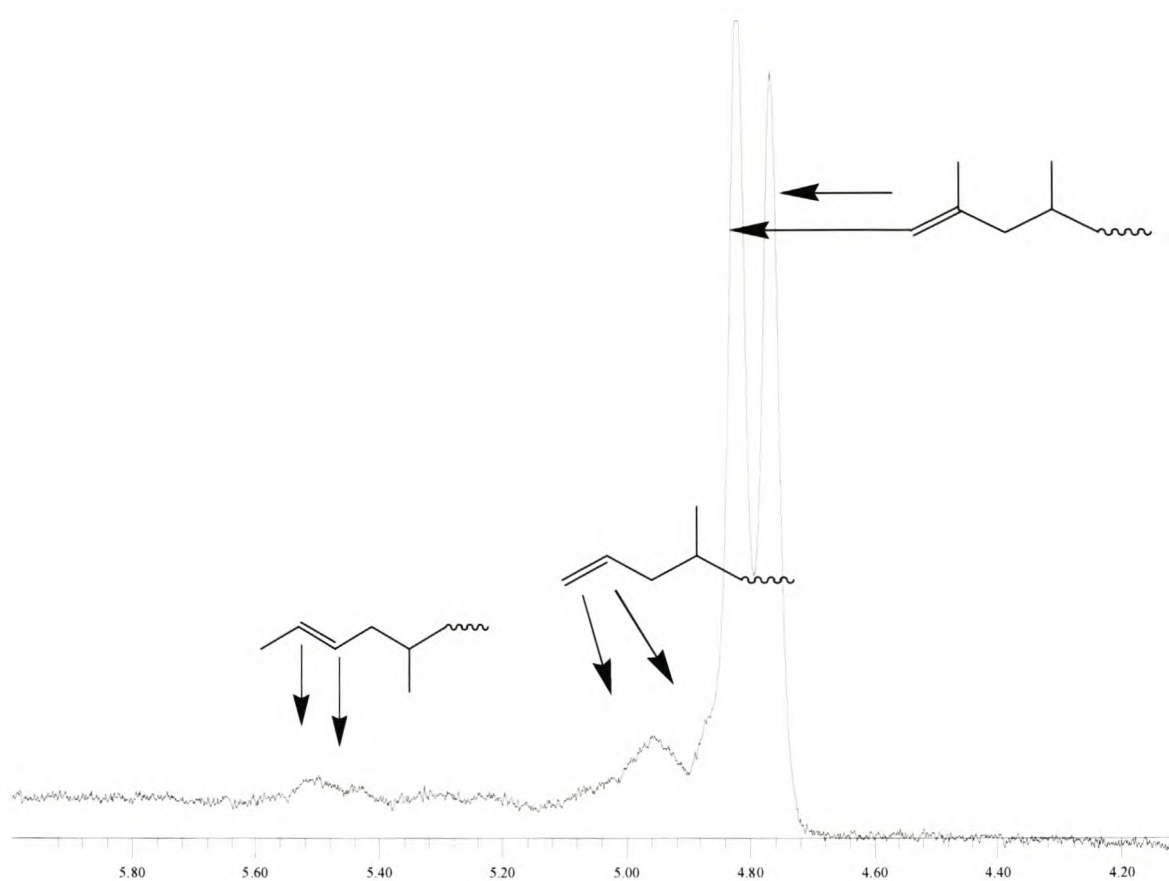


Figure 1. ^1H NMR of an oligomer prepared with the MBI catalyst; vinylidene, vinyl and 2-butenyl endgroups are indicated.

In the case of the above oligomer, there originally appeared to be a discrepancy between the “vinylidene” methylys and the “n-propyl” methylys (0.6:1), which indicated that some of the chain transfer reactions were not only due to β -hydrogen transfer after 1,2-insertion of propylene (see Chapter 4).

The evidence of small amounts of vinyl endgroups could be found in a number of oligomers, but were completely absent in others; there appears to be little or no trend in the appearance of these endgroups; it seems to be independent of catalyst or reaction temperature.

It would be extremely difficult to separate the vinyl-terminated materials from the rest of the oligomers, so it was decided to attempt some polymerization reactions with the oligomers, both by themselves and with ethylene as comonomer. The idea behind this strategy was that it would be possible for those vinyl-terminated oligomers (if they were present) to either (a) homopolymerize or (b) copolymerize with ethylene, leaving the rest of the material unreacted.

Copolymerization reactions were attempted using selected propylene oligomers (described in the previous chapter) and using the metallocene catalysts *i*-propylidene(cyclopentadienyl)(9-fluorenyl) zirconium dichloride (**1**) and (tetramethylcyclopentadienyl)(dimethyl silyl *t*-butylamido) titanium dimethyl (**2**) activated with methyl alumoxane. These catalysts were selected as they are known to be able to incorporate large comonomers more readily than the C_2 -symmetric *ansa*-metallocenes. The copolymerization reactions were carried out while varying conditions such as amount and molecular weight of oligomers, polymerization temperatures and time, as well as the partial pressure of ethylene.

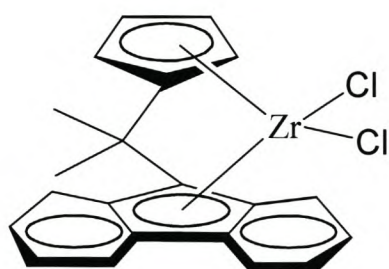
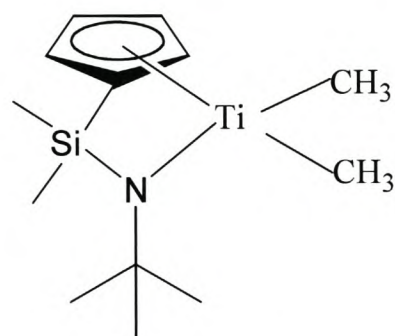
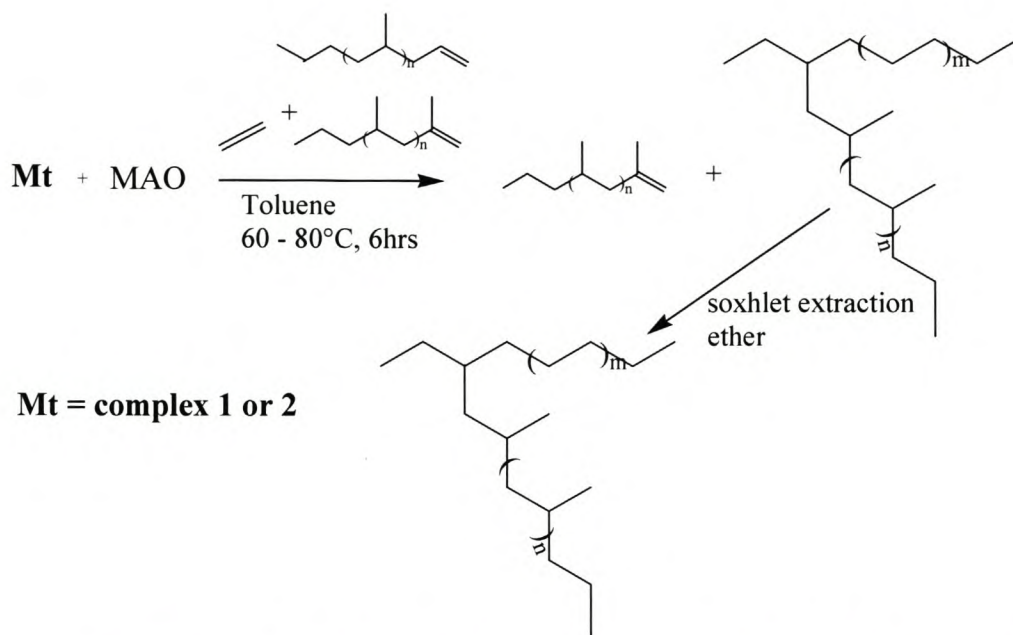
**1****2**

Figure 2: Catalysts used for the copolymerization reactions.



Scheme 2: Copolymerization of ethylene with propylene oligomers.

Table 1: Attempted copolymerization of propylene oligomers with ethylene using catalyst 1.

Run	Oligomer Mw	Amount oligomer (g)	Ethylene (Mpa)	Tp (°C)	Tm (°C)	t (h)	Mw	Mw/Mn	Yield (g)
173	2 560	5	2.5	70	134.4	14			8
272	4 400	5	3	80/60	135.8	12	487 349	3.08	6.3
274	4 500	5	3	70/80	135.2	12	433 678		6.9
281	4 500	7.5	3	70	133.7	12	468 949	3.223	7.8
282	3 400	3	3	70	131.8	6	455 673	13.78	5.6
289	3 400	5	3	80	135.6	6	36 911	5.669	3.8
295	3 400	7.5	3	60	132.2	6	310 726	11.37	4.5
296	2 800	7.5	3	70	134.6	6	396 658	8.57	5.0
297	2 800	7.55	3	80	133.2	6	293 303	9.07	5.6
4	0	0	3	70	134.2	3	800 000	5.503	

Polymerization was done using $[\text{Zr}] = 4.4 \mu\text{mol}$ and $\text{Al}:\text{Zr} = 3\ 000:1$

Table 2: Attempted copolymerization of oligomers with ethylene using catalyst 2.

Run	Oligomer mw	Amount olig (g)	Ethylene (Mpa)	Tp (°C)	Tm (°C)	Mw/Mn	Mw	Yield (g)
302a	3 109	5	1.5	R/t	130.1	5.138	209 268	1.3
306	3 420	3	3	60	130.6	3.59	118 442	3.4
307	2 700	5	3	25	131.6	5.3	573 304	1.4
308	3 200	5	2	R/ t	130.8	3.96		2.3
346	325	5	2	60	131.5	2.832	426 132	3.5
347	1 615	5	2	60	125.7	2.74	336 240	1.8
348	1 615	3	3	60	132.6	2.154	333 449	4.9
357	1 461	5	2.5	70	133.1	2.401	440 585	3.2
358	1 461	5	2	70	130.8	3.338	641 750	2.4
359*	1 461	4.5	2	70	129.9	3.414	643 244	1.9
360	1033	10	0	60	80.3	3.952	10 000	0.8
3	0	0	2.5	R/t	131.6	3.655	241 951	4.0

Polymerization was done using [Ti] = 5.6 μmol , and Al:Zr ratio of 3 000:1, and reaction time was 6 hrs. * After charging the reactor with oligomer, catalyst and cocatalyst solutions, the polymerization was delayed for 1 hour before charging with ethylene monomer.

5.2 Products and yields

From the reactions done with catalyst **1**, it would seem, on the evidence of the melting temperatures, that very little co-oligomer was introduced during the copolymerization reactions. The polyethylene produced (run 4), had a crystalline melting temperature of 134.2°C, and there was practically no difference in any of the other materials produced. The only visible difference was in the molecular weights (as measured by GPC), with the polymer produced in the absence of oligomer having a molecular weight of 800 000 $\text{g}\cdot\text{mole}^{-1}$. The other materials had noticeable lower values of M_w and generally higher values of polydispersity. This prompted the closer inspection of the materials. It needs to be emphasized that all products were extracted initially with diethyl ether, as the original oligomers were found to be soluble in diethyl ether. It was thought that these extractions would get rid of all unreacted oligomeric materials.

The ^{13}C NMR spectra of some of the materials are shown below.

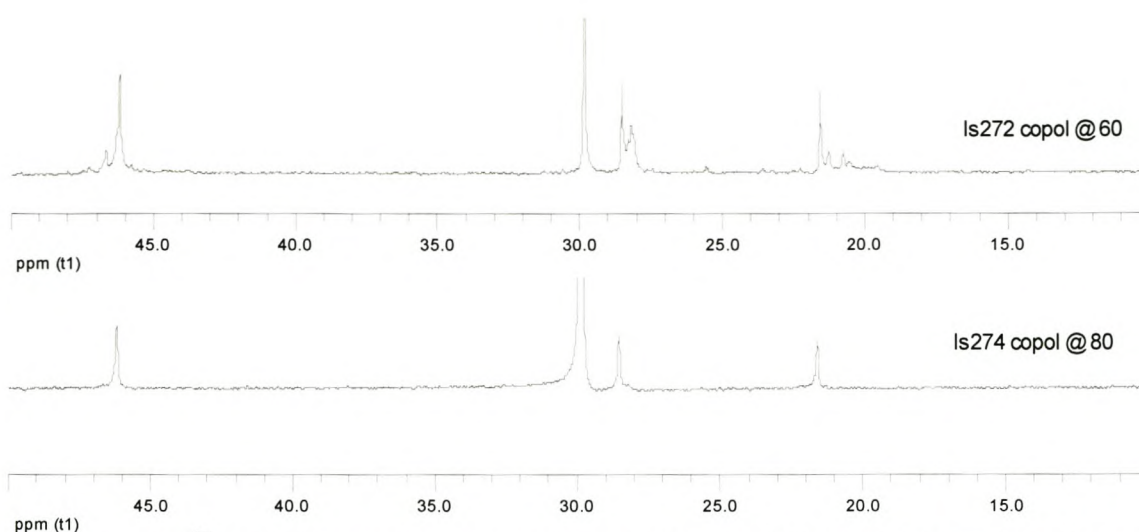


Figure 3: ^{13}C NMR spectra of reaction products 272 and 274 (Table 1); no extraction.

Figure 3 shows the products for runs 272 and 274, in this case the oligomer used was the same, only the reaction temperature varied from 60 to 80°C. From the ^{13}C NMR spectra it would appear as though some of the oligomer has been incorporated into the copolymer, yet the thermal analyses seem to suggest otherwise.

Similarly, for runs 282 and 295:

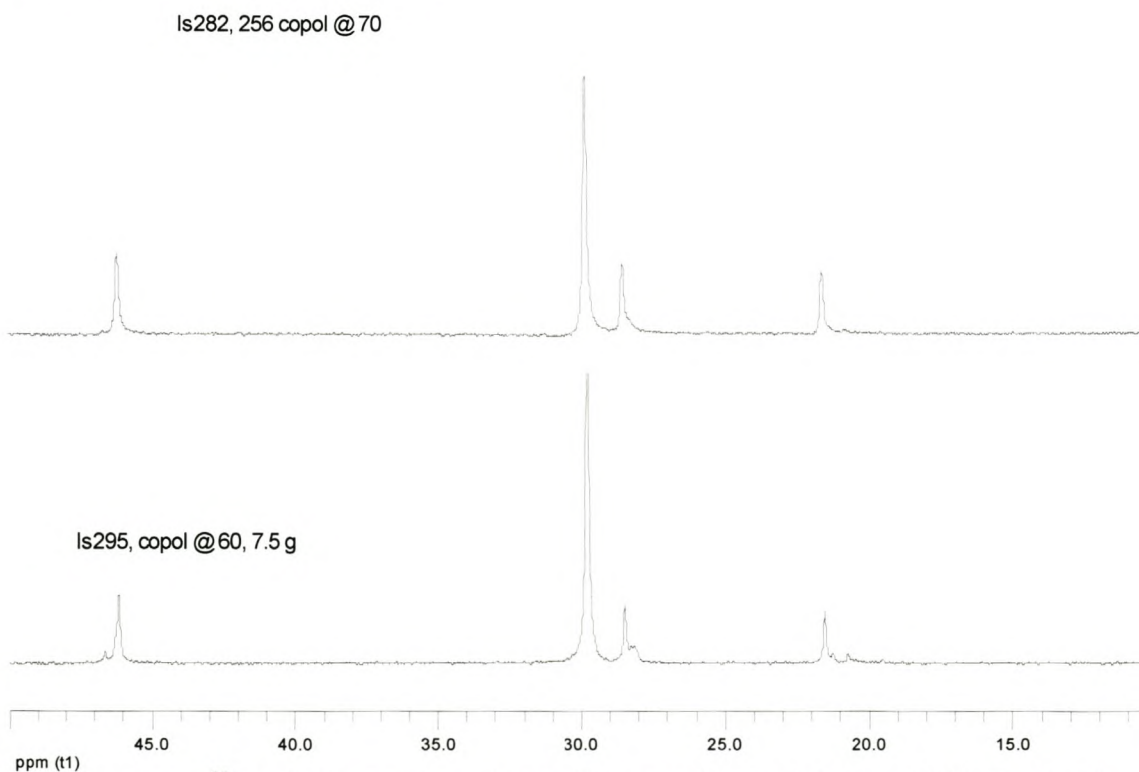


Figure 4: ^{13}C NMR spectra of reaction products 282 and 295 (Table 1).

In this case, the spectrum suggests some oligomer present, yet the peak melting temperatures are the same as for the PE homopolymer. Another clue here was the extremely broad polydispersity values, around 14 to 11. This would indicate Mn values of around 30 000 for both the materials. Closer investigation of the GPC traces seems to suggest a bimodal molecular weight distribution. This prompted us to attempt an extraction by hexane, to see if there was, in fact, two polymeric species present.

Taking another attempted copolymer as example, below are shown the polymer (run 174) before and after hexane extraction:

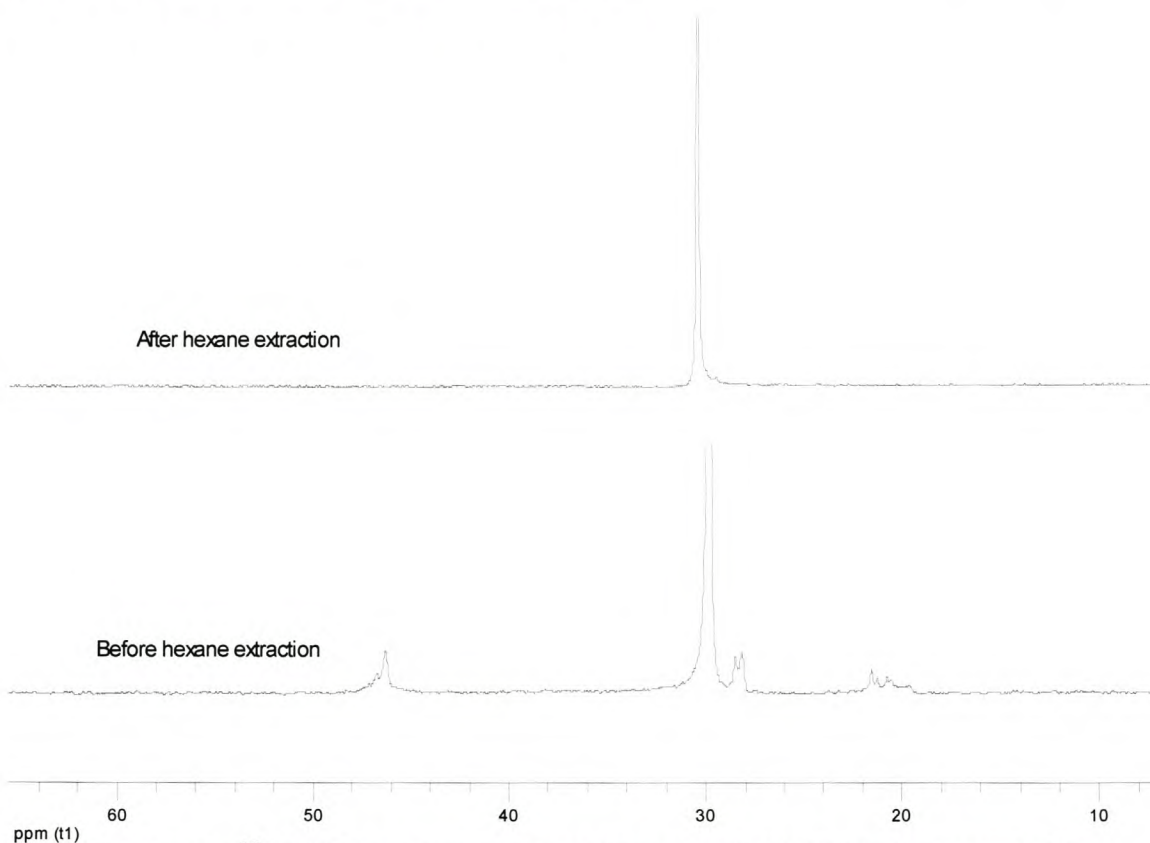


Figure 5: ^{13}C NMR spectra of reaction product 174 before and after extraction with hexane.

In this ^{13}C NMR spectrum it can clearly be seen that after extraction there appears to be only polyethylene left. The extractant, however, yielded some interesting results:

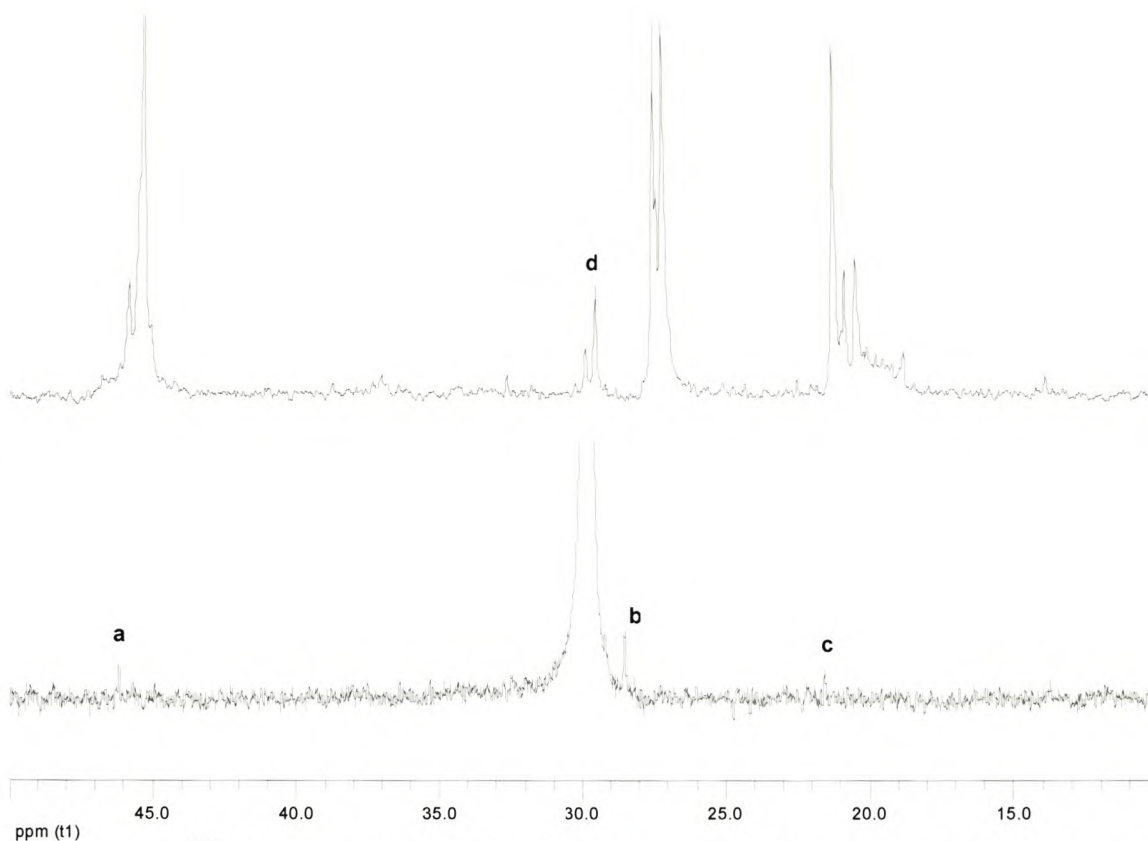


Figure 6: ^{13}C NMR spectra of hexane extract (top) and remaining material (bottom) of product 174.

From this spectrum, two things are clear; the extracted material still has some evidence of ethylene incorporation (peak **d**), and if we expand the spectrum of the extracted polymer greatly, we see a that there still appears to be some oligomer present in the spectrum (peaks **a**, **b** and **c**).

Similarly, if we examine the results for the CGC catalyst, we see that, apart from some larger values for the polydispersity, there seems little evidence of copolymerization reactions having taken place. After extraction with ether and hexane, some spectra were recorded of the resultant material. For run 302, the spectrum is shown below:

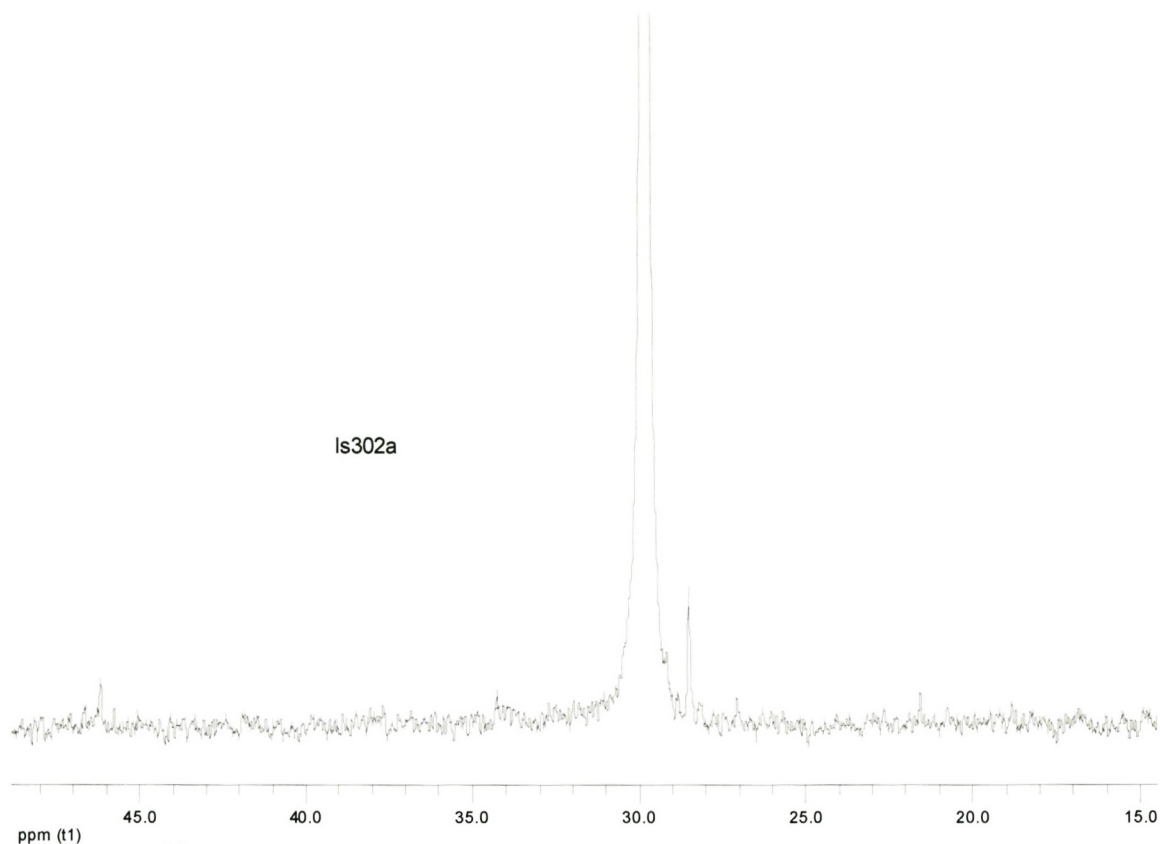


Figure 7: ^{13}C NMR spectrum of reaction product 302 (Table 2).

We can see evidence of a very small amount of oligomer present. This is obviously not enough to affect the bulk properties of the material very much. The same applies to run 306:

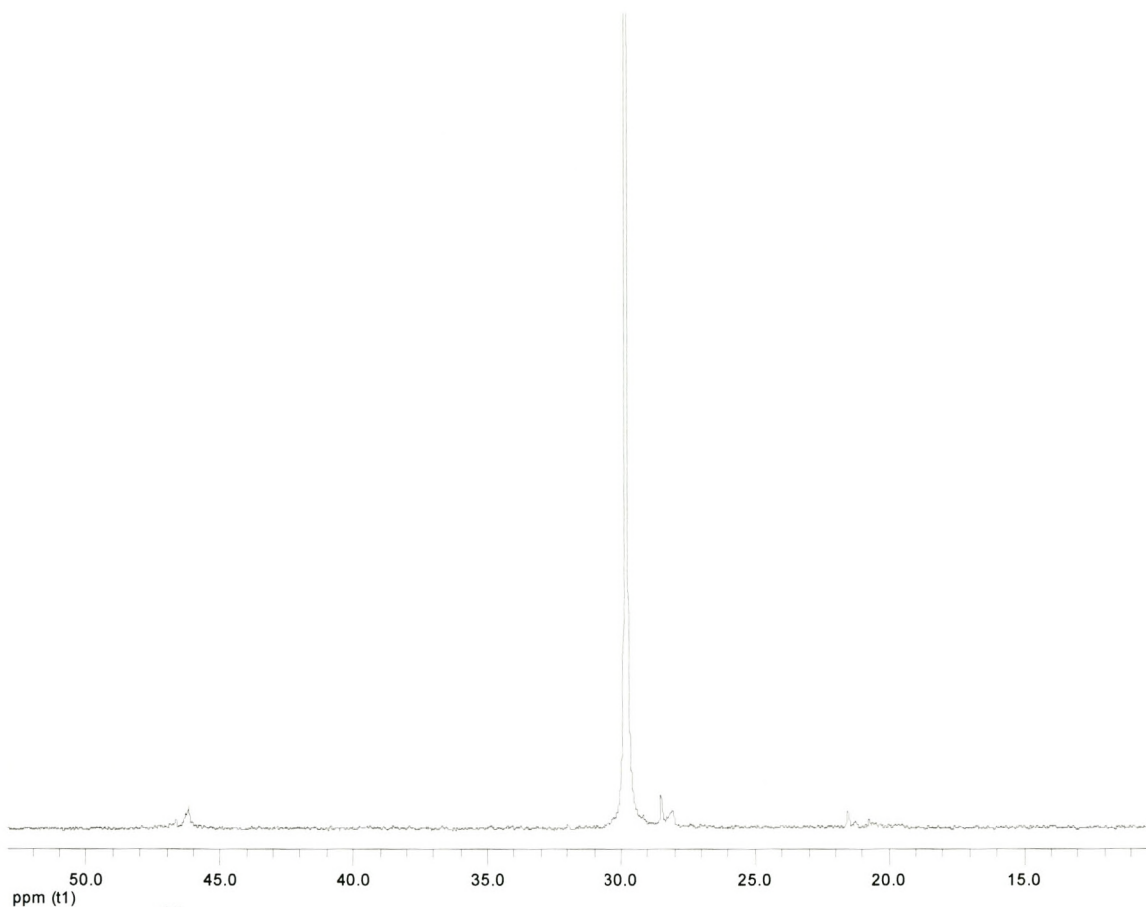


Figure 8: ^{13}C NMR spectrum of reaction product 306 (Table 2)

Minimal inclusion of oligomer is evident. To further illustrate this point, the ^{13}C NMR spectra of the product of run 307 both before and after hexane extraction is shown:

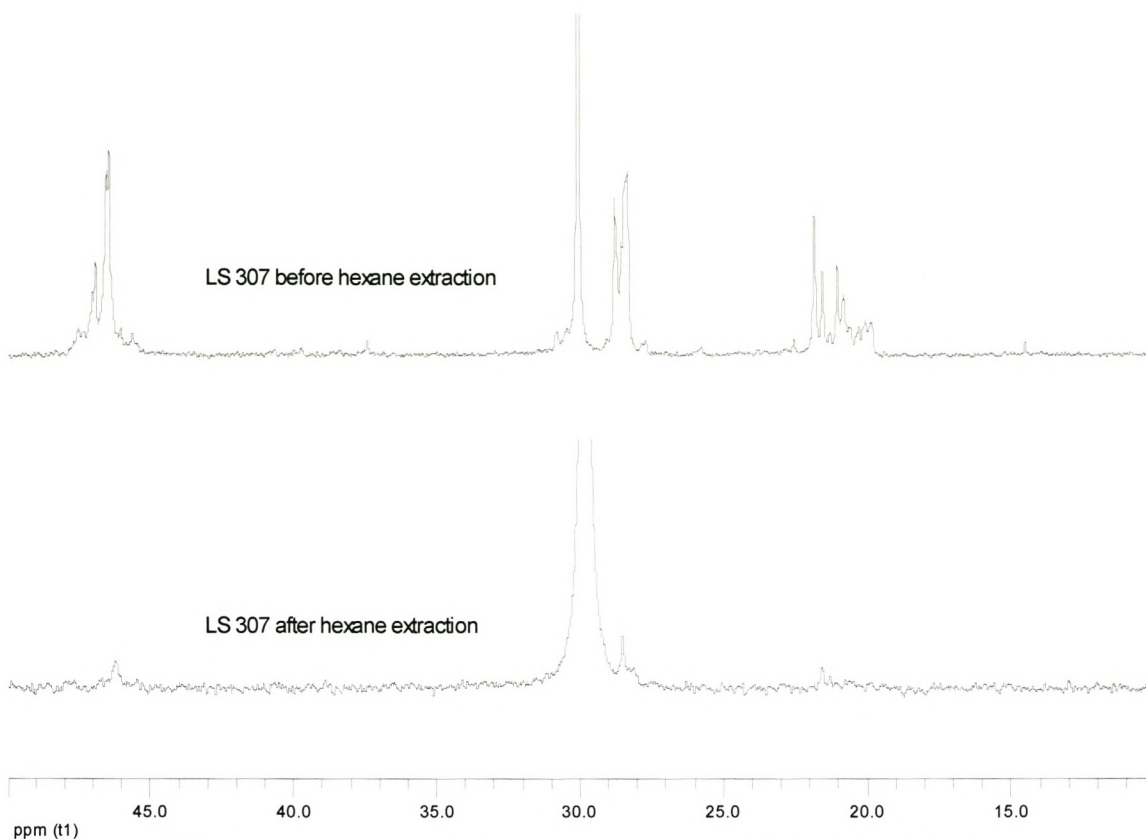


Figure 9: ^{13}C NMR spectra of reaction product 307 (Table 2) before and after hexane extraction.

There seems to be an indication that a broad molecular weight distribution is an indication of some oligomer copolymerization. If we examine the polymer produced in run 347:

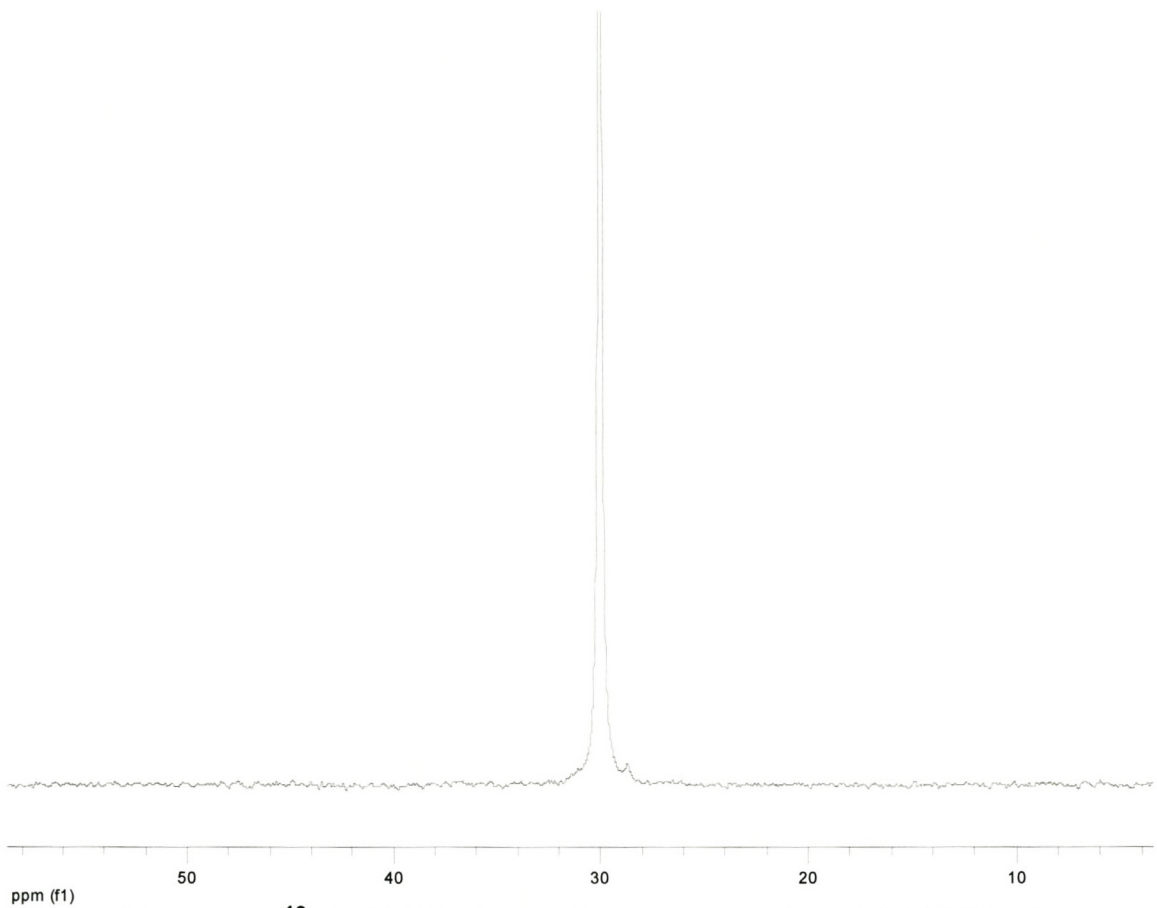


Figure 10: ^{13}C NMR spectrum of reaction product 347 (Table 2).

In this case the polymer produced is essentially polyethylene. The same applies to runs 348 and 357. For runs 358 and 359 (see Table 2) the PDI values are above 3, and if we study the spectra of the extracted materials we see some evidence of oligomer inclusion:

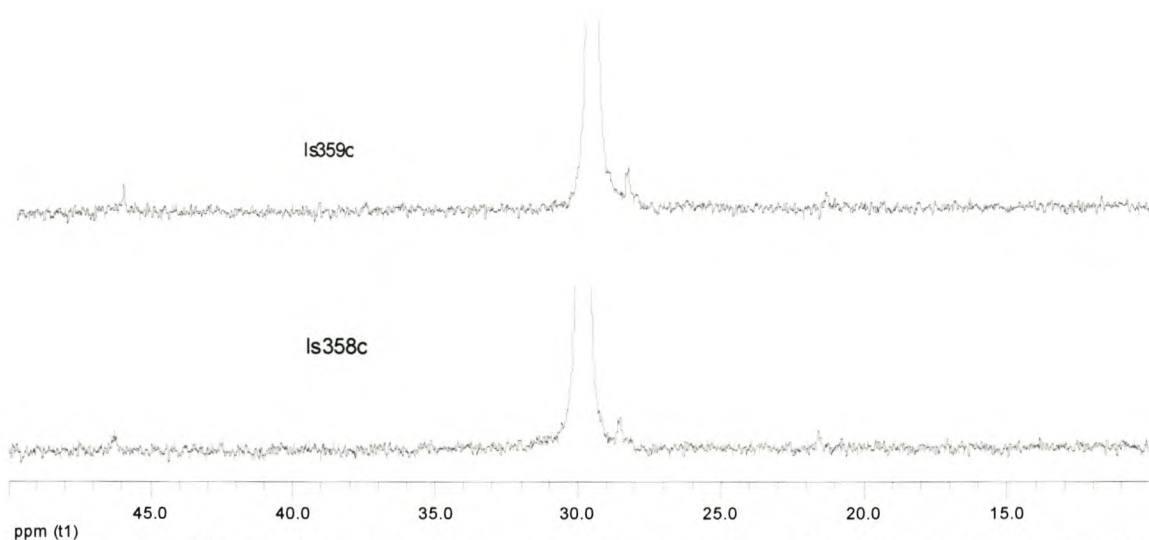


Figure 11: ^{13}C NMR spectra of reaction products 358 and 359 (Table 2) after hexane extraction.

What is of the most interest in this section is the attempted homopolymerization of an oligomer. This experiment proves that some vinyl endgroups must be present in the oligomers, otherwise no polymerization would be possible.

An attempt was made to homopolymerize the propylene oligomer using the constrained geometry catalyst. This reaction had very low yield and produced an essentially atactic product. Crystaf analysis could, for instance, not be done for this homopolymer

The ^{13}C NMR spectrum of the homopolymer showed broader peaks than the ones observed in the spectra of the oligomers. The broadening of the peaks could have been caused by growing of polymer by the oligomers which lack stereoregularity hence resulting in an oligo-oligomer ($M_w = 10\ 000$) with little or no stereoregularity. Shown in Figure 6, the disappearance of the end-group methyl carbon in the spectrum of the homopolymer, which was previously observed in the spectrum of the oligomer indicates the formation of a polymeric compound.

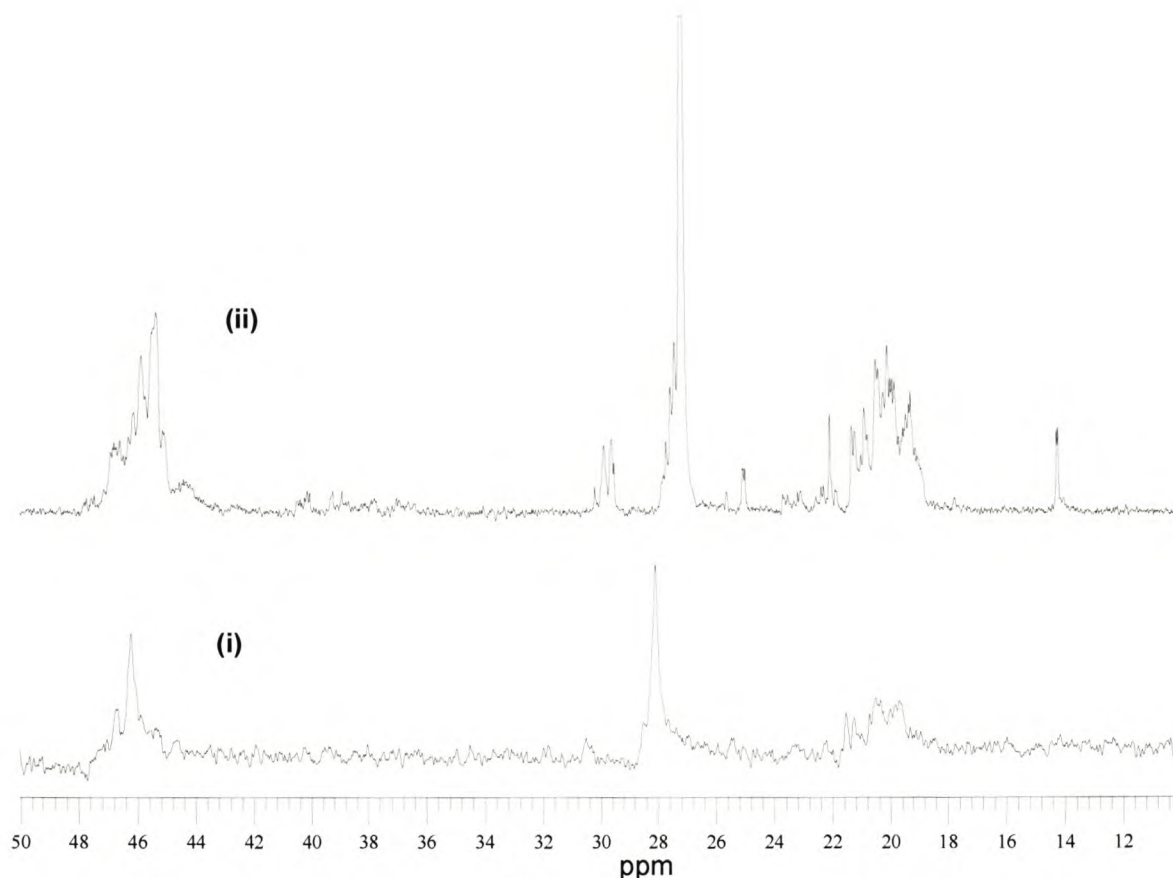


Figure 12: ¹³C NMR spectra of the oligomer (ii) in deuterated chloroform, and its homopolymer (i) in trichlorobenzene synthesized using catalyst (2).

5.3 Copolymer Molecular weight

The molecular weights shown in Table 1 (catalyst **1**) are, with one exception, all very high, albeit lower than the homopolymer with ethylene. There does not appear to be any relationship between amount of oligomer used, T_p , oligomer molecular weight and the molecular weight of the copolymer. The same applies to the MWD, although some very broad molecular weight distributions are recorded, mostly because of bimodal distributions. The molecular weights of the copolymers were analyzed using high temperature size exclusion chromatography (GPC). The GPC curves showed that all the high molecular weight polymers have substantial low molecular weight content. The polydispersities of some copolymers produced by both the syndiospecific catalyst (**1**) and constrained geometry catalyst (**2**) were bimodal. A representative GPC trace is shown in Figure 13.

The observed molecular weight curves, were usually broad for the copolymers synthesized using catalyst (1) and the resultant molecular weight distribution was very high. However, in some bimodal curves, the polydispersities were analyzed for each individual curve, and it revealed narrow polydispersity. The copolymers synthesized by the constrained geometry catalyst (2), generally had narrower MWD's compared to the ones of copolymers synthesized by the syndiospecific catalyst (1).

The polydispersities of the polymers probably varied as a result of the inclusion of co-oligomers in the material or not. It is thought that inclusion of the vinyl-terminated oligomers into copolymers resulted in two different species being synthesized, those in which early inclusion of oligomer resulted in chain transfer and termination leading to low molecular weight materials, and those where the inclusion occurred at a later stage, whereupon much higher molecular weight materials were obtained. It is assumed that inclusion of the long-chain oligo(propylene) macromonomers would likely lead to dormant species and chain termination due to β -hydrogen transfer⁶.

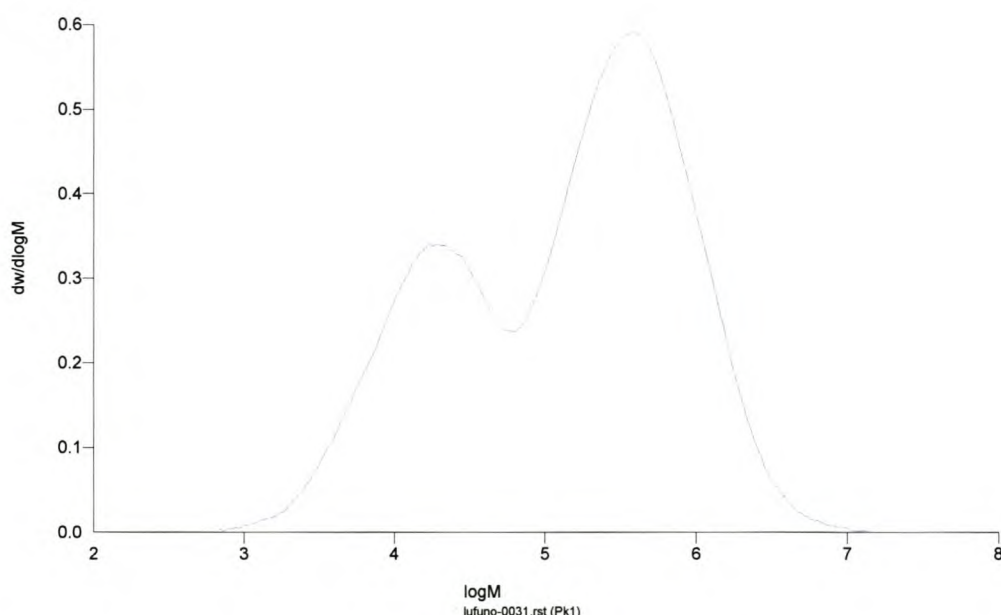


Figure 13: GPC curve of ethylene copolymer with propylene oligomer ($M_w \cong 4\,200$) synthesized using catalyst (1) at 70°C.

The above is particularly true in the situations where a large amount of the oligomer has been used in the polymerization process.

Some of the copolymers which showed large bimodal curves, were dissolved in boiling xylene. The solution was allowed to cool down, and filtered. The NMR study of the xylene soluble polymer revealed a copolymer of ethylene with propylene oligomers. This further indicates that the second molecular weight peak was not only oligomers, but a copolymer of oligomers with ethylene.

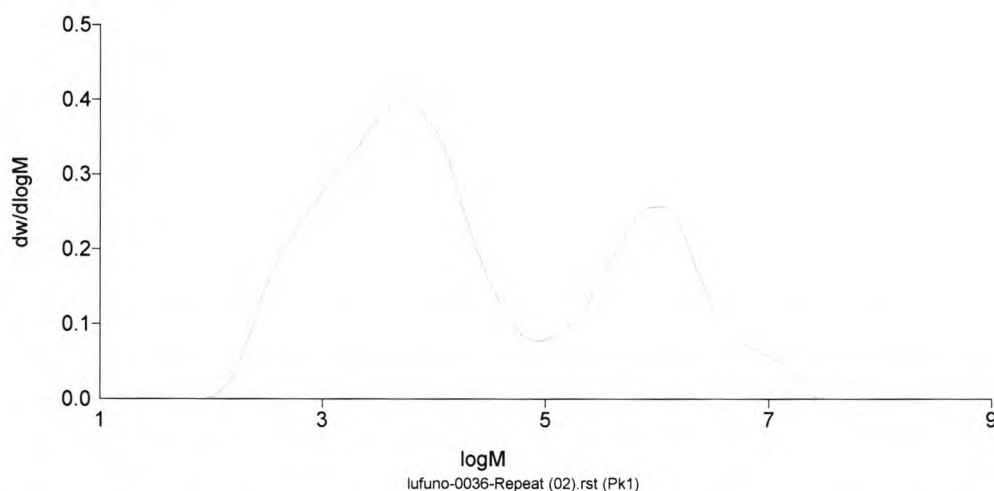


Figure 14: GPC curve of ethylene copolymer with propylene oligomer ($M_w \cong 1\ 800$) using catalyst (2) at 60°C.

The appearance of second molecular weight peaks shown in Figures 12 and 13, implied the presence of two polymer species of different molecular weights. In Figure 12 which shows a copolymer synthesized using catalyst (1) there is a small peak at low molecular weight region, which is in contrast to the one shown in Figure 13, showing a small peak at high molecular weight region for the copolymer which was synthesized using catalyst (2).

5.4. Crystallization analysis by fractionation (CRYSTAF)

The polymers were, after simple ether extraction, dissolved in trichlorobenzene and were heated to above their melting temperatures and then allowed to cool down.

The CRYSTAF traces show peak crystallization temperatures for the copolymers (Figure 14). In addition, it can be seen that the crystallization temperatures vary

with some of the polymers synthesized by catalyst **2**, having lower peak crystallization temperatures than the polymers made by catalyst **1**. In addition, the copolymers seem to have more than 1 crystallization peak, with significant soluble residues (material not crystallizing at 30°C)

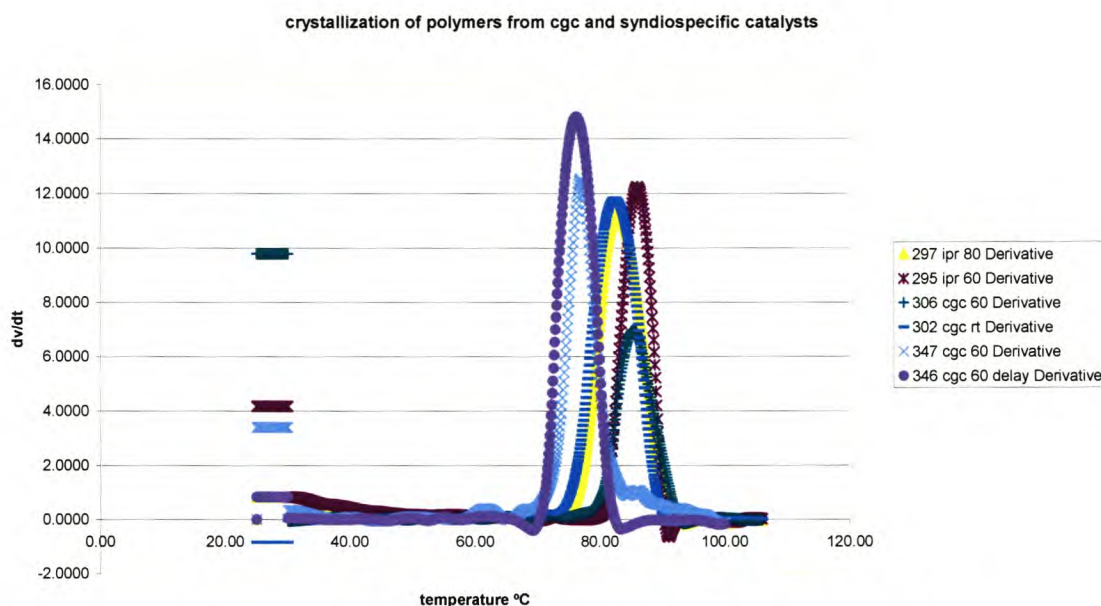


Figure 15: Crystallization curves of the copolymers, Δ and $*$ were synthesized using catalyst 1 at polymerization temperatures of 60 and 80°C, and $+$, o , and x were synthesized using catalyst 2 at 60°C, while $-$ was synthesized using catalyst 1, at room temperature..

It is interesting to note that with all the samples being semi-crystalline, while there is only one large crystallization curve, some shoulders appear either above the crystallization peak (higher T, for example run 302) or below (around 60°C) and the rest of the material appear as a soluble fraction at low temperature. The significance of the soluble fractions is that metallocene catalysts should produce uniform, chemically similar molecules with similar crystallization characteristics. This has been demonstrated by Soares *et al*¹². Yet these polymers obviously have a wide molecular weight and chemical distribution. This indicates that the presence of the oligomers during polymerization leads to a heterogeneous product, possibly due to more facile termination after incorporation of one or more oligomer molecules into the polymer chain.

The amount of the soluble fraction was observed to be higher for the copolymers synthesized at lower temperatures, and these fractions decreased as the copolymerization temperatures was increased. This behavior was observed for both catalysts systems. The explanation for this behavior can be based on the inclusion of the propylene oligomers. The copolymers formed at lower temperatures with catalyst **2** have wider MWD than those synthesized at 60 - 80°C which accounts for a larger low-molecular weight non-crystallizable fraction. Comparison of selected polymers made by catalyst **1** is shown in Figure 15.

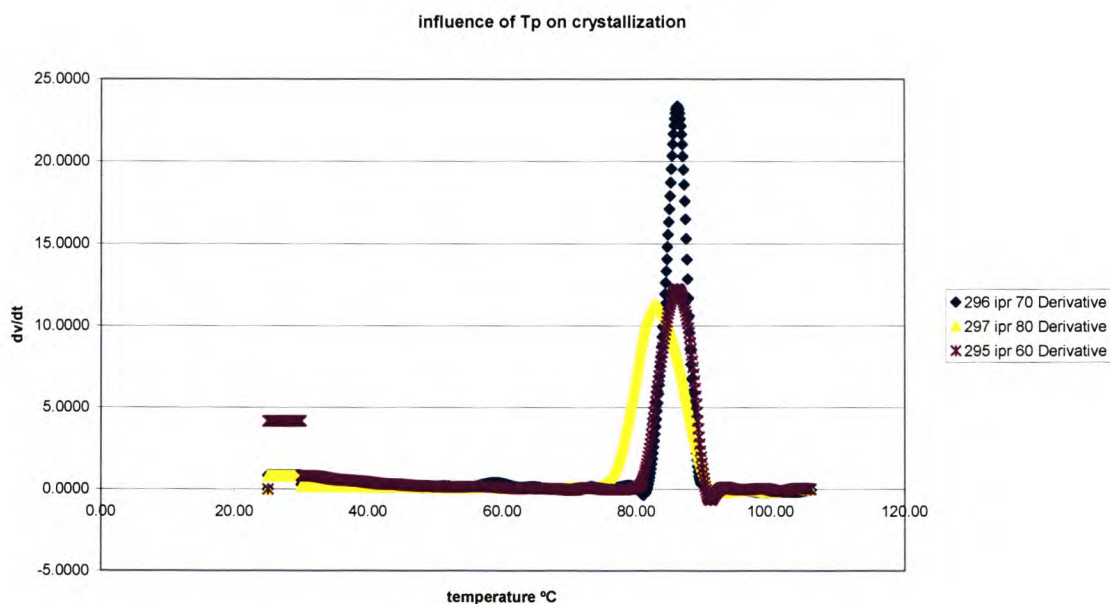


Figure 16: Influence of polymerization temperatures on the crystallinity of the copolymers synthesized using catalyst 1, *, \diamond , Δ at polymerization temperatures of 60, 70 and 80°C respectively.

The temperature at which the copolymers were synthesized had an influence on the crystallization curves of the copolymers and their amount of soluble material. At lower polymerization temperatures, there was a higher amount of soluble material, which can indicate formation of low molecular weight copolymers. This is similar to the results obtained with the catalyst 2, but the reason is not clear, as the molecular weight distributions for the materials made by this catalyst is broad for all the materials, although it is broader (MWD = 11.4) for the lower temperature product than for the other two (MWD = 8.6 – 9.1). All of these three materials

showed a slight bump in the crystallization curves around 60°C, indicating a second, slightly crystallizable fraction.

On the other hand the copolymers synthesized at high temperature had broader crystallization curves than the polymer synthesized at lower temperature and smaller soluble fractions. At higher temperature it is expected that there will be higher incorporation of oligomers in the copolymers. The narrower crystallization curve observed for copolymer synthesized at lower temperature may be explained by incorporation of fewer oligomers in this fraction. Without fractionation of the copolymers this cannot be proven, although the NMR spectrum of a xylene soluble fraction of one of these copolymers does show incorporation of oligomers in this fraction (see Figure 16). The decrease of molecular weight of polymer should be another factor of increasing polymer solubility⁸.

The spectrum in Figure 16 shows a high concentration of oligomer in the copolymer, simply by comparing the intensities of the methylene carbons of the ethylene (around 32ppm) with that of the propylene oligomer (around 46 ppm). Also, the appearance of peaks at 23 and 27 ppm are interesting, as these might be due to long-chain branching.

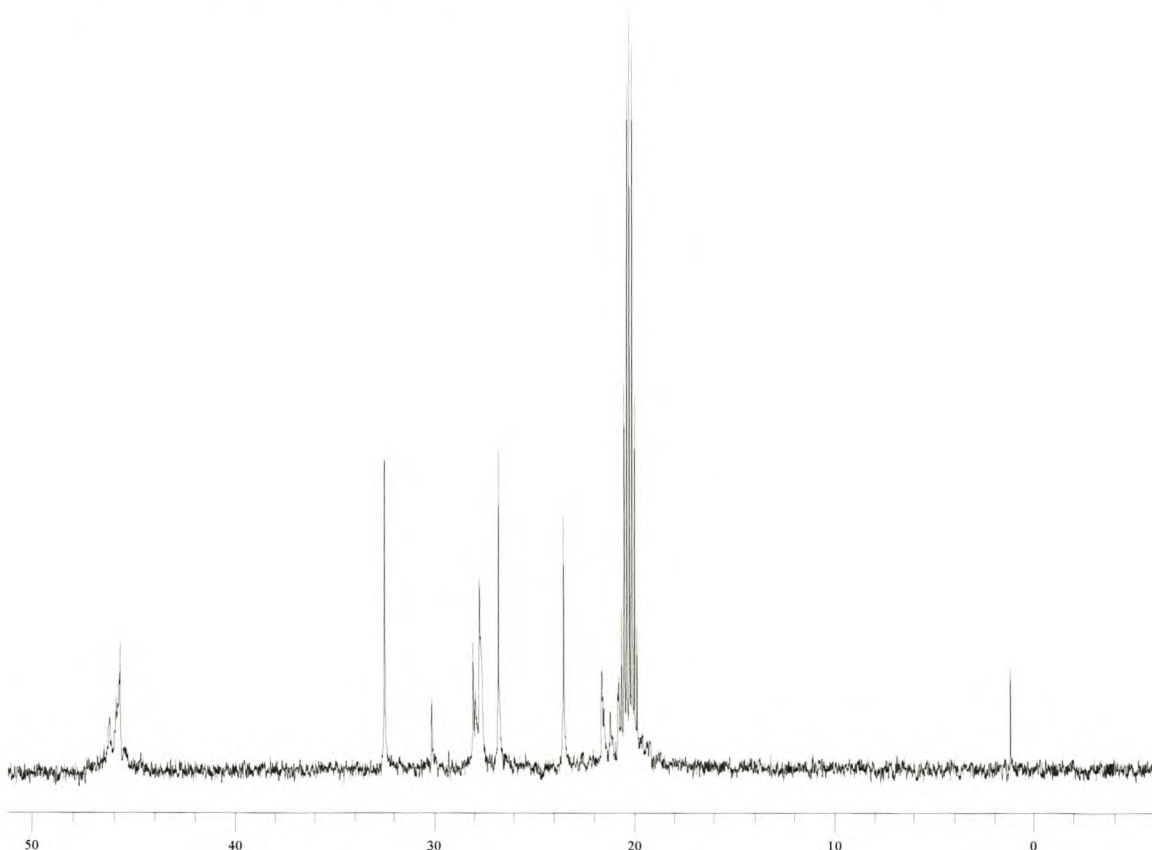


Figure 17: ^{13}C NMR spectrum of xylene soluble fraction of copolymer in toluene- d^8 . The large peak at 20 ppm is due to solvent.

5.5 Thermal characterization

Thermal analysis of the copolymers was done on a Mettler DSC by heating the polymers from room temperature to 180°C, and taking the reading from the second heating scan.

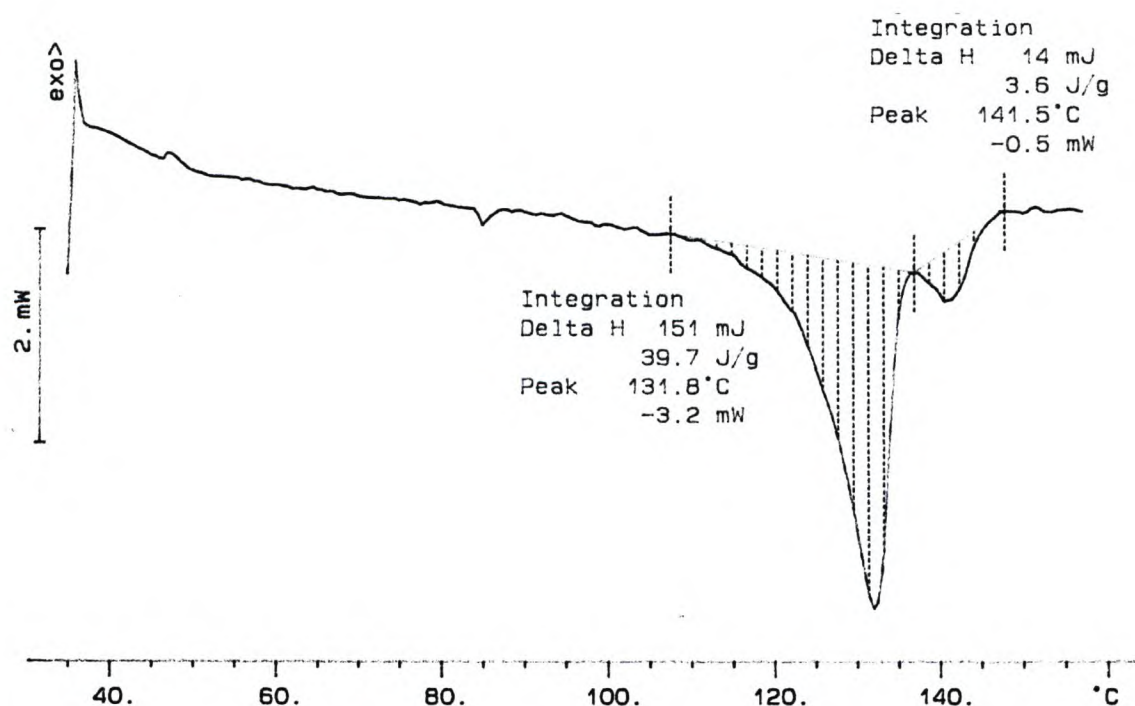


Figure 12: DSC thermogram of the ethylene copolymer with propylene oligomer ($M_w \cong 4\,500$) synthesized using catalyst 1 at 70°C.

These copolymers produced broader melting temperatures than the polyethylene homopolymers under similar conditions. The melting temperatures of these copolymers ranged from 126°C – 136°C. The corresponding enthalpy values (Table 3) started from as low as 39.8 J/g to high values of 135 J/g. For copolymers synthesized with the syndiospecific catalyst this low melting temperatures and enthalpy values represent a decrease in crystallinity of the polymers compared to the polyethylene homopolymers⁹. It may be attributed to

longer side chain branches in ethylene copolymer causing disorder and irregular crystal structure¹⁰.

Table 4: Enthalpy values of copolymers from DSC and their melting temperatures.

Run	Oligomer Mw	Polymerization temperature	Melting temperature (°C)	ΔH (J/g)
3*	0	60	131.4	129.2
4 ⁺	0	60	134.8	170.4
274	4 200	80	135.2	74.9
282	4 800	70	131.8, 141.5	39.7, 3.6
295	4 800	60	132.2	65.9
297	4 300	80	133.2	118.7
302 ^Δ	1 800	60	131.1	124.3
308 ^Δ	1 800	25	130.8	46.1
346 ^Δ	500	60	131.5	60.2
347 ^Δ	600	60	126.9	23.6
348 ^Δ	600	60	132.6	92.2
357 ^Δ	1 600	70	133.1	108.0
358 ^Δ	900	70	130.4	70.1
359 ^Δ	900	70	129.9	57.2

* and + were polymers synthesized without oligomers using catalyst **1** and **2** respectively. Δ were copolymers synthesized using catalyst **1**, and the other copolymers were synthesized using catalyst **2**.

In overall the copolymers produced by the constrained geometry catalysts displayed lower heats of fusion than the copolymers synthesized using the syndiospecific catalyst. The low melting temperatures and their corresponding heat of fusion were lower than for polyethylene homopolymers with long chain branching prepared using the constrained geometry catalyst (135°C and 180 J/g)¹¹.

In both catalyst systems the melting temperatures increased with decreasing the amount of the oligomer in the polymerization feed. Copolymerization with oligomers of very low molecular weight resulted in copolymers with a lower melting temperature, and the baseline was decreased during the measurement of the melting temperature.

5.6 Conclusions

¹H NMR spectra appear to show some signs of endgroups other than the predominant vinylidene type. Selected copolymerization reaction with ethylene seems to indicate that the vinyl-terminated oligomers could selectively copolymerize with ethylene using two different metallocene catalysts, while leaving the vinylidene-terminated oligomers unreacted. This appears to be the case where copolymers with very wide PDI are found. Crystallization studies (Crystaf) and DSC, in conjunction with ¹³C NMR analyses of materials extracted with hexane indicate that there appears to be different molecular species present in the copolymers. This is borne out by the GPC results. It is possible that, where vinyl-terminated oligomers are included in the polymer chain, the inclusion is followed immediately by β -H abstraction and chain termination, leading to low-molecular weight materials with low crystallizability. The latter is borne out by the presence of a considerable amount of soluble material evidenced by the Crystaf analyses. In addition it is noticeable that the molecular weight of the products obtained during the polymerization of ethylene in the absence and presence of oligomer were distinctly different. This indicates some reaction of the oligomers during the polymerization reaction.

Limited amounts of low-molecular weight homopolymer were also obtained when the oligomers were reacted with catalyst in the absence of ethylene as a comonomer. This also indicates the presence of some vinyl endgroups in some of the materials, as the vinylidene endgroups are not polymerizable with transition metal catalysts.

5.7. References

1. W. J. Wang, E. Koldka, S. Zhu, A. E. Hamielec; *J. Polym. Sci. A: Chem.*, **37**, **1999**, 2949.
2. H. G. Alt, E. Samuel; *Chem. Soc. Rev.*, **27**, **1988**, 323.
3. M. Eskelinen, J. V. Seppala; *Eur. Polym. Journal*, **32**, **1996**, 331.
4. E. Koldka, W. J. Wang, P. A. Charpentier, S. Zhu, A. E. Hamielec; *Polymer*, **41**, **2000**, 3985.
5. C. Li Pi Sahn, J. B. P. Soares, A. Penlidis; *Polymer*, **43**, **2002**, 773.

6. D. Harrison, I. M. Coulter, S. Wang, S. Nistala, B. A. Kuntz, M. Pigeon, J. Tian, S. Collins; *J. Mol. Cat. A: Chem.*, **128**, **1998**, 65.
7. S. Lieber, H. H. Brintzinger; *Macromolecules*, **33**, **2000**, 9192.
8. I. Kim, S. Y. Kim, M. H. Lee, Y. Do, M. S. Won; *J. Polym. Sci: A, Chem.*, **37**, **1999**, 2763.
9. H. G. Alt, M. Jung, *J. Organomet. Chem.*; **568**, **1998**, 87.
10. K. J. Chu, T. H. Park; *Mater. Lett.*, **31**, **1997**, 11.
11. D. Yan, W. J. Wang, S. Zhu; *Polymer*, **40**, **1999**, 1737.
12. D.M.Sarzotti, J. B. P Soares, A., J Pendelis,. *Polym. Sci. Part B, Polym. Phys.*, **40**, **2002**, 2595.

Chapter 6

Functionalization and block copolymerization reactions of propylene oligomers

6.1 Introduction

In this chapter, the introduction of functional groups into the oligomer via the reactive chain-ends is discussed. The first step was the conversion of vinylidene end-groups of the propylene oligomers to hydroxyl groups. The second step was the reaction of the resultant hydroxyl groups on the propylene oligomers with acrylic and methacrylic acid chlorides to form acrylate and methacrylate esters. The (meth)acrylate esters of propylene oligomers were homopolymerized and copolymerized with methyl methacrylate using free radical initiators. These reactions should result in poly(meth)acrylates with oligopropylene blocks incorporated.

In the early 90's, Mulhaupt et al.¹ reported the on the functionalization of vinylidene terminated propylene oligomers with various functional groups such as maleic anhydride, silane, epoxy, thiols and borane. The presence of borane functional groups afforded further conventions to other functional groups such hydroxy group. These oligomers were copolymerized with MMA to give propylene-b-MMA polymers.

6.2 Hydration of oligomers

The propylene oligomers, which were described in Chapter 4, were reacted with mercuric acetate to yield oligomers with hydroxyl end-groups. The resultant product was obtained via the conversion of vinylidene end-groups in the propylene oligomers to hydroxyl groups by oxymercuration-demercuration reaction process^{2,3}. This method brings about the hydration of the alkenes with regioselectivity that obeys Markovnikov's rule. This results in the introduction of a tertiary hydroxyl group in the oligomer.

6.2.1 NMR Studies

6.2.1.1 ¹H NMR

The hydrated oligomers were dissolved in deuterated chloroform and TMS was used as an internal reference. The ^1H NMR spectra of an oligomer before and after hydration are shown in Figure 1.

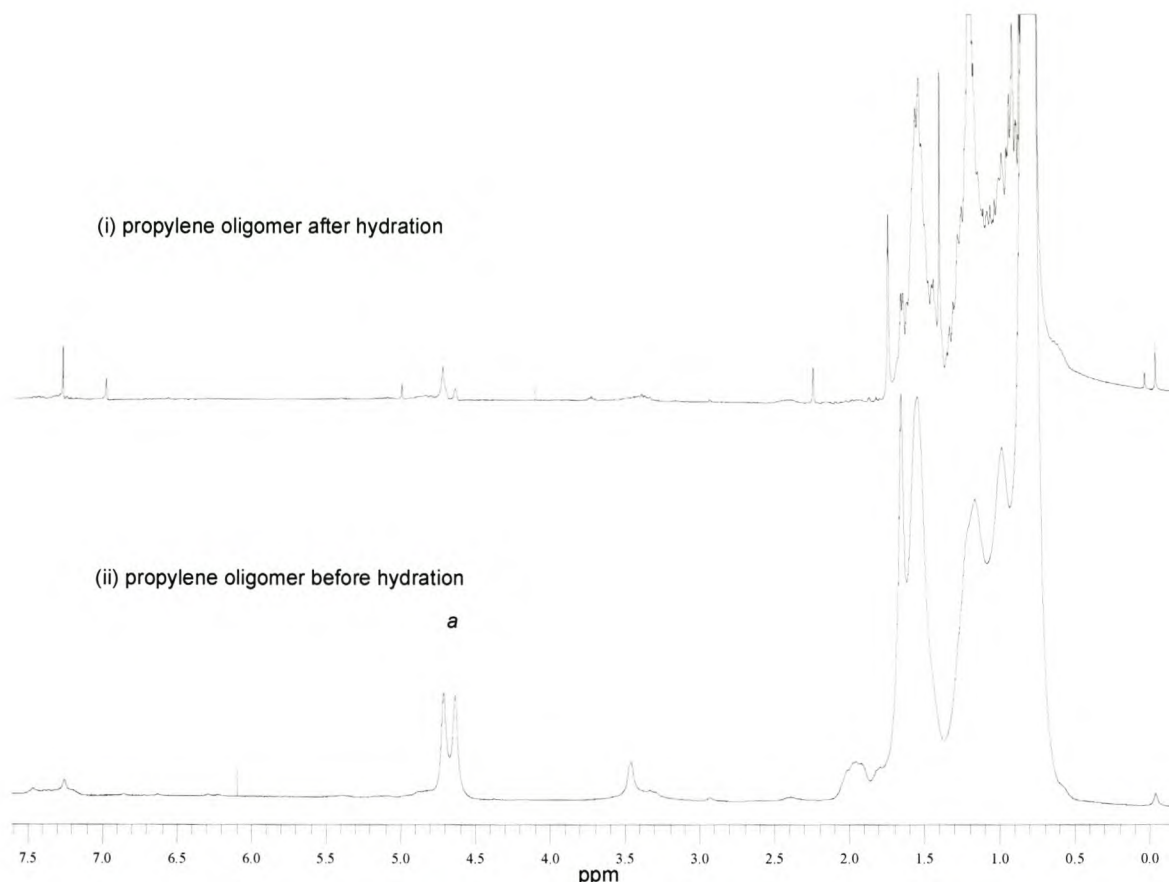


Figure 1: ^1H NMR spectra of propylene oligomers ($M_w \approx 500$) : (i) after hydration and (ii) before hydration.

From the above figure it can be observed that the hydration process was not completely effective. The peaks in the spectrum representing the vinylidene chain end-groups, (depicted by the letter *a*, at 4.75 and 4.85 ppm) of the oligomer have almost, but not completely, disappeared after the hydration reaction. The presence of signals from the protons adjacent to the hydroxyl group cannot easily be detected as their resonances are in the same region as the peaks associated with the backbone of the oligomers.

A range of propylene oligomers with varying molecular weights were hydrated using this process (see Table 6.1). The product yield during the hydration process depends on the molecular weight of the propylene oligomer. For low molecular

weight oligomers ($M_w \leq 1\ 000$) the conversion was greater than 85%, but the conversion decreased with increased molecular weight of the oligomer. With oligomers having $M_w \cong 2\ 500$, the hydration process was difficult to complete, and this resulted in products which were extremely difficult to isolate. For low molecular weight material separation of the product was much easier than it was for high molecular weight material. The ^1H NMR of the high molecular weight oligomer showed very little evidence of successful hydration reactions.

Table 1: The molecular weights of the oligomers which were hydrated.

Oligomer molecular weight	Success of hydration
350	Very good
500	Very good
700	Very good
1 000	Good
1 500	Good
2 000	Poor
2 500	Very poor

6.2.1.2 ^{13}C NMR

The samples were dissolved in deuterated chloroform with TMS as internal reference. ^{13}C NMR spectra of an oligomer before and after hydration are shown in Figure 2.

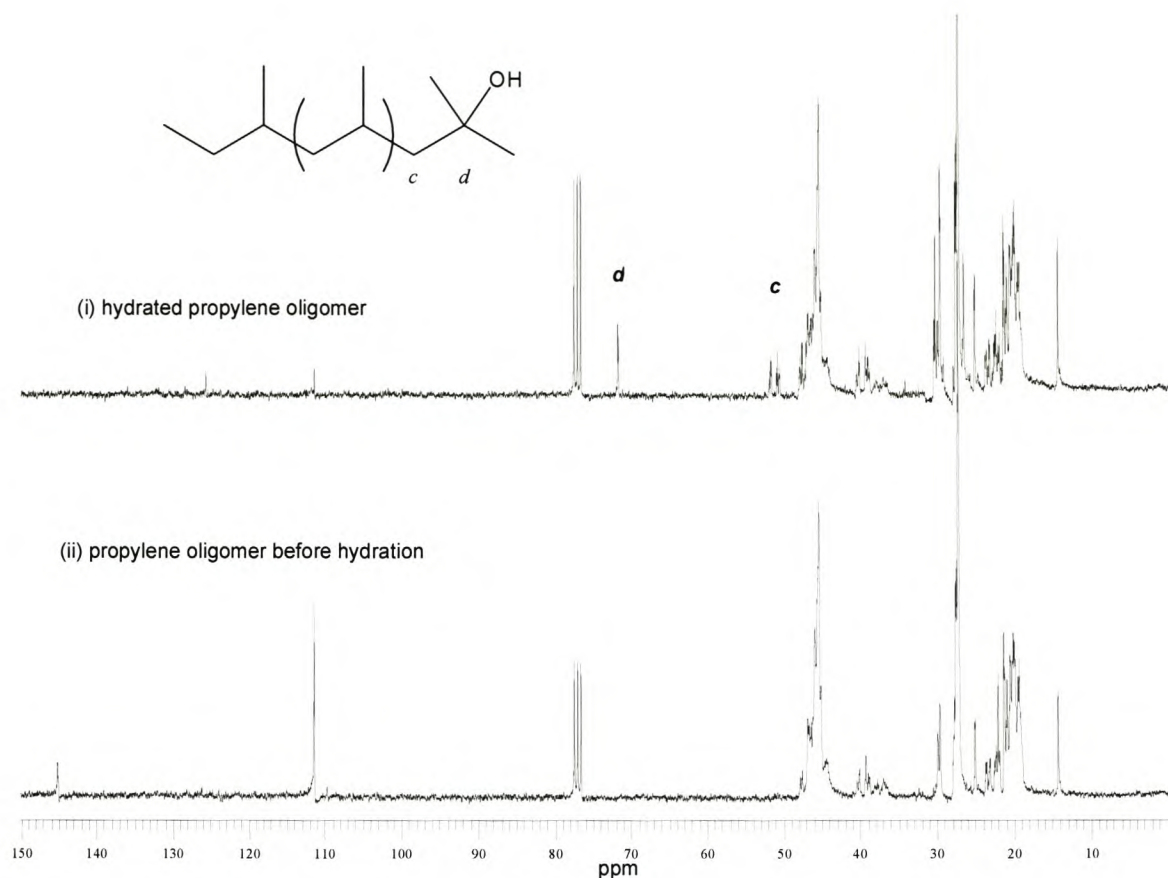


Figure 2: ¹³C NMR spectra of propylene oligomers ($M_w \cong 500$): (i) shows the spectrum of the oligomer after it was hydrated and (ii) before it was hydrated.

The spectra shown in Figure 2 confirms the evidence of the ¹H NMR spectrum for the same oligomer (Figure 1). The vinylidene carbon peaks are at 111 and 144 ppm. The spectrum of the hydrated oligomer (i) shows a decreased intensity of the peak at 111 ppm quite clearly. A peak appears at 71 ppm in spectrum (i) (labeled *d*). This represents the formation of a tertiary carbon containing a hydroxyl group. There are also new peaks (marked as *c*) which appear at 52 – 51 ppm, and these peaks represent the carbon adjacent to the hydroxyl group. The prominent appearance of these peaks as doublets can be the result of the stereochemistry of the hydroxyl group.

6.2.2 Infrared spectra

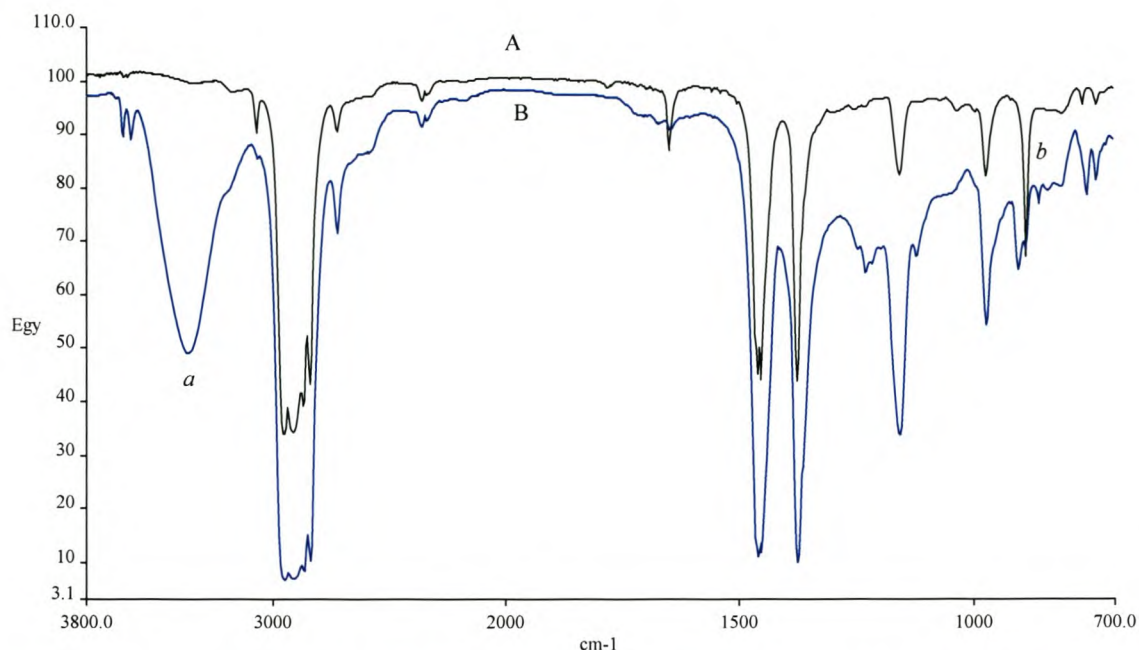
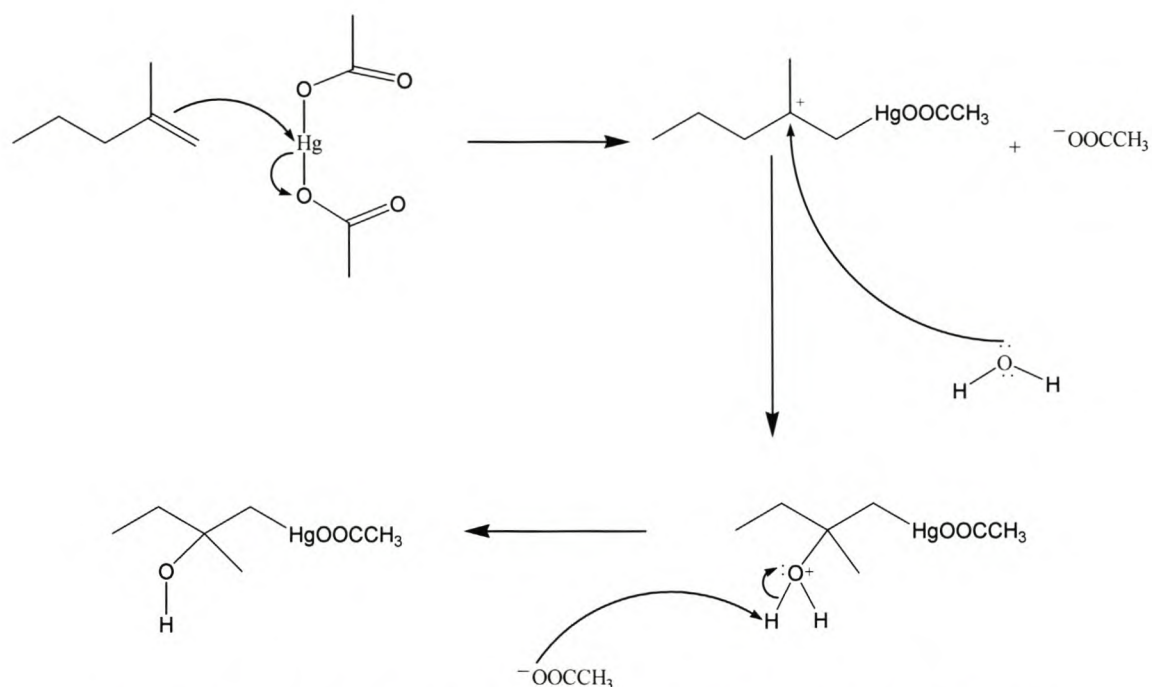


Figure 3: Infrared spectra of propylene oligomers ($M_w \cong 700$), (A) before hydration and (B) after hydration process.

Figure 3 shows the FTIR of hydrated (B) and non-hydrated (A) propylene oligomers. The emergence of the OH stretch between 3300 cm^{-1} and 3500 cm^{-1} marked as (a) confirms the conversion of the vinylidene group in the oligomer to hydroxyl group. The bending vibrations of the protons attached to the terminal vinylidene groups at 840 cm^{-1} and 980 cm^{-1} marked as (b) became strongly suppressed^{2,3}. However owing to the bulky size of the oligomer chain, it is difficult to have complete hydration of the vinylidene group, and this can be observed in the spectra of the hydrated product, traces of the alkene groups can still be observed. This can also be seen in the ^1H and ^{13}C NMR spectra of the hydrated oligomers.

6.2.3 Mechanism of hydration

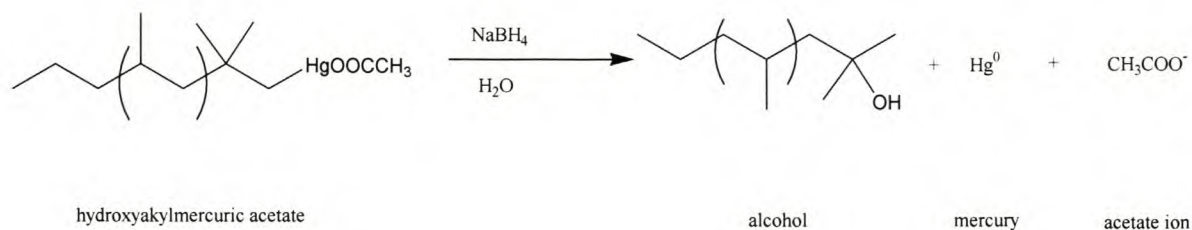
Scheme 1 shows a schematic of the hydration process. The reaction starts with the formation of a mercury-carbon bond³.



Scheme 1: Hydration of oligomers using mercuric acetate¹.

The carbocation formed in this step is of special kind, stabilized by the presence of the mercury substituent on the carbon adjacent to the positively charged one. These carbocations are readily formed, are relatively stable and do not rearrange. Because these reactions were carried out in the presence of water, the resulting compounds are known as hydroxyalkylmercuric acetates. This reaction is known as oxymercuration.

The solvent mixture in this reaction is water and tetrahydrofuran. The choice of the solvent mixture is based on the ability of water to mix with tetrahydrofuran in all proportions, and THF is a good solvent for organic compounds. Water acts as a nucleophile toward the mercury-substituted carbocation intermediate. The water molecule attacks the carbocation formed in the earlier step.



Scheme 2: Removal of mercury from the oligomers.

The hydroxyalkylmercuric acetate formed in the oxymercuration step is not normally isolated but is instead treated directly with sodium borohydride (NaBH_4) as shown in Scheme 2. Sodium borohydride converts the hydroxylmercuric acetate to an alcohol. This step is called demercuration. The carbon-mercury bond of the hydroxyalkylmercuric is replaced by a carbon-hydrogen bond.

6.3 Esterification of the hydrated oligomers

The presence of the hydroxyl group in the oligomer allows modification of the oligomer endgroup to other functional groups. In this section two methods based on the modification of Schotten-Baumann reactions that were used to obtain the (meth)acrylate esters of the oligomers (oligopropenyl(meth)acrylates) are described. The first attempt was to use THF as solvent under low temperatures and the second method was based on the use of ether as the solvent under even lower temperatures.

6.3.1. Reactions of methacryloyl chloride in THF

The hydrated propylene oligomer was reacted with methacryloyl chloride in THF as the solvent medium.

This method was found to be only partially effective in the sense that, although the conversion of the hydroxyl groups to the corresponding acrylate ester was evident from both the NMR and IR spectra, there was a large amount of the unreacted hydroxylated oligomer present, which remained in the product. Owing to the nature of the oligomers used, separation of the product from the unreacted hydroxyl-containing oligomer was not possible.

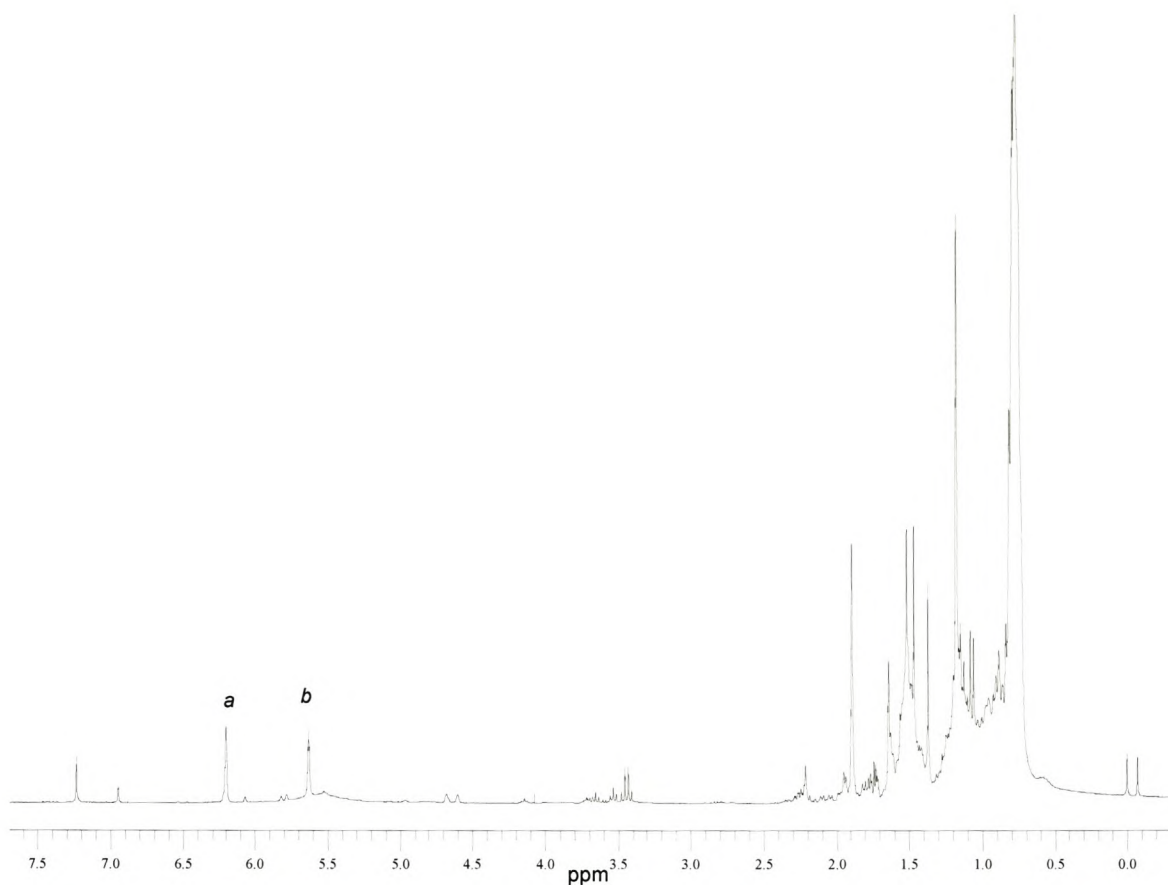
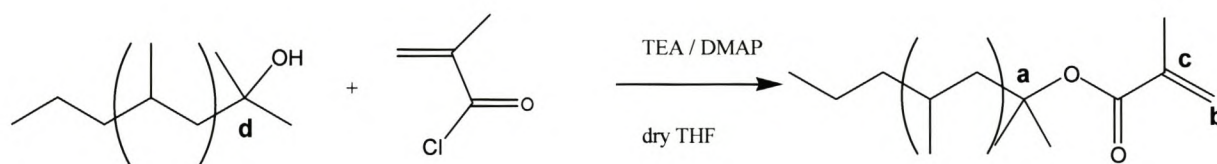


Figure 4: ^1H NMR of the methacrylate ester of a propylene oligomer ($M_w \cong 800$).

Figure 4 shows the ^1H spectrum of a hydrated propylene oligomer after reaction with methacryloyl chloride. Appearance of peaks (a) and (b) at 6.3 ppm and 5.8 ppm respectively is the result of inclusion of the vinyl protons of the methacryloyl ester. Several attempts to purify the product were not successful. This is evident by the presence of other peaks in the upfield region.



Scheme 3: Esterification of oligomers using methacryloyl chloride⁴.

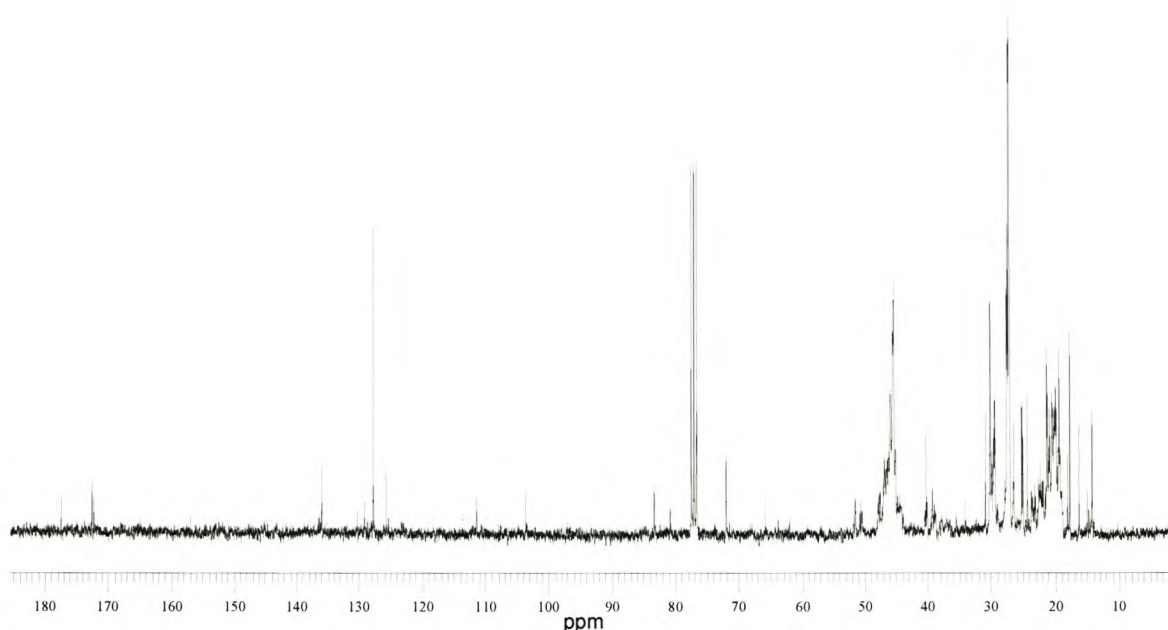


Figure 5: ^{13}C NMR spectrum of the methacrylate ester of a propylene oligomer ($M_w \cong 800$).

Figure 5 shows a ^{13}C NMR spectrum of propylene oligomer after being converted to the methacrylate ester. In the above spectrum the presence of the methacrylate ester group is confirmed by presence of chemical shift at 83 ppm, which arises from the carbon designated **a** in Scheme 3. Further downfield, peaks which show chemical shifts 172 ppm and 176 ppm arises due to the presence of the carbonyl group.

The appearance of multiple peaks at 172 and 176 ppm region can be assigned to the stereochemistry of the product. The peaks, which show chemical shifts at 128 ppm and 137 ppm, are associated with the vinylic carbons of the methacryloyl ester (**b** and **c** in Scheme 3). As it can be clearly seen in this spectrum, the presence of the characteristic peak at 71 ppm (**d** in Scheme 3) indicates that this method was not effective and a substantial amount of the propylene oligomer did not react with the methacryloyl chloride

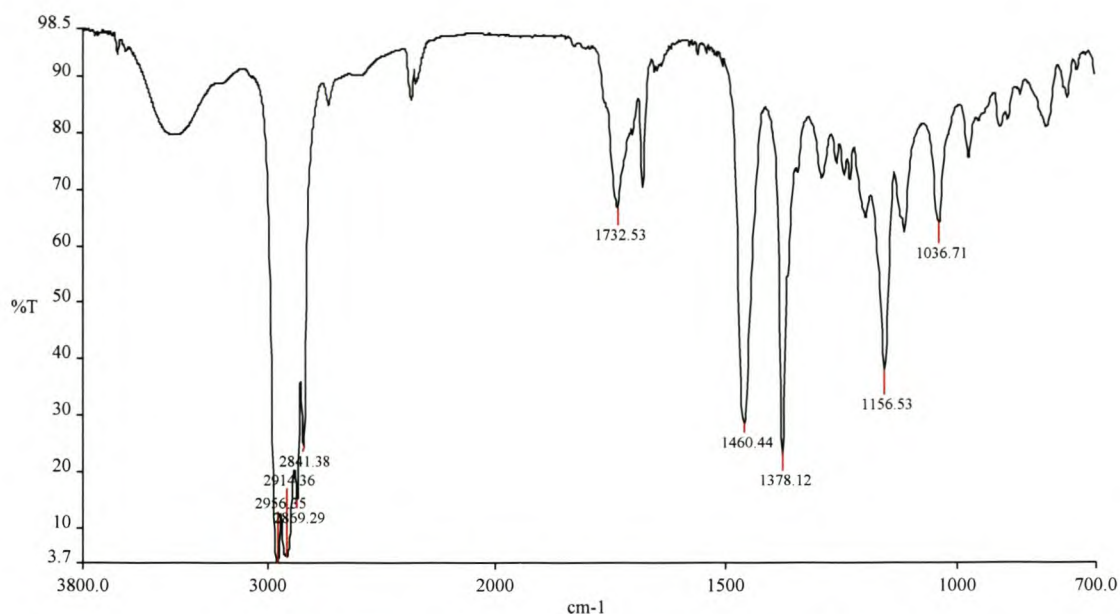


Figure 6: Infrared spectrum of the methacrylate ester of the propylene oligomer ($M_w \approx 800$).

In Figure 6, the FTIR spectrum of the hydrated propylene oligomer after it has been converted to a methacrylate ester via a reaction with methacryloyl chloride is shown. This reveals further evidence that this method was not very successful, the presence of the hydroxyl group peak is clearly observed in the spectrum. The carbonyl stretching peaks are observed at 1732 cm^{-1} and they show weak absorptions. Evidence from both NMR and IR thus confirms the lack of success with this type of reaction.

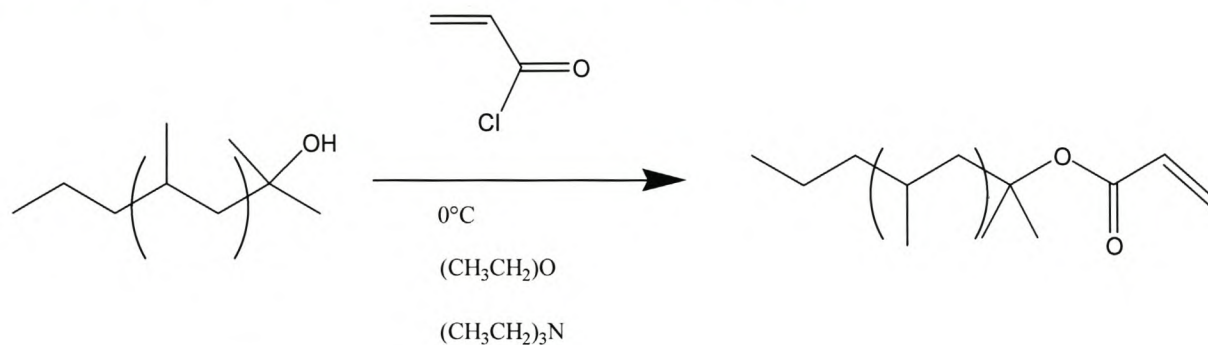
6.3.2 *The reaction of acryloyl chloride with oligomer in ether as a solvent*

After the reaction in THF proved to be unsuccessful (Section 6.3.1), a different approach was tried. This method involved reaction of the (meth)acrylic acid chloride with the hydrated oligomer using ether as a solvent⁵. Acryloyl chloride reacted much more readily with the hydrated oligomer and showed fewer byproducts than during the reactions of the hydrated oligomer with methacryloyl chloride.

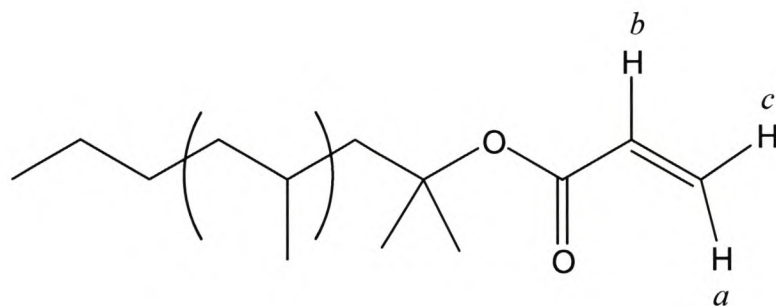
Furthermore it can be stated that the esterification of acid chlorides is strongly affected by the steric hindrance. Bulky groups on either reaction partner slow down the rate of reaction considerably, resulting in a reactivity order among

alcohols of primary > secondary > tertiary. Taking the above into account it can be understood why the reactivity of the high molecular weight oligomers are low.

It is clear that two factors will lead to a decrease in the reactivity of the oligomers: the fact that the hydroxyl group is tertiary and the size of the oligomer. The latter will affect mobility and accessibility of the hydroxyl groups.



Scheme 4: Reaction of hydrated oligomer with acryloyl chloride⁶.



Scheme 5: Assignment of vinyl protons of the acrylate ester of propylene oligomer.

Scheme 5 shows the assignment of vinyl protons in the acrylate ester of the propylene oligomer, which results from the reactions of the hydrated oligomer with acryloyl chloride.

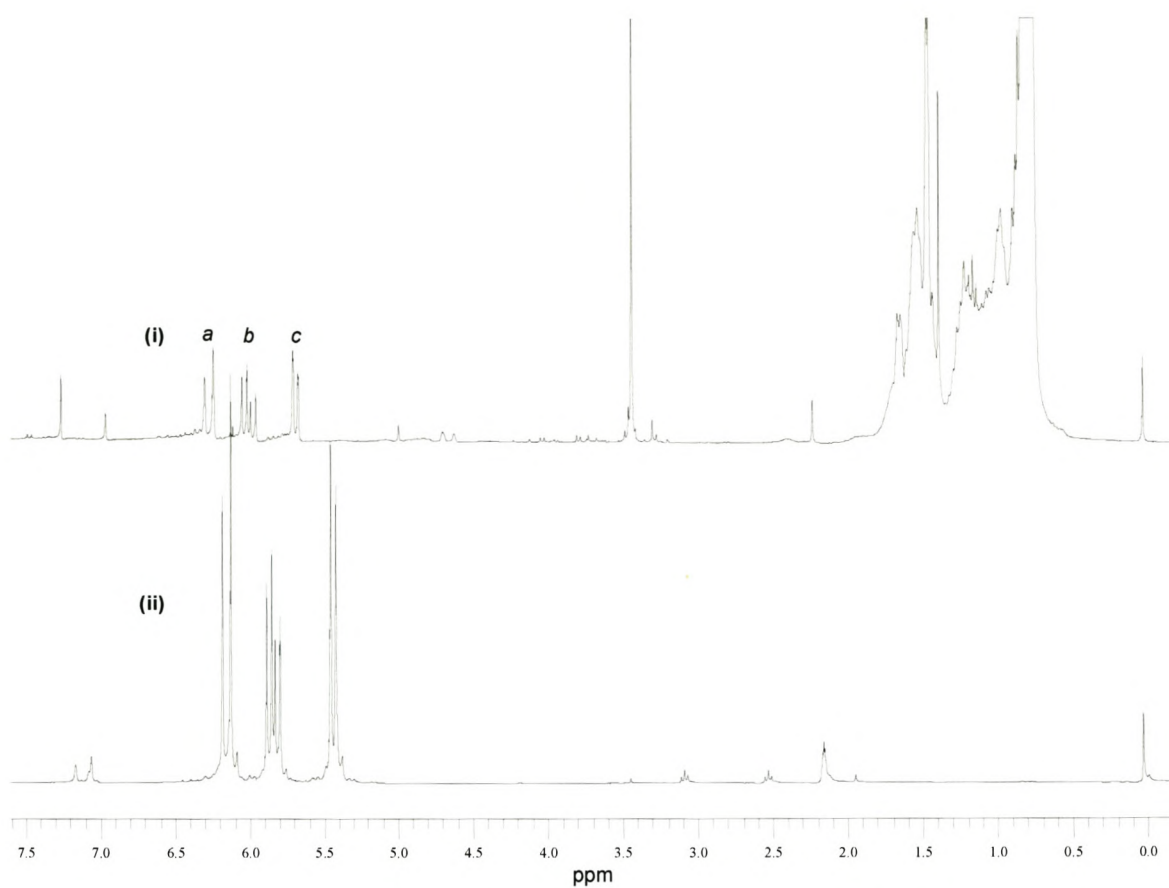


Figure 7: ¹H NMR spectra comparing the unreacted acryloyl chloride (ii) and acrylate ester of a propylene oligomer (i) ($M_w \cong 350$).

In Figure 7 the ¹H NMR spectra of acryloyl chloride (ii) and a propylene oligomer (i) after esterification with acryloyl chloride in ether, are shown. The presence of the acrylate group can be observed by the presence of the vinyl peaks from acryloyl chloride (see Scheme 5) at 5.7, 6.1, 6.3 ppm for protons *a*, *b* and *c* respectively.

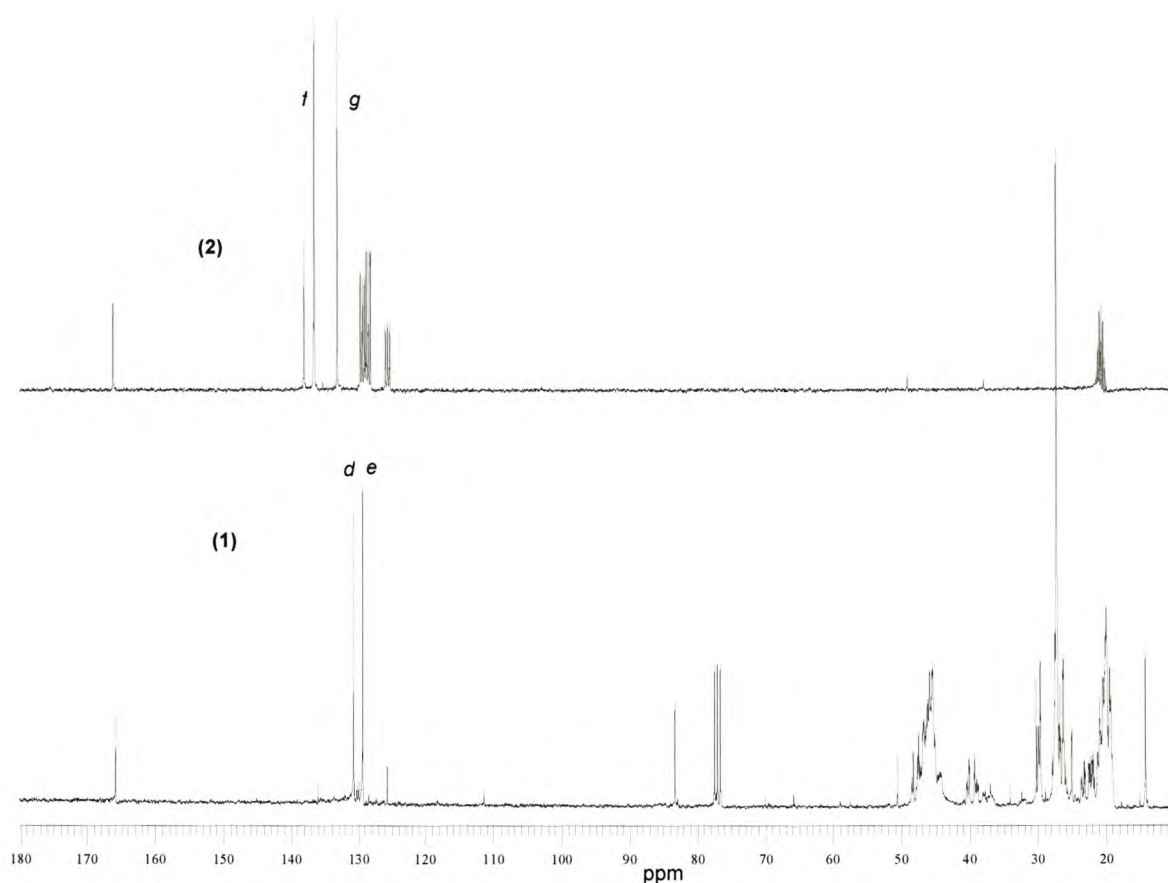


Figure 8: ¹³C NMR spectra of acryloyl chloride (2) in toluene-*d*₈ and the acrylate ester of propylene oligomer (1) (Mw ≅ 350) in CDCl₃.

In Figure 7 it is clear that the peaks of the acryloyl chloride have shifted downfield after reaction. The peaks associated with the acryloyl chloride before the reaction, were at 5.4, 5.85, and 6.18 ppm respectively. The stereochemistry around the vinyl protons of this acrylate group results in the split of chemical shift of these protons. This is also observed in the spectrum of the unreacted acryloyl chloride.

Figure 8 shows a comparison of the ¹³C NMR spectra of acryloyl chloride (2) and that of the acrylate ester of propylene oligomer (1), after reaction with acryloyl chloride. The conversion of the hydroxyl group to an acrylate ester is observed by complete disappearance of the hydroxyl carbon and a new peak is observed at 83 ppm, which is the tertiary carbon bonding the propylene oligomer to the acrylate group. Downfield at 168 ppm is a sharp carbonyl peak, which is confirming the incorporation of the acrylate ester. Another interesting feature in the above spectra is the shift of the vinyl carbons *f* and *g*; in the acryloyl chloride they appeared downfield at 133.2 ppm and 136.5 ppm and they shifted upfield to 129.3 and 130.8 ppm respectively, shown by peaks *d* and *e* respectively.

In this study, attempts were made to carry out the esterification of methacryloyl chloride with oligomers of $M_w \cong 1\,500$. With oligomers of such high molecular weight, the esterification does take place, however the rate of converting the alcohol to the ester is much slower. After 48 hours of reaction time, there is still a large amount of the unreacted hydroxylated oligomer present. Evidence of that could be clearly observed from the IR spectrum showing hydroxyl absorption peak, and the NMR showing the C- bonded to the OH and a smaller peak of the C bonded to the COO.

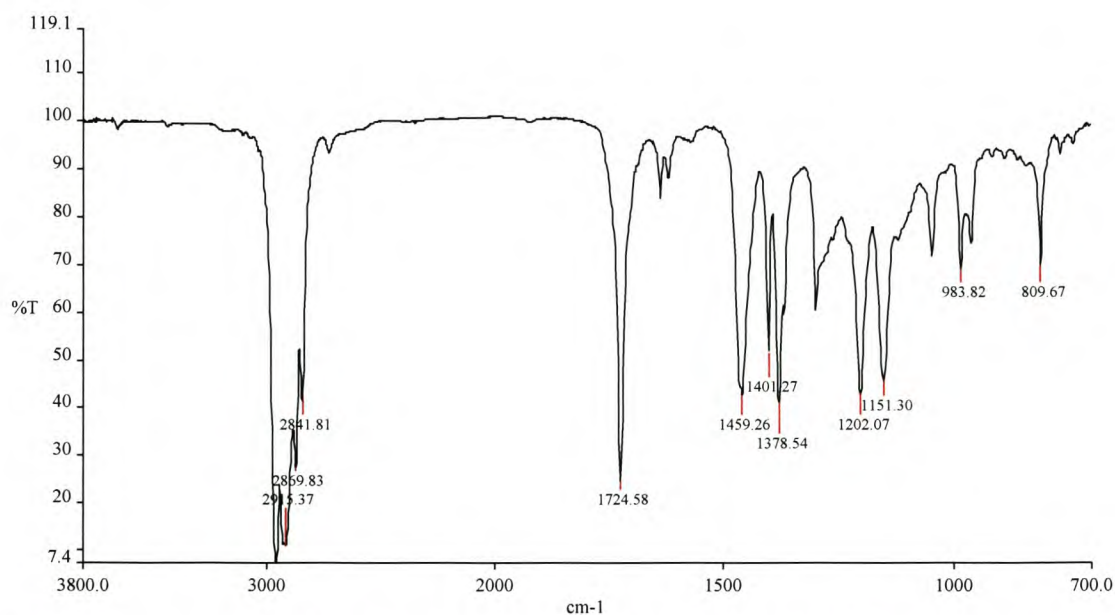


Figure 9: Infrared spectrum of the acrylate ester of a propylene oligomer ($M_w \cong 350$).

The above figure shows an FTIR spectrum of a hydrated oligomer ($M_w = 350$) after esterification with acryloyl chloride. The esterification process appears to have occurred to 100% conversion as there is no hydroxyl group absorption peak observed. From the above spectrum the presence of the ester carbonyl group can be easily observed with a sharp absorption at the wavenumber of $1\,724\text{ cm}^{-1}$. The terminal alkene groups are also observed from stretching of the protons bonding to the C=C group at the wavelength of 809 and 980 cm^{-1} . The C-O stretching is also observed at $1\,202$ and $1\,150\text{ cm}^{-1}$.

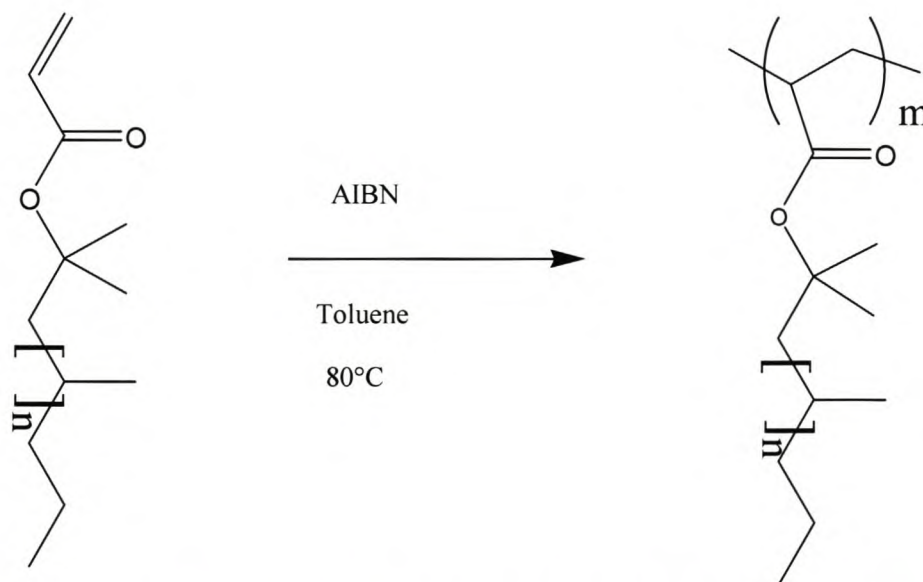
Overall the reactivity of the methacryloyl chloride in comparison to the acryloyl chloride was very poor, and it is suspected that the methacryloyl chloride could

have converted to the free acid upon contact with the atmospheric oxygen. The other most likely reason could be the purity of the methacryloyl chloride. The product was not obtained in its pure state and this could have resulted in the lack of reactivity and increased side reactions.

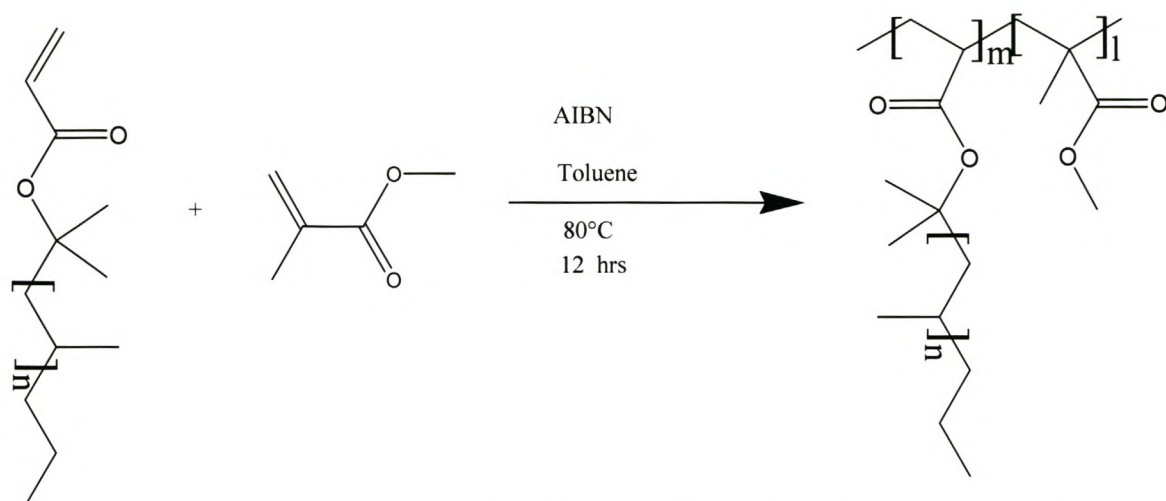
Another method, which was explored to incorporate the acrylate group to the oligomer, has been the use of phase transfer reactions of the hydrated oligomer with methacrylic anhydride. This method yielded no encouraging results and was discontinued.

6.4 Polymerization of the acrylate ester oligomer

The oligomers were polymerized using a free radical initiator at 80°C. For the homopolymerization (Scheme 6), the degree of polymerization was low, ranging from 5 to 15 repeat units. The polymer was a thick sticky non-crystalline material. However, when these oligomers were copolymerized with methyl methacrylate (Scheme 7), higher molecular weight polymers were obtained. The copolymers were a solid material. The molecular weight of the poly(methyl methacrylate) was found to be reduced by introduction of the acrylate propylene oligomer in comparison to the homopolymers of poly(methyl methacrylate).



Scheme 6: Homopolymerization of acrylate ester of oligomer with AIBN.



Scheme 7: Copolymerization of acrylate ester of oligomer with methyl methacrylate.

6.4.1 ^{13}C NMR of the polymer

Figure 10 shows the ^{13}C NMR spectra of oligopropenylacrylate before (i) and after (ii) polymerization using free radical initiators. It can be seen that the oligomer has undergone some degree of polymerization noting the carbonyl peak, which is downfield at 176 and the peak of the carbon at 81 ppm, has broadened. These peak show broad resonances which are typical of polymer molecules.

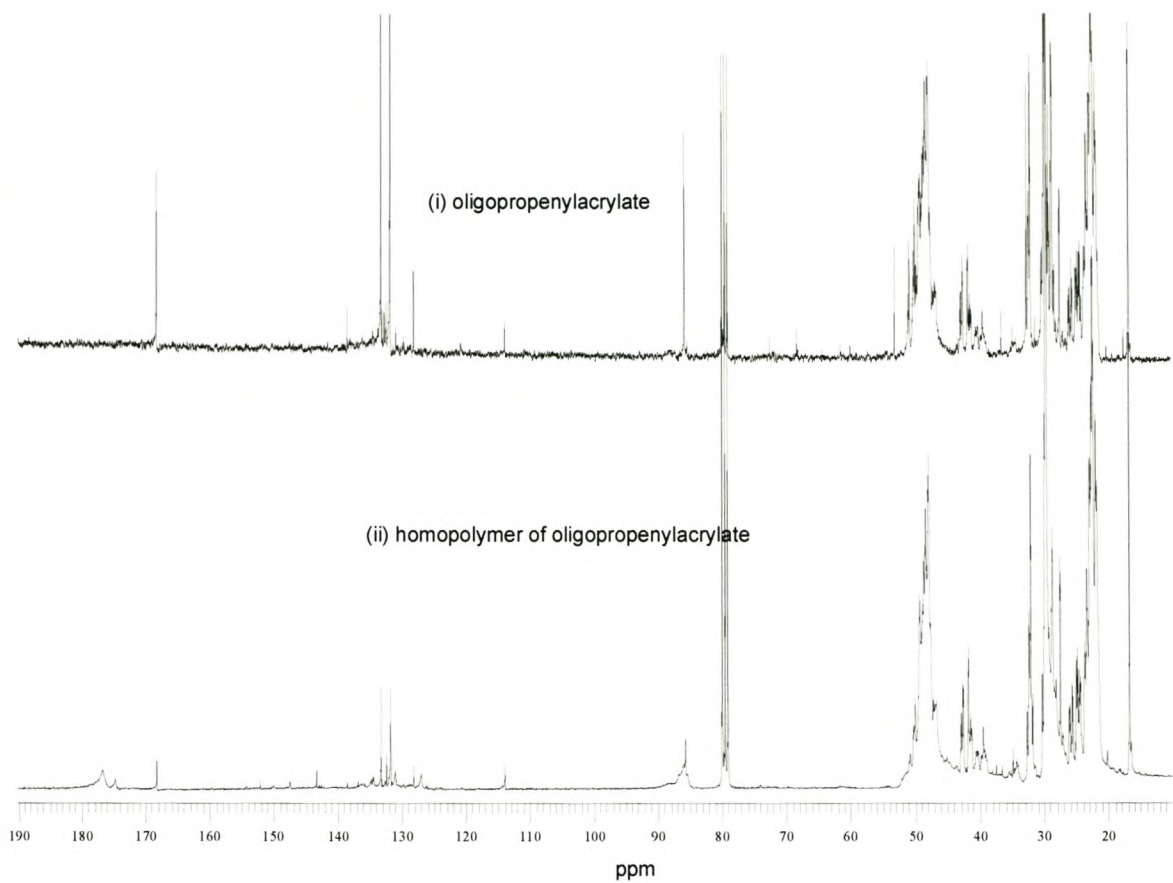


Figure 10: ^{13}C NMR spectra of the oligopropenylacrylate (i) and its homopolymer (ii).

6.4.2. Molecular weight of polymers

The homopolymer and copolymer of oligopropenylacrylate with methyl methacrylate show interesting GPC curves. From Figure 11, it can be seen that in the GPC of the homopolymer of the acrylate ester of the propylene oligomer, one single curve could be observed indicating that the polymerization occurred in one stage.

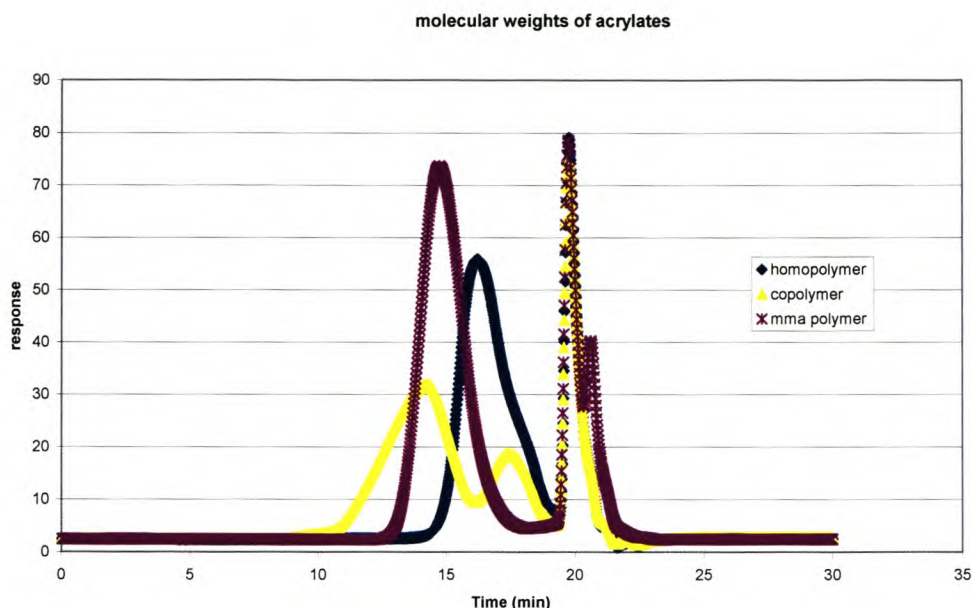


Figure 11: GPC curves of the acrylates synthesized using AIBN at 80°C, \diamond is the homopolymer of the acrylate ester of propylene oligomer, Δ is the copolymer of acrylate ester of propylene oligomer and \times is the homopolymer of MMA.

The copolymer of the acrylate ester and methyl methacrylate gave a bimodal molecular weight distribution. This bimodal curve is either due to formation of two homopolymers or due to two different species of copolymer. As the poly(oligopropenyl acrylate) has a low molecular weight and obviously chain-terminates easily, it is possible that during the copolymerization of the acrylate with the methacrylate addition of the oligopropenylacrylate could be shortly followed by chain termination.

The molecular weight of the higher molecular weight fraction of the copolymer is higher than that of the homopolymer of MMA prepared under similar conditions. The low molecular weight peak is probably due to polymer formed when the oligopropenylacrylate was incorporated early in the reaction.

The peaks at the lower end of the graph (longer times) are the residual monomer which remained after polymer work-up.

6.4.3 Dynamic mechanical properties

The copolymer of oligopropenylacrylate with methyl methacrylate was analyzed by a dynamic mechanical analyzer, and results compared to that of the poly(methyl methacrylate) homopolymer. Figure 12 shows two overlaid curves of the polymers.

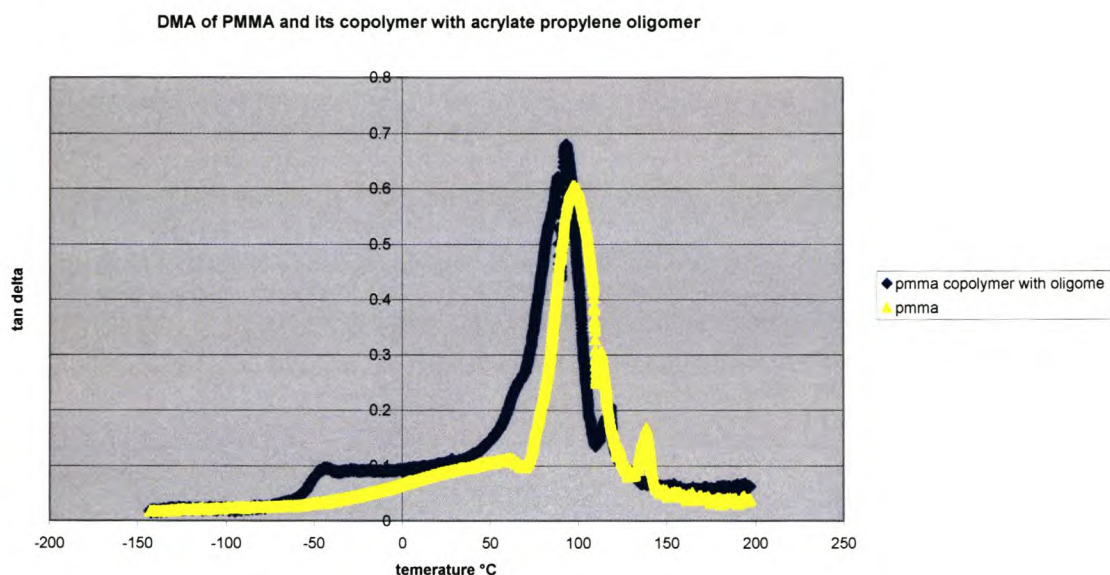


Figure 12: DMA curves of the PMMA (Δ) and a copolymer of PMMA with oligopropenylacrylate (\diamond).

In the above figure, subtle changes in the mechanical properties of the oligomers can be observed at low temperatures. While the $\tan \delta$ peak for both the homo- and copolymer is around 100°C (T_g of PMMA fractions), there is a slight decrease in the T_g for the copolymer. Interestingly at around -50°C in the curve of the copolymer a second transition becomes visible, which is likely due to a transition of the oligopropenyl phase. There can be little doubt that these two phases of the polymer would phase-separate, leading to two separate, observable T_g's. In addition a shoulder appears on the main chain $\tan \delta$ peak of the copolymer that was not there in the homopolymer.

6.5. References

1. R. Mulhaupt, T. Duschek, B. Rieger; *Makromol. Chem. Macromol. Symp.*, **48/49**, **1991**, 317.
2. H. C. Brown, P. J. Geoghegan; *J. Org. Chem.*, **35**, **1970**, 1844.
3. F. A. Carey, *Organic Chemistry*, McGraw-Hill Book Company, New York, **1987**, 219.
4. B. S. Funnis, A. J. Hannaford, V. Rogers, P. W. G. Smith, A. R. Tatchel; *Vogel's Text Book of Practical Organic Chemistry*, 4th Edition, Longman Incorporation, New York, **1989**, 1414.
5. H. Y. Acar, J. J. Jensen, K. Thigpen, J. A. McGowen, L. J. Mathias, *Macromolecules*, **33**, **2000**, 3855.
6. S. Balasubramanian, B. S. R. Reddy; *Eur. Polym. Journal*, **32**, **1996**, 1073.

Chapter 7

Conclusions and recommendations

7.1 Introduction

This chapter will serve as summary of the work which has been discussed in Chapters 4, 5 and 6 and recommendations for future work will be made.

7.2 Oligomerization

Successful oligomerization of propylene with three different catalysts in combination with MAO as a cocatalyst were demonstrated. Oligomerization was controlled by catalyst concentration, temperature of reaction, catalyst/cocatalyst ratio and reaction time.

The appearance of the oligomers ranged from fully liquid materials with molecular weights of less than 1 200 g/mol, to viscous gel-like materials with molecular weights between 1 500 to 3 400 g/mol.

The use of the catalyst $\text{Et}(\text{Ind})_2\text{ZrCl}_2$ (EBI) in conjunction with MAO lead to lower molecular weight oligomers than in the case of the $\text{Me}_2\text{Si}(2\text{-Me-4,5-Benzolnd})_2\text{ZrCl}_2$ (MBI) catalyst under similar conditions. Molecular weight could be controlled to anywhere in the region of 500 to 1 500 g/mole.

The microstructure of the oligomers were investigated using ^{13}C and ^1H NMR. Three aspects were of importance: the tacticity of the oligomers, the type of endgroups produced, the amount of 2,1-misinsertions and the type of stereoerrors found.

- The tacticity (expressed as $mmmm\%^1$) was very low for the C_{2v} -symmetric catalyst (as expected) and varied between 12 and 25% for the EBI catalyst systems and between 25 and 50% for the MBI catalyst (the latter being C_2 -symmetric metallocenes).
- With all the catalysts there were predominantly vinylidene endgroups produced, although some evidences of 2-butenyl endgroups and vinyl endgroups were found. This indicates that the predominant method of chain transfer was β -H transfer to catalyst.

- The level of 2,1-misinsertions were dependent on the type of the catalyst used (MBI > EBI > Cp₂ZrCl₂). Similarly the temperature of reaction also played a role, with higher temperatures resulting in levels of up to 9.5% of 2,1-misinsertions. Despite this, very little evidence of 2-butenyl endgroups were found (which would be due to β-methyl abstraction after 2,1-misinsertion), indicating β-H abstraction after a “normal” or 1,2-insertion.
- Stereoerrors over the whole spectrum of possible errors were found. This indicates enantiomorphic site control only becomes effective with an increase in molecular weight. This was also indicated by comparing a series of propylene reaction products made by the same catalyst at elevated temperatures with molecular weight varying between 800 and 400 000 g/mole.

Some propylene oligomerization reactions were conducted in the absence of solvent. These reactions resulted in polymers which were semi-crystalline and only soluble in chlorinated aromatic solvent at high temperatures. These polymers showed broad melting temperatures (DSC), and their crystallization curves were broad (Crystaf).

7.3 Copolymerization of oligomers with ethylene using metallocene catalysts

Copolymerization reactions of the oligomers with ethylene was attempted using two different metallocene catalysts; the C_s-symmetric catalyst (*i*-propylidene-(cyclopentadienyl)(9-fluorenyl)zirconium dichloride) the “constrained geometry” catalyst tetramethylcyclopentadienyl(dimethylsilyl-*t*-butylamido)titanium dimethyl.

The reaction products varied in composition. In general the following could be concluded:

- The reaction products had significantly lower molecular weights than poly(ethylene) produced by the same catalysts under similar conditions.
- In many cases the polydispersities of the materials were very broad.
- In all cases the melting temperatures of the formed materials varied very little from the ethylene homopolymers, but the melting endotherms as

observed by DSC were broader and the melting enthalpies lower than for the ethylene homopolymers.

- Extraction of the formed products with hexane was used to extract unreacted oligomer, indicating that the only oligomer to react was the vinyl terminated materials.
- The polymers with broad polydispersities could be shown to be essentially two materials; (i) an ethylene rich copolymer with very limited inclusion of oligomer, and (ii) an amorphous, low molecular weight material comprising essentially oligomer with a limited amount of ethylene included.
- Materials with broad polydispersities also had significant amounts of soluble (non-crystallizable) material, as evidenced by the Crystaf results.
- GPC results indicated bimodality in all of the materials where inclusions of the oligomers were observed after hexane extraction. This indicates the presence of two different types of copolymers.

In the homopolymerization of the oligomer, a low molecular weight solid material was obtained. This material had a very low degree of polymerization of about 10 repeat units. This homopolymer (or oligo-oligomer) did not exhibit any thermal transitions, but degraded when heated during thermal analysis.

7.4 Functionalization and block copolymerization

7.4.1 Hydration of propylene oligomers

The reactions of the propylene oligomers with mercuric acetate afforded hydrated products that obeyed Markovnikov's rule. The hydration of the oligomers was much easier for the oligomers which had low molecular weight, affording more than 90% conversion of the vinylidene endgroups to the hydroxyl group. Hydration of oligomers which had molecular weight of over 1 500 afforded less than 55% conversion whereas for those oligomers which had molecular weights of above 2 500 yielded less than 20% conversion of alkenes to hydroxyl groups. In general the oligomers which were synthesized using the EBI catalyst were easily hydrated whereas the oligomers synthesized using the MBI catalyst were not easily hydrated.

7.4.2 Synthesis of oligomer acrylate esters

The hydrated oligomers were converted to acrylate esters by reactions with acryloyl chloride or methacryloyl chloride. The conversion of the hydrated propylene oligomers from an alcohol to an acrylate ester was easily carried out using acryloyl chloride than when using methacryloyl chloride. Low molecular weight oligomers afforded an almost complete conversion of the hydroxyl group to an acrylate ester. NMR and IR spectroscopy were used to identify the corresponding acryloyl ester groups in the products.

7.4.3 Polymerization of acrylate esters

The derived oligomer acrylate esters were successfully polymerized using a free radical process. In the homopolymerization process the degree of polymerization was low but it increased when a comonomer was included. The presence of the oligomer acrylate ester in the copolymerization of methyl methacrylate was significant in the way that the copolymers had lower molecular weight than the methyl methacrylate homopolymers.

The resultant low molecular weight of the copolymers can be associated with the bulkiness of the oligomer which in turn block the incoming monomers to the growing polymer chain.

The presence of the oligomer acrylate ester in methyl methacrylate copolymers resulted in the appearance of a small peak in the DMA scan at lower temperatures. This implies that with proper control of the polymerization process; the mechanical properties of the copolymers of MMA with these functionalized oligomers can be changed. It is assumed that if a higher amount of the oligomer was used in the copolymerization reaction; it would have resulted in a shift of the T_g peak of the copolymer. Hence it is recommended that further studies be made on the copolymerizing MMA with these oligomers and attention be paid to the resultant mechanical property characteristics of these copolymers.

7.5 Recommendations

The following areas should be further investigated:

- The mechanical testing of copolymers of ethylene with low amounts of propylene oligomer present, to see if the apparent disruption of crystallinity affects polymer material properties.

- Preparative fractionation (like TREF) could be utilized to separate the ethylene copolymers into crystallizable fractions and non-crystallizable materials, and in so doing gain full picture of the molecular make-up of these polydisperse materials.
- The work on the acrylate macromonomers should be expanded. These materials have the potential to be useful in changing the properties of the traditionally glassy, brittle like PMMA and polystyrene.
- The preparation of primary alcohol terminated oligopropylene by borane chemistry on the vinylidene terminated endgroup would produce an oligomeric alcohol that will more readily react with MMA in order to prepare an MMA terminated polypropylene.

7.6 References

1. L. Resconi, L. Cavallo, A. Fait, F. Piemontesi; *Chem. Rev.*, **100**, **2000**, 1253.